

NP-8237

CONTRACT NO. 62558-(24)-1770.

NP-8237 R.126/4.

FINAL REPORT.

068-001

## **DISCLAIMER**

**This report was prepared as an account of work sponsored by an agency of the United States Government. Neither the United States Government nor any agency Thereof, nor any of their employees, makes any warranty, express or implied, or assumes any legal liability or responsibility for the accuracy, completeness, or usefulness of any information, apparatus, product, or process disclosed, or represents that its use would not infringe privately owned rights. Reference herein to any specific commercial product, process, or service by trade name, trademark, manufacturer, or otherwise does not necessarily constitute or imply its endorsement, recommendation, or favoring by the United States Government or any agency thereof. The views and opinions of authors expressed herein do not necessarily state or reflect those of the United States Government or any agency thereof.**

## **DISCLAIMER**

**Portions of this document may be illegible in electronic image products. Images are produced from the best available original document.**

FULMER RESEARCH INSTITUTE LTD.

Contract No. 62558-(24)-1770.

R.126/4/JUNE 1959.

PART A

THE MISCIBILITY GAPS IN THE U-Nb AND U-Nb-Zr SYSTEMS

by

B.S.Berry, M.Sc., Ph.D.

and

G.J.Partridge, B.Sc.,

SYNOPSIS.

The miscibility gap in the U-Nb system has been established using metallographic and X-ray techniques. The monotectoid temperature is placed at  $640^{\circ} \pm 2^{\circ}\text{C}$  and the composition limits at that temperature are 65-70 a/o Nb and  $17.5^{\circ} \pm 1$  a/o Nb, the monotectoid.

The  $700^{\circ}$ ,  $650^{\circ}$  and  $600^{\circ}\text{C}$  isothermal sections of the U-Nb-Zr system have also been investigated. Each of the miscibility gaps present in the limiting binary sections was found to be closed by additions of the third element. At  $700^{\circ}\text{C}$  the U-Zr gap is closed by addition of less than 5 a/o Nb. The behaviour of the Zr-Nb gap is less certain owing to the sluggish reactions close to this binary system but the gap appears to be closed by about 15 a/o U. The U-Nb gap has been studied in more detail and is closed by 14 a/o Zr. To a near approximation the ternary U-Nb gap can be considered to be bounded by the composition lines 33 a/o U, 14 a/o Zr and about 20 a/o Nb depending on temperature. A notable feature is that at Nb and Zr compositions approximately corresponding to a line of minimum lattice distortion, the  $\gamma$  phase at  $600^{\circ}\text{C}$  bulges towards the U corner.

As a result of the closure of the gaps the  $\gamma$  phase is stable over a large area of the diagram at temperatures down to at least  $600^{\circ}\text{C}$ .

I. INTRODUCTION.

The object of this research was to determine and account for the effect of zirconium on the miscibility gap in the uranium-niobium system. In view of the lack of agreement<sup>1</sup> on the size and shape of the the gap at the time this work was initiated, a new determination has been made, which agrees fairly well with the recently published findings of other workers<sup>2-4</sup>. Concurrently, the U-Nb-Zr isothermal sections at 700°, 650° and 600°C have been examined, and these also are found to be in overall agreement with the independent recent work of Dwight and Mueller<sup>5</sup>.

II. ALLOY PREPARATION.

(a) Materials.

1 Uranium.

The uranium was supplied by Harwell as rolled rod. A typical analysis is as follows:-

p.p.m.			
C	Fe	N	Mn
270	50	45	20

The 1" diameter rod was hot-rolled to 3/16" diameter and conveniently sized pieces sheared off. These were pre-melted in the arc furnace before alloying. The microstructure of the final premelted slugs is shown in Figs. 4 & 5, the major impurities being carbides.

2. Niobium.

The niobium was received from Murex Ltd., as ductile sheet offcuts containing ~2% Ta and an estimated O<sub>2</sub> content of 0.11 w/o.

### 3. Zirconium.

Zirconium pellets were prepared by arc melting low Hf sponge supplied by A.E.R.E. Harwell, and having the following batch analysis:-

Fe .....	0.02%
N <sub>2</sub> .....	0.005%
Cr .....	0.002%
Pb .....	<0.05%
Mg .....	<0.01%
Hf .....	0.03 $\pm$ 25%
Al .....	510 p.p.m. $\pm$ 15%
O <sub>2</sub> .....	750 p.p.m. mean range 500-1000 p.p.m.

#### (b) Selection of Alloy Compositions

The U-Nb diagram proposed by Sawyer <sup>1</sup> was used as a first guide to selecting the compositions of the binary alloys. Further alloys were then prepared in the light of the results obtained.

The appearance of the ternary diagram will be dominated by the behaviour of the miscibility gaps which are a feature of each of the limiting binary systems, and alloy compositions were chosen with this in mind to determine the limits of these miscibility gaps in the ternary systems. Further alloys were selected to locate more accurately the limit of the U-Nb miscibility gap. The compositions of the binary and ternary alloys are given in Tables 1 and 2, while their positions on the ternary diagram are shown in Fig. 6.

(c) Melting.

Alloy buttons weighing about 10 gm. were prepared in a multiple hearth argon arc furnace, taking special care to minimise melting losses. Segregation was avoided by remelting each button at least ten times.

(d) Homogenisation.

Care was taken to ensure that dendritic structure was removed from arc cast buttons by a thorough homogenising treatment. Where alloys had solidus temperatures below 1250°C they were Ta wrapped and annealed in evacuated silica capsules, while all other alloys were annealed in the high temperature vacuum furnace 15, at 50-100°C below their estimated solidus or 1550°C whichever was the lower. Figs 7 and 8 show the structures of a 50 a/o Nb alloy before and after annealing  $5\frac{1}{2}$  hours at 1400°C and  $90\frac{1}{2}$  hours at 1340°C.

(e) Working.

After homogenisation, some of the alloys were forged by hand at 650-750°C in an attempt to promote more rapid attainment of equilibrium on subsequent final annealing. There is evidence that this was successful in some alloys, but some tended to crack and working of others was not attempted.

(f) Compositions of Alloys.

Some of the more critical ternary alloys have been analysed, and while no binary alloys have been analysed, there is little doubt that the nominal and actual percentages are very close in view of a very small melting loss during alloying.

**III. EXAMINATION OF ALLOYS.**

**(a) Metallographic Technique.**

Specimens were mounted in bakelite, wet ground to 600 paper, and polished with 0-1  $\mu$  diamond dust and slow cutting alumina. For high U alloys the most generally useful etch was 10% aqueous oxalic acid, used electrolytically at 3-6 volts. For Nb-rich alloys a polish-attack method was used with slow cutting alumina and solutions of nitric and hydrofluoric acids in various proportions.

**(b) X-ray Technique.**

All X-ray photographs were obtained from the block metallographic specimens, using a 14 cm diameter camera in which the specimen is oscillated and rotated with respect to a beam of filtered Co K  $\alpha$  X-radiation. The majority of the binary alloys and the more important ternary compositions were examined.

**IV. RESULTS.**

**(a) The Miscibility Gap in the U-Nb system.**

The U-Nb miscibility gap, drawn in accordance with present metallographic and X-ray results, is presented in Fig. 9. The monotectoid is placed at 17.5 a/o Nb and 640°C, and the gap extends at 640°C to  $\sim$  65 a/o Nb. The procedure used in establishing the gap was to decompose the alloys at low temperatures (640 - 660°C), and to locate the phase boundaries by observing the phase changes produced on reheating to higher temperatures. This approach avoids the difficulty of the sluggish  $\gamma_1 + \gamma_2$  decomposition from  $\gamma$  at temperatures above 700°C, as reported by P.C.L. Pfeil <sup>4</sup>. The structures encountered in the various phase fields are described in turn below.

**1. The  $\gamma$  field.**

In alloys with less than 20 a/o Nb, the stable  $\gamma$  phase could not be retained on quenching to room temperature. Alloys containing up to 17.5 a/o Nb transformed on quenching either to the  $\alpha'$  or  $\alpha''$  modifications of  $\alpha$ , and some distortion of the b.c.c. pattern was

observed in the quenched 20 a/o Nb alloy. When lightly electrolytically etched with oxalic acid, the microstructure gave no indication of this transformation, and consisted only of structureless equiaxed grains (and impurities). An example is shown in Fig. 10. Longer etching, however, produced considerable broadening of the grain boundaries and acicular markings within the grains (see Fig. 11), which was found by experience to be an indication of the transformation on quenching.

Dwight and Mueller <sup>5</sup> have reported the existence of a body centred tetragonal phase in specimens of near monotectoidal composition. In the present work, this structure has been observed only in the 17.5 a/o Nb alloy, quenched from 1040°C after a homogenising anneal.

The  $\gamma$  phase was retained on quenching alloys containing more than 30 a/o Nb. On resolution of the structure produced by decomposition in the  $\gamma_1 + \gamma_2$  phase field, the grain size of the  $\gamma$  phase was much smaller than in the as-cast and homogenised state, as shown by comparison of Figs. 12 and 13.

## 2. The $\gamma_1 + \gamma_2$ field.

The intersection of the  $\gamma_1/a+\gamma_1$  boundary with the  $\gamma_1/\gamma_1+\gamma_2$  boundary and the monotectoid horizontal places the U rich limit of the  $\gamma_1+\gamma_2$  field at 17.5 a/o Nb, with an estimated accuracy of  $\pm 1$  a/o. Fig. 20 shows the globular type of  $\gamma_1+\gamma_2$  structures observed in the U-20 a/o Nb alloy.

At the Nb-rich end of the gap, as shown in Figs. 15 and 16,  $\gamma_1+\gamma_2$  decomposition was detected microscopically in the U-63 a/o Nb alloy after 21 days at 680°C, but not in the U-66 a/o Nb alloy. On this evidence (which may require modification in the light of longer anneals), the end of the gap is placed at 65 a/o Nb. Using the parameter composition curve for  $\gamma$  alloys obtained by Rogers et al<sup>3</sup>, however, the composition of the  $\gamma_2$  phase in  $a+\gamma_2$  type alloys is thought to be nearer 70 a/o Nb. The present evidence suggests therefore that the end of the gap is located in the region 65-70 a/o Nb.

The rate at which the  $\gamma$  phase decomposes to  $\gamma_1 + \gamma_2$  at 640 - 660°C becomes very much slower in alloys of increasing Nb content. The decomposition occurs on a fine scale and in a characteristic manner, illustrated by Figs. 17 and 18. On heating the  $\gamma_1 + \gamma_2$  structure to higher temperatures, some coarsening takes place as the annealing temperature approaches the  $\gamma/\gamma_1 + \gamma_2$  boundary, as shown in Fig. 19. The peak of the miscibility gap occurs at or near the 50 a/o composition and a temperature of 950°C. The 50 a/o alloy annealed at 960°C for 8 days showed a diffuse ghost structure in parts, but this is tentatively assigned to incomplete diffusion during the anneal, or incipient decomposition on quenching, rather than to the stability of the  $\gamma_1 + \gamma_2$  structure at 960°C.

### 3. The $\alpha + \gamma_1$ field.

The  $\alpha$  phase in the  $\alpha + \gamma_1$  structures tarnishes in air, giving in the unetched condition structures comprising darker globules or plates in a light matrix (Fig. 20). The  $\alpha$ -phase can be darkened further by electro-etching with oxalic acid, or outlined with the 4%  $\text{CrO}_3$ , 1% HF etch.

### 4. The $\alpha + \gamma_2$ field.

The  $\alpha + \gamma_2$  structures encountered were virtually the reverse of the  $\alpha + \gamma_1$  type noted above. The  $\alpha$  groundmass tarnishes characteristically, revealing a light dispersion of  $\gamma_2$  (Fig. 21).

It should be noted that the four structures listed in the key of Fig. 9 appear on the 640°C isothermal, and that this has been interpreted to mean that the monotectoid temperature lies so close to 640°C that inaccuracies of a degree or two in the annealing temperature can result in the structures lying just above and just below the monotectoid line being attributed to the range  $640 \pm 2^\circ\text{C}$ .

## (b) The Ternary U-Nb-Zr Isothermal Sections.

### 1. The Limiting Binary Systems.

- (i) The U-Nb System. The diagram of Fig. 9 has been used, with supplementary information on alloys of high U content taken from the report by Pfeil Brown and Williamson<sup>4</sup>.

(ii) The U-Zr System. The diagram proposed by Summers-Smith<sup>11</sup> apparently requires modification solely in connection with the  $UZr_2(\delta)$  phase, which affects the form of the diagram only below  $606^{\circ}C$ . The diagram assumed is that used by Dwight and Mueller<sup>5</sup>, and comprises the diagram of Summers-Smith above  $606^{\circ}C$ , and that of Rough, Austin, Bauer and Doig<sup>13</sup> below  $606^{\circ}C$ .

(iii) The Zr-Nb System. The diagram put forward by Rogers and Atkins<sup>12</sup> has been used, except where this is inconsistent with the few results obtained in the present investigation on Zr-Nb alloys. The miscibility gap in Rogers and Atkins diagram extends from 18 to 87 a/o Nb at the monotectoid temperature of  $610^{\circ}C$ . A minor discrepancy between this and the present results is that the 85 a/o Nb alloy in the present work is single phase at temperatures of  $600^{\circ}$ ,  $650^{\circ}$  and  $700^{\circ}C$ . The more serious discrepancy concerns the location of the monotectoid horizontal; alloys annealed at  $600^{\circ}$ ,  $650^{\circ}$  and  $700^{\circ}C$  in this investigation decomposed within the miscibility gap, indicating that the horizontal lies below  $600^{\circ}C$ . The present results are consistent with those of Bichkov<sup>14</sup> et al, who state the monotectoid composition and temperature to be 12 a/o Nb and  $560^{\circ}C$ , respectively.

## 2. The Isothermal Sections.

The isothermal sections at  $700^{\circ}$ ,  $650^{\circ}$  and  $600^{\circ}C$  are presented in Figs. 22, 23, 24 respectively, and will be discussed in that order. It will be observed that each of the binary miscibility gaps closes within the ternary composition triangle, so that above the peaks of the binary gaps, U, Nb and Zr are soluble in all proportions in the  $\gamma$  b.c.c. solid solution. Over much of the central region of the composition triangle the stability of the  $\gamma$  phase extends to below  $600^{\circ}C$ .

The results shown in Figs. 22, 23, and 24, are based upon the microstructures obtained after annealing periods of between  $40\frac{1}{2}$  and 20 days. The more critical of those annealed for short times were later annealed for a further 66 days after which the microstructures confirmed those already observed.

(i) The Isothermal Section at  $700^{\circ}\text{C}$ . (Fig.22)

The terminal phases present at  $700^{\circ}\text{C}$  are  $\beta\text{U}$ ,  $\alpha\text{Zr}$ , and  $\gamma_2$  (Nb-rich b.c.c. solid solution). The section at  $700^{\circ}\text{C}$  intersects the miscibility gaps in all three binary systems, and the limits of these and other phase fields in the binary systems are marked with the symbol X in Fig. 22 (a similar procedure is used in Figs. 23 and 24).

The  $\gamma_2 + \gamma_3$  decomposition in the Zr-40 a/o Nb and Zr-60 a/o Nb binary alloys was incomplete, indicating sluggish transformation kinetics. As shown in Fig. 25, decomposition occurs preferentially at the grain boundaries, and the manner of decomposition is reminiscent of that found within the U-Nb miscibility gap.

The most striking feature of this section is the closure of each of the miscibility gaps on extending into the ternary. At  $700^{\circ}\text{C}$ , the U-Zr gap closes with additions of less than 5 a/o Nb. The extent to which the Zr-Nb gap extends into the ternary is not known with certainty. Alloys 17 and 41, for example, have been assigned to the  $\gamma$  phase, though as shown in Figs. 29 and 30, their microstructures obviously contain a second phase. However, the dispersion of this phase does not resemble the  $\gamma_2 + \gamma_3$  decomposition in the binary Zr-Nb alloys, and further, the amount appears to vary erratically between alloys of different compositions. Due to the sluggishness of transformations in this region of the composition triangle, much longer annealing times will be required to settle this part of the diagram conclusively.

The closure of the gap in the U-Nb binary system has been studied in more detail using a bracketing technique. About 14 a/o zirconium was sufficient to close the gap but the limiting isothermal was not symmetrical. The latter was drawn giving weight to the amount of second phase found in bi-phase alloys and is well established except at the uranium-rich end. It is of interest to note that precipitation took place mainly within the grains in the uranium-rich alloys whilst it was confined to grain boundaries in niobium-rich alloys. The main feature is that up to 5% zirconium had little effect on the width of the gap e.g. in the binary system the two-phase region extended from 20-65 a/o Nb, at 5% Zr from  $17\frac{1}{2}$  - 62 a/o Nb, and at 10 a/o Zr from 20 - 57 a/o Nb. Beyond 5 a/o the gap was closed sharply. It is however possible to regard the results as follows. At the uranium-rich end the isothermal ran close to the 20 a/o Nb line up to 10 a/o Zr i.e. zirconium preferentially replaces uranium atoms initially. On the other hand at the niobium-rich end the isothermal runs close to the 62 a/o uranium line i.e. zirconium predominately replaces niobium atoms.

Examples of the type of microstructure obtained at  $700^{\circ}\text{C}$  are illustrated in Figs 25 - 32 and 34.

(ii) Isothermal Section at  $650^{\circ}\text{C}$ . (Fig.23)

This differs significantly from that at  $700^{\circ}\text{C}$  in two respects only. Firstly  $650^{\circ}\text{C}$  is below the monotectoid temperature of the U-Zr system and the section intersects the  $\alpha + \gamma$  phase field in that system. Secondly whilst the width of the binary miscibility gap increases in size as the temperature is lowered, the amount of zirconium required to close it remains constant at about 14 a/o. The niobium-rich end of the limiting isothermal remained the same as at  $700^{\circ}\text{C}$  whilst the uranium-rich end extends to higher uranium contents. Again the first 5 a/o of zirconium has little effect on the width of the gap the main effect occurring with the addition of over 10 a/o.

(iii) Isothermal Section at 600°C. (Fig. 24).

This temperature lies below the monotectoids in both systems and the isothermal represents the limit of solubility of uranium in the Nb - Zr rich BCC solid solution. The niobium-rich part of the isothermal (with  $> 40$  a/o Nb) is similar to that at higher temperatures. With up to 10 a/o Zr it lies close to the 33 a/o U line and then turns between 10 and 14 a/o Zr to lie parallel to the U - Nb axis. With less than 40 a/o Nb, the effect of the monotectoids with a predominates.

VI DISCUSSION.

(1) U-Nb Binary System.

Three investigations of the U-Nb system have been reported since this work was undertaken, and a comparison of the present diagram with the results of other workers is given in Table 3.

TABLE 3  
Characteristics of the miscibility gap in the U-Nb system.

Investigators	Monotectoid Temp. °C	Composition limits (a/o) at the monotectoid	the Nb rich end	Composition at peak a/o	Peak Temp. °C
Sawyer <sup>1</sup>	656	11	78	68	1020
Dwight <sup>2</sup>	$634 \pm 2$	$18.2 \pm 1$	-	-	-
Rogers et al <sup>3</sup>	647	14.5	73	54	960
Pfeil et al <sup>4</sup>	$650 \pm 5$	14	70	50	950
Present work	$640 \pm 2$	$17.5 \pm 1$	65-70	50	950

Agreement on the peak temperature, peak composition, and Nb rich limit of the gap is considered satisfactory. Taking the limits of error into account, the agreement on the monotectoid temperature is also considered satisfactory, whereas the differences in the monotectoid composition appear more serious. In this connection, the presence of different amounts of C in the basis U does not appear to be an adequate explanation. It is observed that U-Nb alloys contain a white impurity phase which is not present in either the U or Nb starting materials, and which may reasonably be supposed to be NbC. However, even if all C forms NbC, an alloy of intended composition 15 a/o Nb made from U containing as much as 500 ppm C would in fact have an effective composition 14.3 a/o Nb, a difference which is not as large as those between the various monotectoid compositions in Table 5. The faint extra lines found on some of the X-ray photographs have not been positively identified. They do not correspond either to NbC or  $UO_2$ . As another line of thought, segregation in the alloys would have the effect of broadening the miscibility gap and moving the eutectoid to lower Nb contents.

(ii) U-Nb-Zr Ternary System.

The work on the U-Nb-Zr system has revealed the large range of stability of the  $\gamma$  phase due to the closure of each of the miscibility gaps in the binary systems. In order of potency, Nb exerts the strongest influence, closing the U-Zr gap on addition of less than 5 a/o Nb. The extent of the penetration of the Zr-Nb system into the ternary has not been established with certainty, and longer annealing times appear necessary to do so. However, it seems probable that addition of U to the Zr-Nb system is the least effective of the 3 combinations in restriction of the miscibility gap.

In their work on the ternary system, Dwight and Mueller<sup>5</sup> concentrated their investigations on the U-rich corner of the diagram. Their investigation of the U-Nb and U-Zr miscibility gaps was very limited and their proposed phase boundary is supported by only two of three alloys. However, where comparison between their results and the present work is possible, the agreement is very good, particularly at 600°C where their work is rather more detailed.

The more detailed study of the closure of the gap in the U-Nb system has shown that the isothermal does not form a smooth regular curve but comprises three separate parts. For small additions of zirconium up to 5 - 10%, the isothermal approximated to a constant uranium content at the niobium rich end (approx. 33 a/o) and to lines of constant niobium content at the uranium-rich end. At higher zirconium contents the isothermal changes direction sharply and approximates to the 14 a/o zirconium line particularly at 650°C. The examination has not been sufficiently detailed to determine how accurate this approximation is particularly at the U-rich end. For example it is possible to make the contrary suggestion that the first 5 a/o of zirconium have little effect on the width of the miscibility gap.

The results confirm the general interpretation of miscibility gaps in terms of size factor, namely that the occurrence is dependent on the balance between strain energy favouring immiscibility and the entropy effect which increases with temperature and favours miscibility<sup>4</sup>. The atomic diameters of U, Nb, & Zr expressed as the closest distance of approach in the body centred cubic lattice (extrapolated to RT in the case of Zr) decrease in the order Zr > U > Nb giving size factors with respect to uranium of +2% for Zr and - 5% for Nb. Thus niobium causes more lattice strain in uranium and gives rise to a more pronounced miscibility gap than does zirconium. Hence relatively small amounts of niobium (< 5 a/o) were required to eliminate the weak gap due to zirconium whilst more zirconium (14 a/o) was required to eliminate the stronger U-Nb gap. The small amounts of Zr and Nb required to eliminate these two gaps arises in part from the fact that they strain the uranium lattice in opposite senses. Uranium is intermediate in size with respect to niobium and zirconium and larger amounts would be expected to eliminate the Zr-Nb gap.

The bulge of the  $\gamma$  isothermal at 600°C towards the uranium - corner indicates that at this proportion of niobium and zirconium, the distortion of the uranium lattice is a minimum thus allowing stable  $\gamma$  to exist with as much as 55 a/o U. It is probable that in alloys with this proportion of niobium to zirconium (about 3:2) metastable  $\gamma$  can be retained on quenching in alloys with much higher uranium contents than in either binary system and it is probable that alloys with Nb/Zr atom ratios of 3:2 would give maximum thermal stability of  $\gamma$ .

Acknowledgements.

The authors wish to thank their colleagues particularly Mr. G.B.Brook for helpful discussions. Special acknowledgement is due to Miss C.Knight for the X-ray examinations.

BSB/GJP/AK.  
16-6-59.

068 015

REFERENCES.

1. H.A. Saller and F.A.Rough. U.S. A.E.C. Document, BMI.1000, June 1955.
2. A.E.Dwight. U.S. A.E.C. " TID.7523 (Pt.1) Dec. 1956.
3. B.A.Rogers, D.F.Atkins, E.J.Manthos and M.E.Kirkpatrick. Paper No. 57 - N.E.S.C. 5 2nd Nuclear Eng. & Sci. Conference.
4. P.C.L. Pfeil, J.D.Browne, and G.K. Williamson. A.E.R.E. M/R 2498, 1958.
5. A.E.Dwight & M.H. Mueller. U.S. A.E.C. Document, ANL.5581, 1957.
6. W. G. O'Driscoll and G.L. Miller. Jl. Inst. Metals, 1956-57, 85, 379.
7. D.A. Sutcliffe, J.I.M.Forsyth, and R.L.Bickerdike. R.A.E. Tech Note, Met.121, 1950.
8. R.W.Nichols. Nuclear Eng., 1957, 2, (18), 355.
9. B.W.Mott and H.R.Haines. Jl. Inst. Metals, 1952, 80, 621.
10. C.R. Tottle. " " " 1956-57, 85, 375.
11. D. Summers-Smith. " " " 1954-55, 83, 277.
12. B.A.Rogers and D.F.Atkins. " " " 1955, 7, 1034.
13. Rough, Austin, Bauer and Doig. U.S.I.A.E.C. Document, B.M.I. 1092.
14. Yu. F. Bichkov, A.N.Rozanov, D. M. Skorov. J. Nuclear Energy, II, 1957, 5, 402.
15. B.S.Berry. F.R.I. Report. R126/3.

-----oOo-----

068 016

TABLE 1

Nominal Compositions of Binary Alloys.

Ref No.	A/O			W/O		
	U	Nb	Zr	U	Nb	Zr
1	89	11	-	95.40	4.60	-
26	87	13	-	94.49	5.51	-
8	85	15	-	93.56	6.44	-
27	82.5	17.5	-	92.36	7.64	-
2	80	20	-	91.12	8.88	-
28	70	30	-	85.68	14.32	-
3	60	40	-	79.36	20.64	-
4	50	50	-	71.94	28.06	-
5	40	60	-	63.09	36.91	-
29	37	63	-	60.11	39.89	-
30	34	66	-	56.93	43.07	-
6	32	68	-	54.67	45.33	-
31	31	69	-	53.54	46.46	-
32	28	72	-	49.94	50.06	-
7	25	75	-	46.07	53.93	-
42	-	85	15	-	85.23	14.77
19	-	60	40	-	61.44	38.56
43	-	40	60	-	40.53	59.47

TABLE 2.  
COMPOSITIONS OF TERNARY ALLOYS.

Ref No.	A/O			W/O		
	U	Nb	Zr	U	Nb	Zr
9	15	75	10	31.19	60.84	7.96
10	24	60	16	43.98	44.72	11.23
11	36	40	24	58.55	26.45	14.95
12A	47.5	21	31.5	69.72	12.53	17.71
#13	52.7	10.9	36.5	74.0	6.0	19.7
14	57	5	38	77.49	2.76	19.79
#16	33.0	56.9	10.2	56.0	37.8	6.6
17	15	60	25	30.63	49.83	19.55
21	92	3	5	96.68	1.281	1.967
22	87	5	8	94.52	2.21	3.33
23	75	10	15	88.59	4.61	6.79
24	63.68	15.09	21.19	81.98	7.577	10.46
25	25	10	65	46.33	7.536	46.14
33	80	5	15	91.23	2.229	6.554
34	70	15	15	85.78	7.171	7.042
35	65	20	15	82.73	9.936	7.316
#36	56.1	27.8	16.1	76.6	14.8	8.4
#37	44.0	39.3	16.7	66.8	23.3	9.7
38	35	50	15	58.09	32.37	9.537
39	15	70	15	31.21	56.82	11.96
40	25	40	35	46.27	28.88	24.82
#41	24.1	37.9	38.0	45.1	27.7	27.3
#46	38.8	49.8	11.4	61.7	30.9	6.9
47	45	50	5	67.74	29.38	2.88
#48	34.7	60.3	5.0	57.6	39.0	3.2
49	38	60	2	61.11	37.66	1.23
#50	59.0	29.1	11.8	78.4	15.1	6.0
#51	64.5	25.2	10.2	82.5	12.6	5.0
#52	74.1	14.6	11.4	88.5	6.8	5.2
#55	67.1	21.08	11.9	84.39	10.35	5.73
#56	52.3	35.75	11.93	74.11	19.76	6.47
#57	48.1	37.1	14.8	70.8	21.36	8.35
58	35.5	55	7.5	60.63	34.72	4.65
#59	33.3	54.1	12.7	56.5	35.91	8.24

■ Analysed specimens.

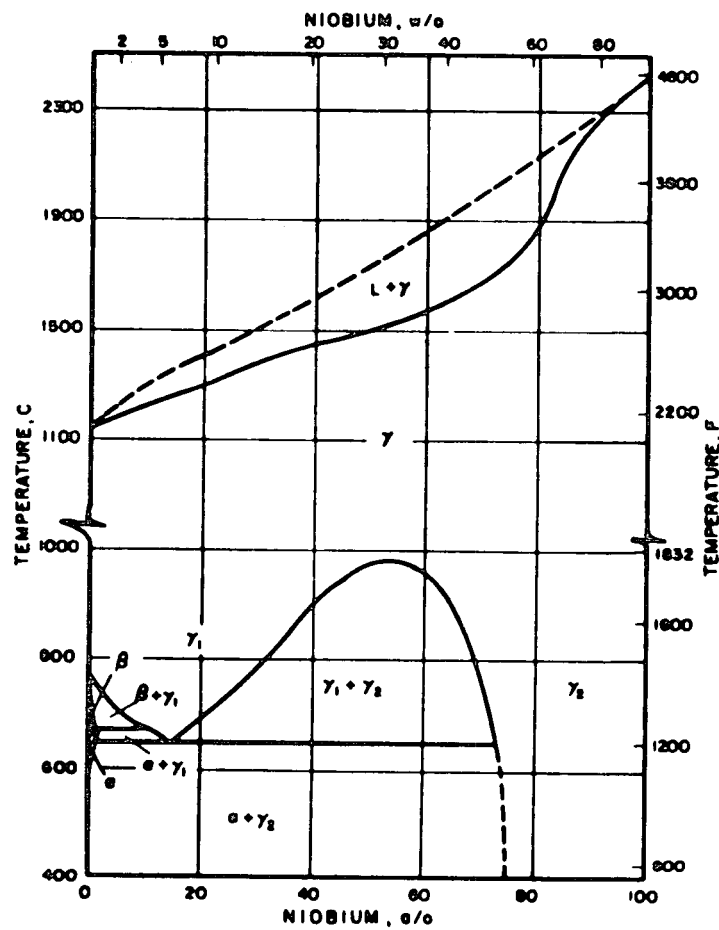


FIG. 1. The U-Nb Phase Diagram as published previously to this work in B.M.I.-1300 (1958).

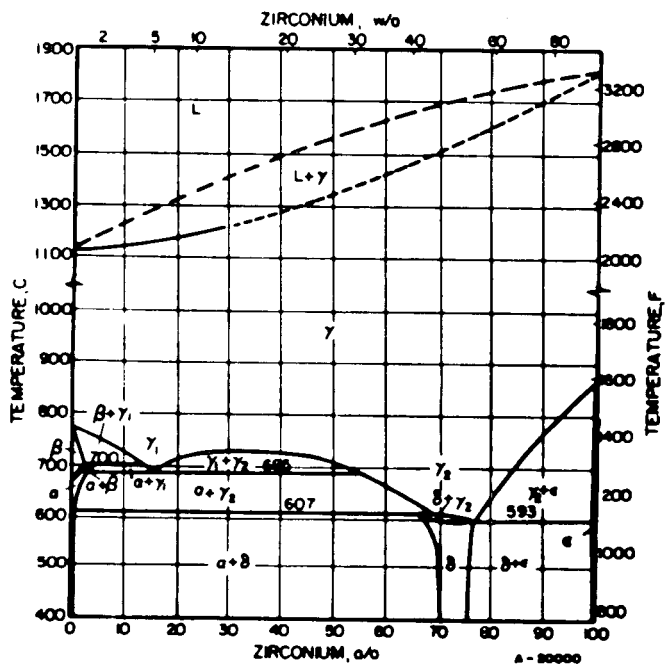


FIG. 2. The U-Zr Phase Diagram from B.M.I.-1300 (1958).

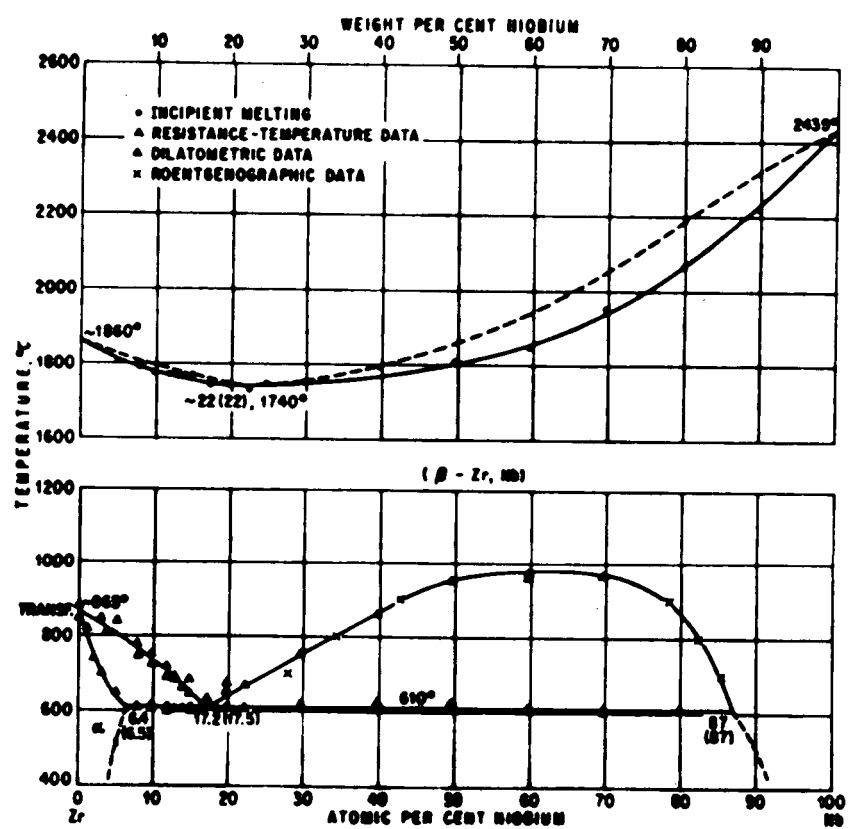


FIG. 3. The Nb-Zr Phase Diagram from "Constitution of Binary Alloys" by M. Hanson. (1958).

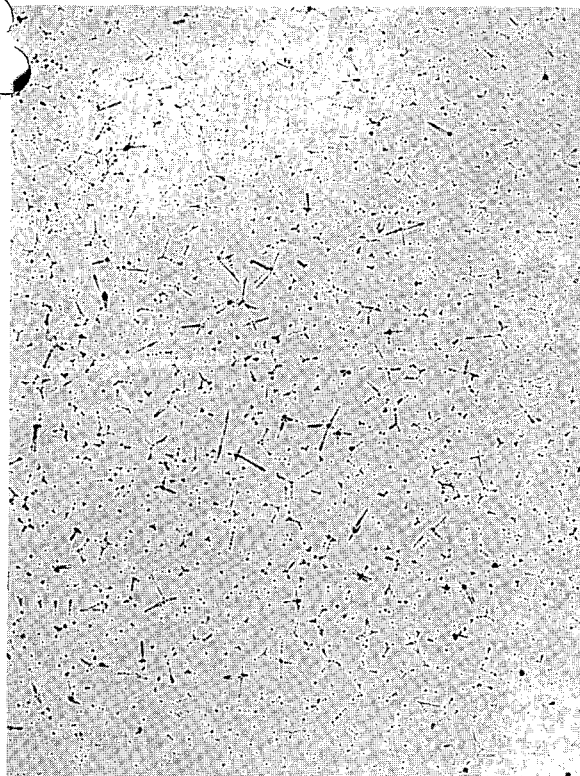


Fig.4 x150  
Uranium after arc melting -  
electrodeposited.



Fig.5. x150  
As Fig.4. Polarised light.

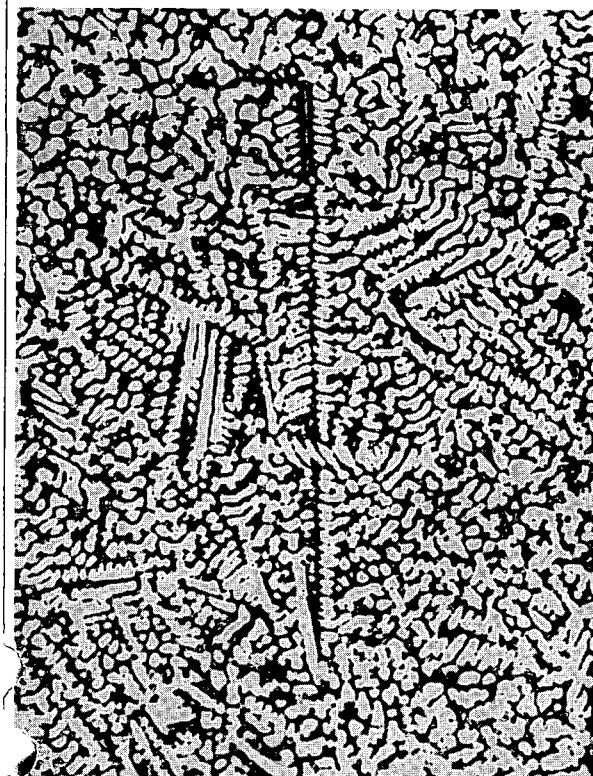


Fig.7 x150  
U-50 a/o Nb as cast -  
oxalic acid etch.

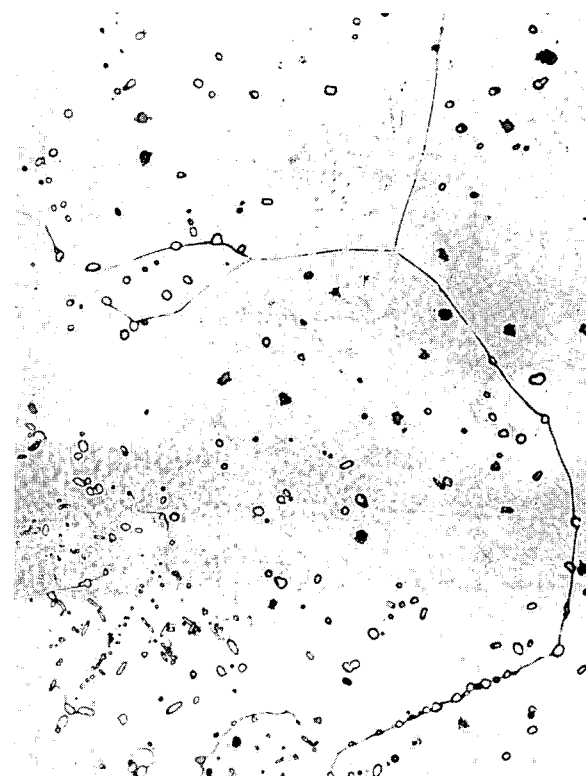


Fig.8 x150  
U-50 a/o Nb after 90 hrs 8 °C  
1340°C - polish attack

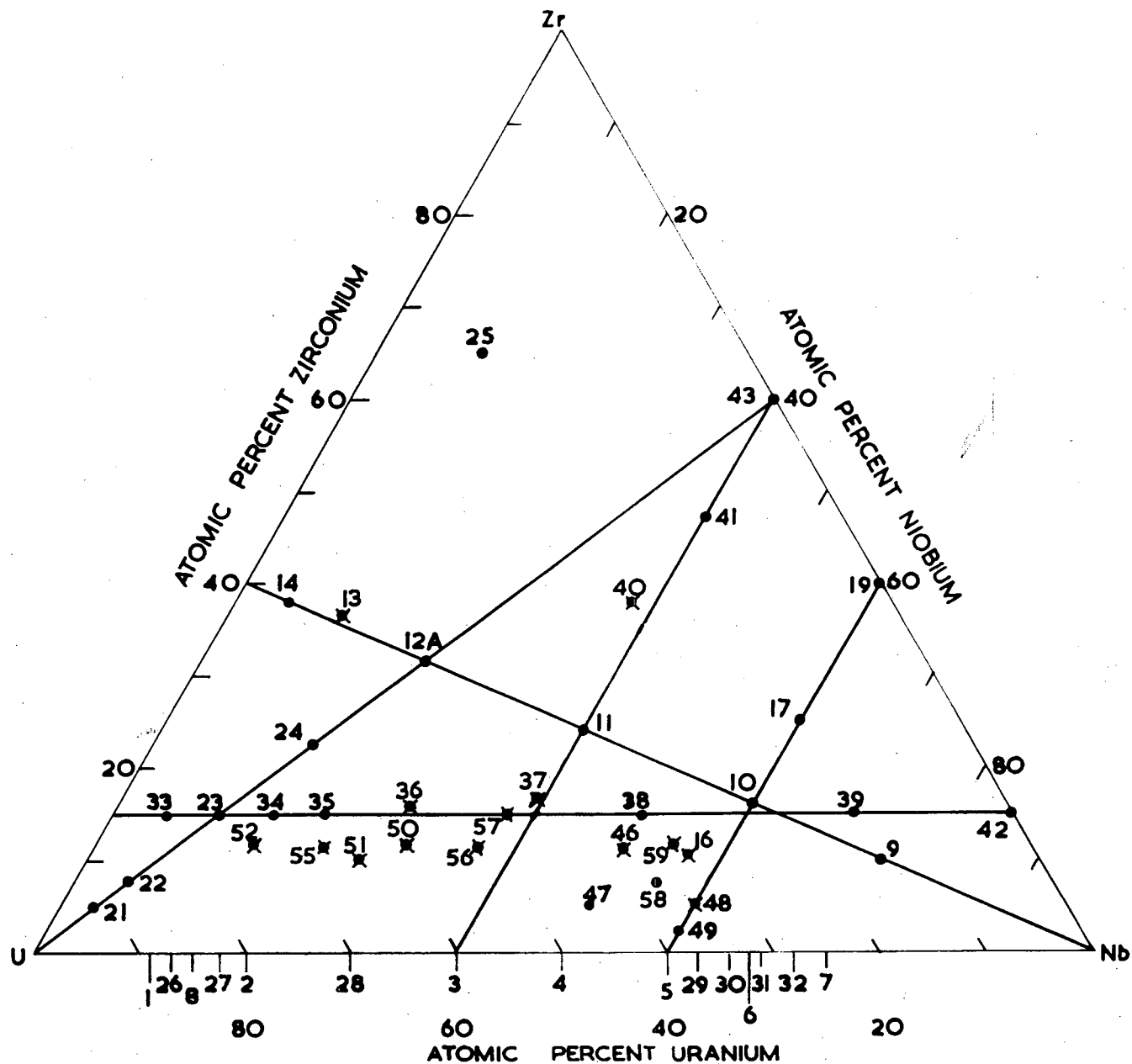


FIG. 6. LAYOUT OF ALLOYS IN THE COMPOSITION TRIANGLE.  
 X — ANALYSED SPECIMENS

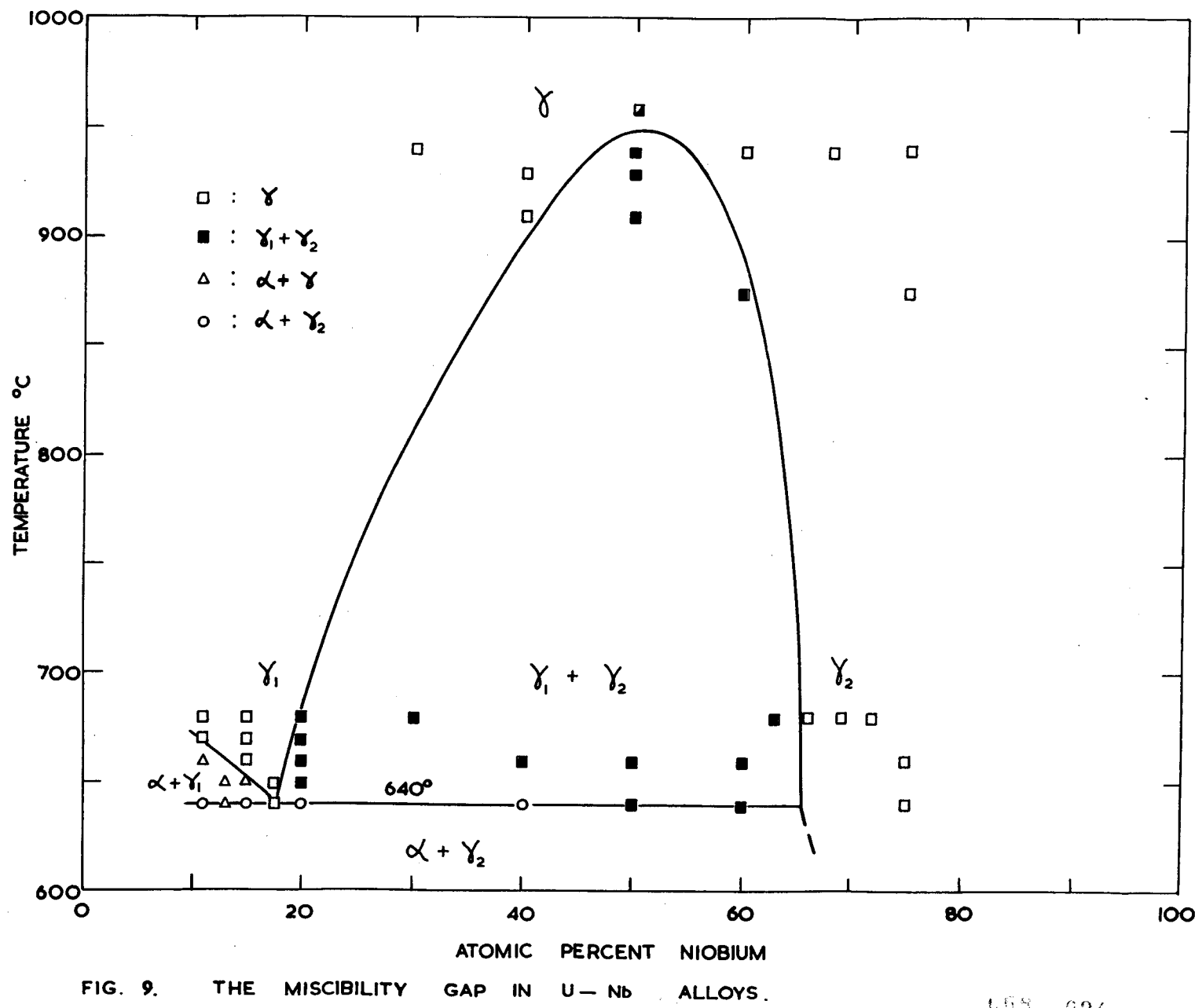
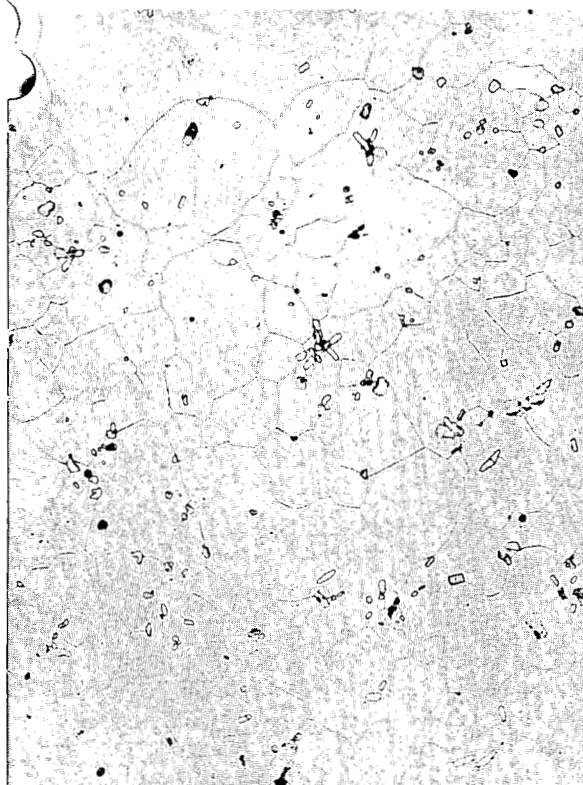
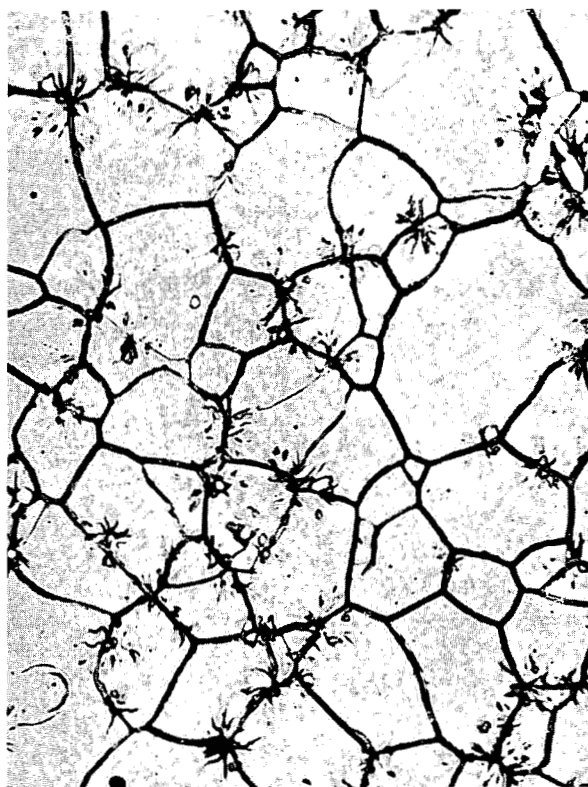


FIG. 9. THE MISCIBILITY GAP IN U-Nb ALLOYS.



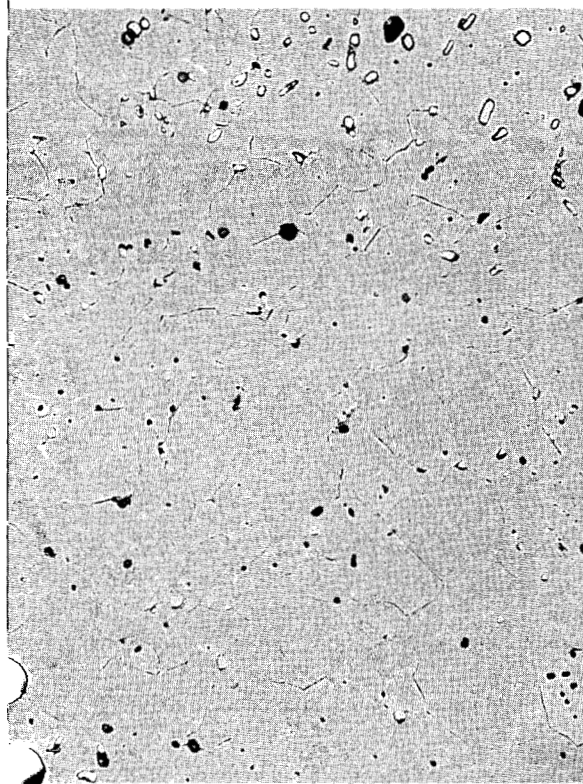
F374

Fig.10. x150  
U-15 a/o Nb-18 d 670°C w.q.  
oxalic acid etch.



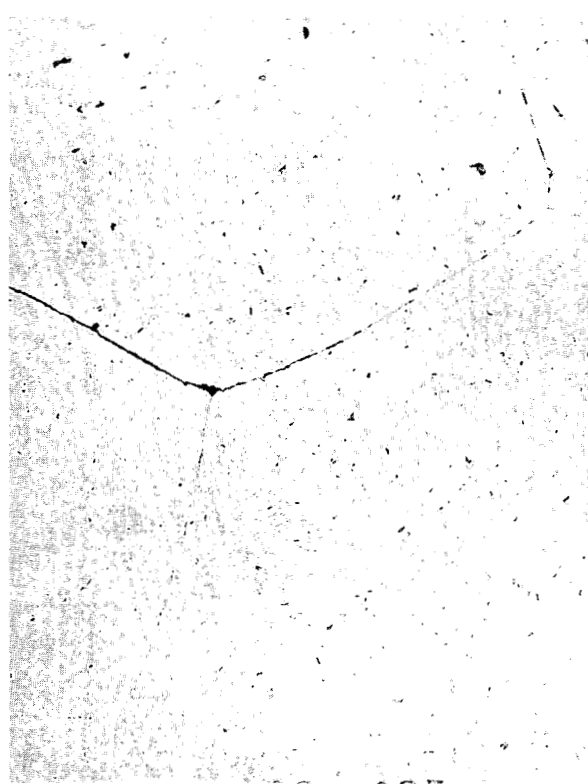
F274

Fig.11. x500  
U-15 a/o Nb + 8d at 660°C w.q.  
oxalic acid etch.



F440

Fig.12 x150  
U-40 a/o Nb-17 d 910°C w.q.  
polish attack.



F416

Fig.13 x150  
U-75 a/o Nb-18 d 875°C w.q.  
polish attack.

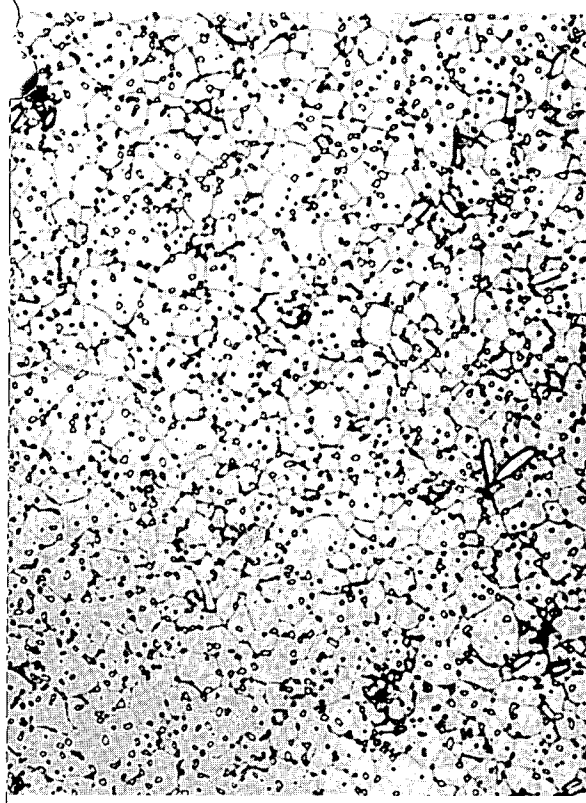
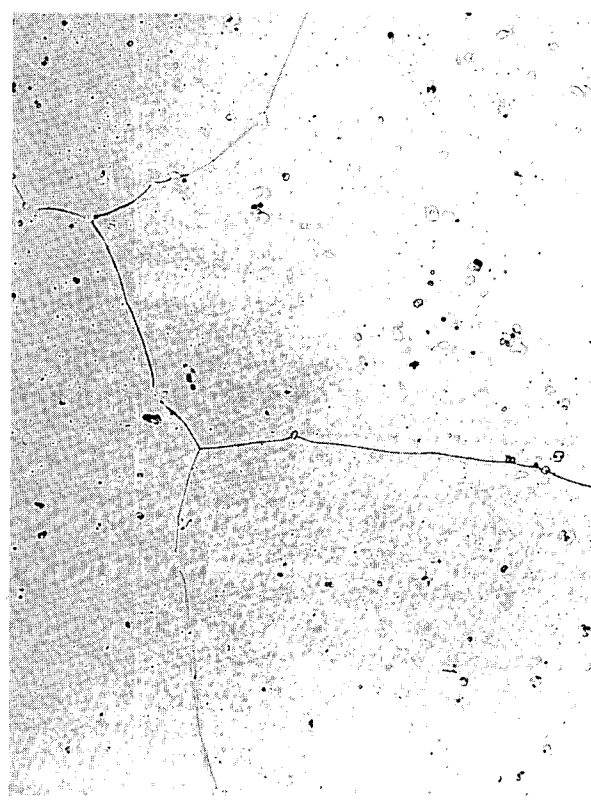


Fig. 14 x500  
U-20 a/o Nb-18 d 600°C w.q.  
oxalic etch.

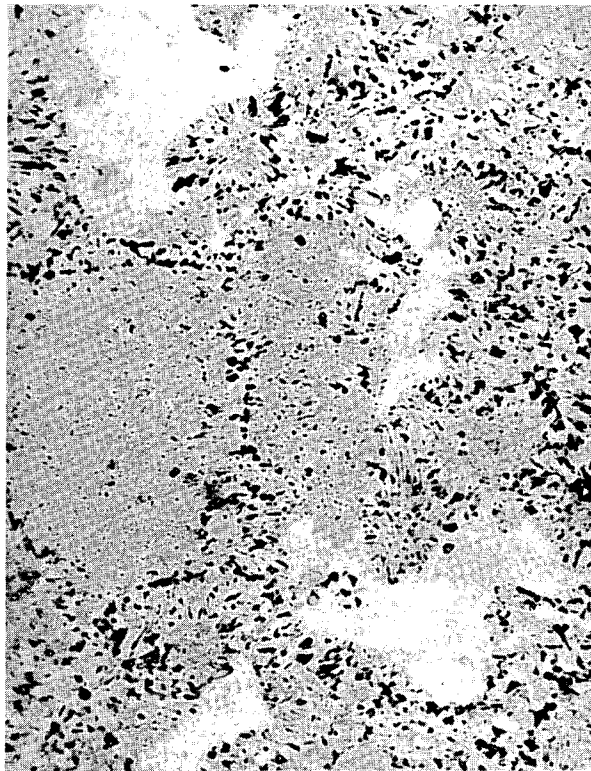
F266



F339

Fig. 15 x150  
U-13 a/o Nb-17 d 1040°C w.q.  
oxalic etch.

F401



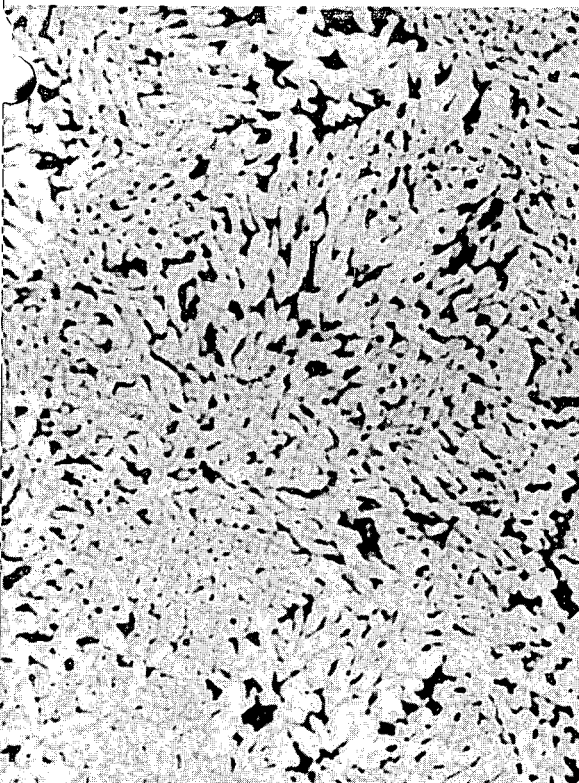
F143

F226

Fig. 16 x150  
U-66 a/o Nb 3 wks 680°C w.q.  
polish attack.

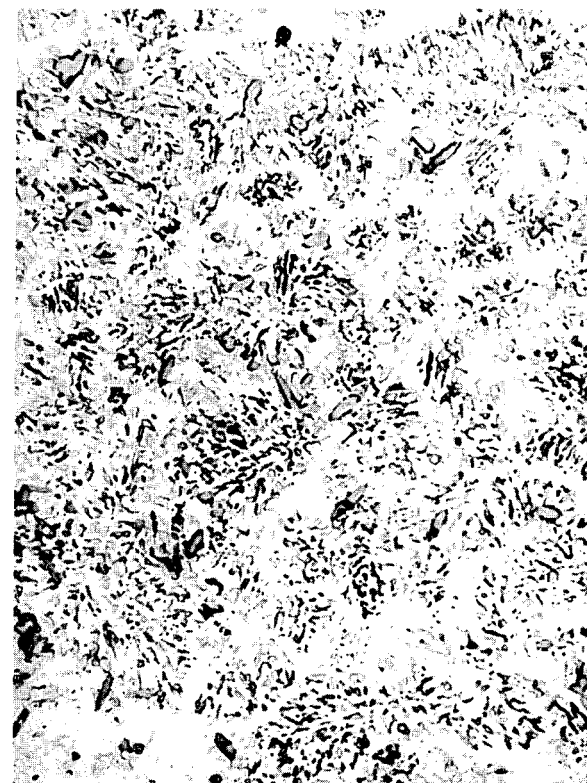
F226

Fig. 17 x500  
U-50 a/o Nb 24 d 640°C w.q.  
oxalic acid etch.



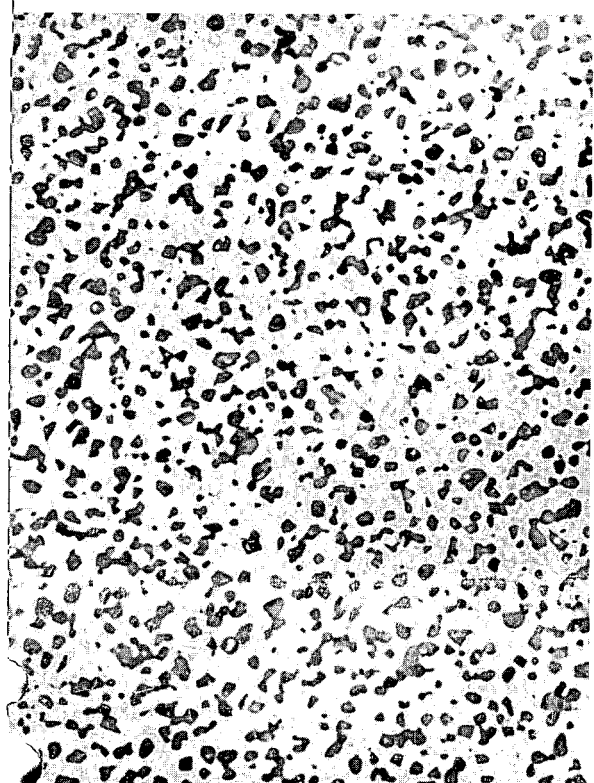
F255

Fig. 18 x1500  
U-50 a/o Nb 40 d 660°C w.q.  
oxalic acid etch.



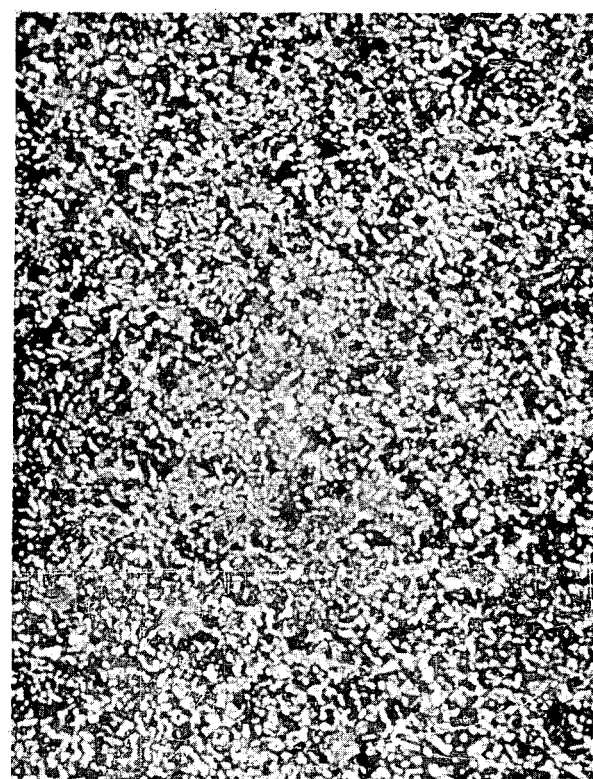
F476

Fig. 19 x500  
U-50 a/o Nb 8 d 940°C w.q.  
polish attack.



F213

Fig. 20 x500  
U-11 a/o Nb 18 d 650°C w.q.  
atmospheric etch.



F131

627

Fig. 21 x500  
U-11 a/o Nb 24 d 640°C w.q.  
atmospheric etch.

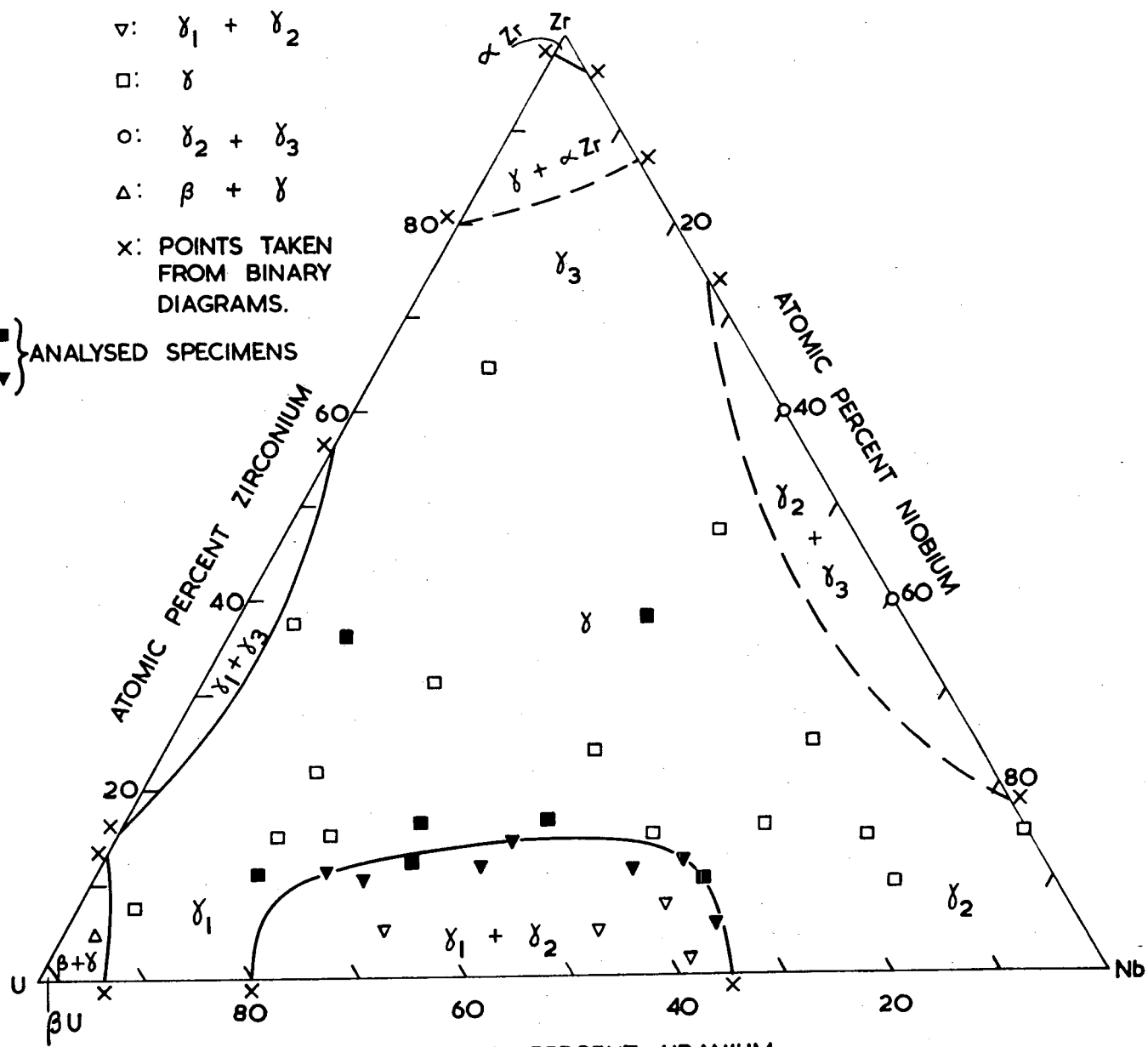


FIG. 22. U - Nb - Zr ISOTHERMAL SECTION AT 700°C.

▽ :  $\gamma_1 + \gamma_2$   
 □ :  $\gamma$   
 ○ :  $\gamma_2 + \gamma_3$   
 △ :  $\alpha + \gamma_1$   
 X : POINTS TAKEN FROM  
 BINARY DIAGRAMS.  
 ■ : ANALYSED SPECIMENS

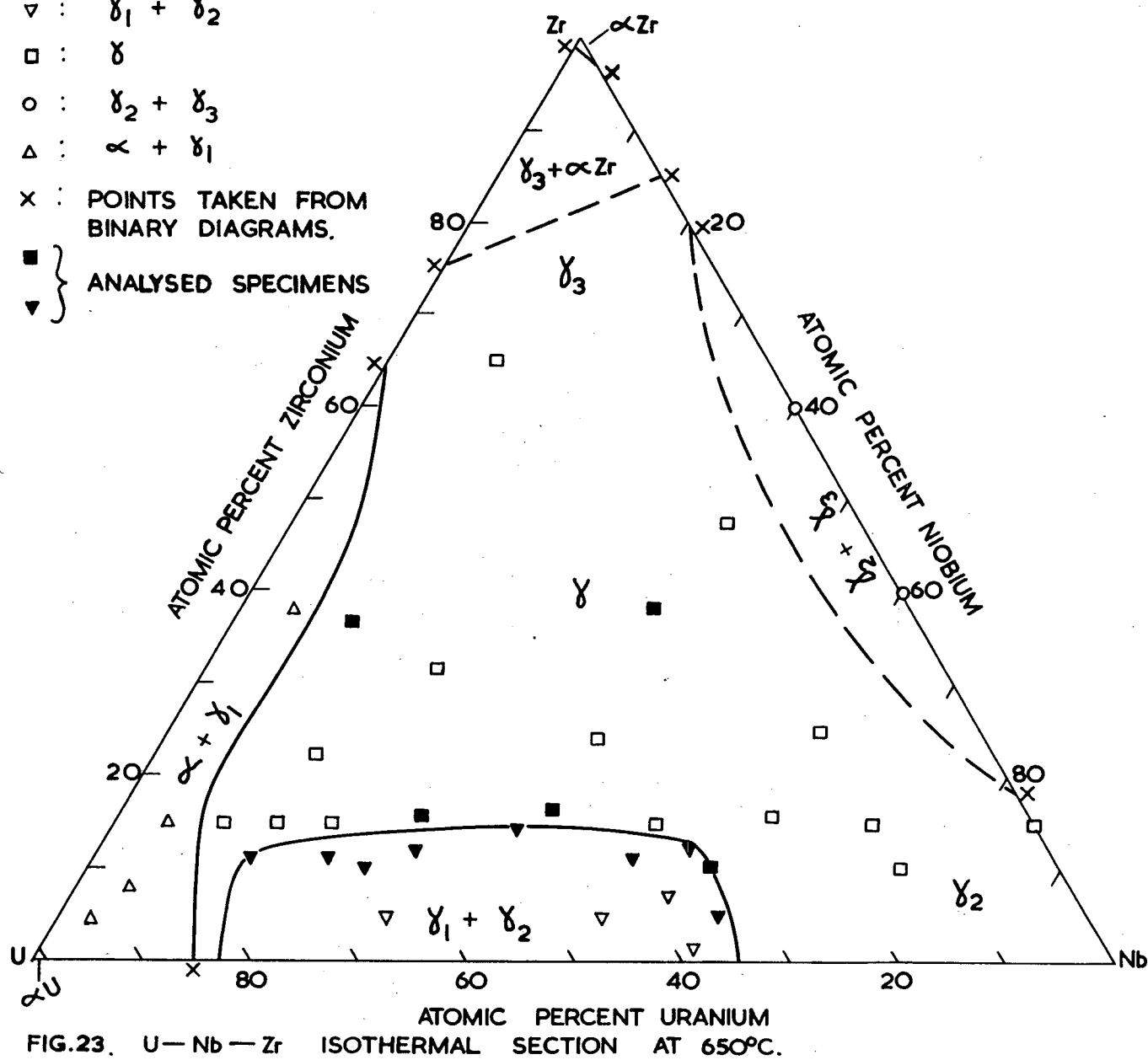


FIG.23. U—Nb—Zr ISOTHERMAL SECTION AT 650°C.

□ : SINGLE PHASE ALLOYS

**Δ : TWO (OR MORE) PHASE ALLOYS.**

X : POINTS TAKEN FROM BINARY  
DIAGRAMS

■ } ANALYSED SPECIMENS

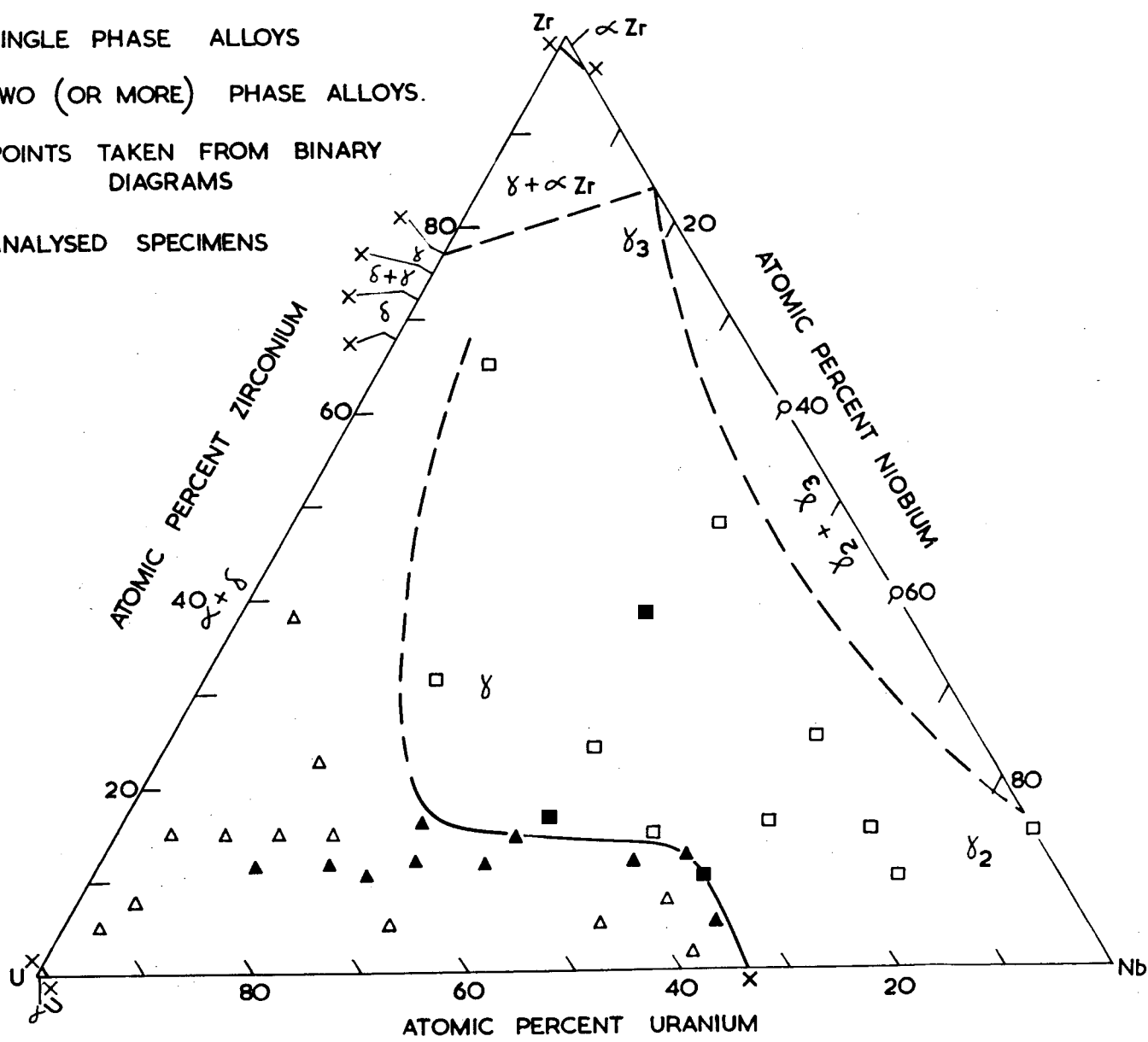
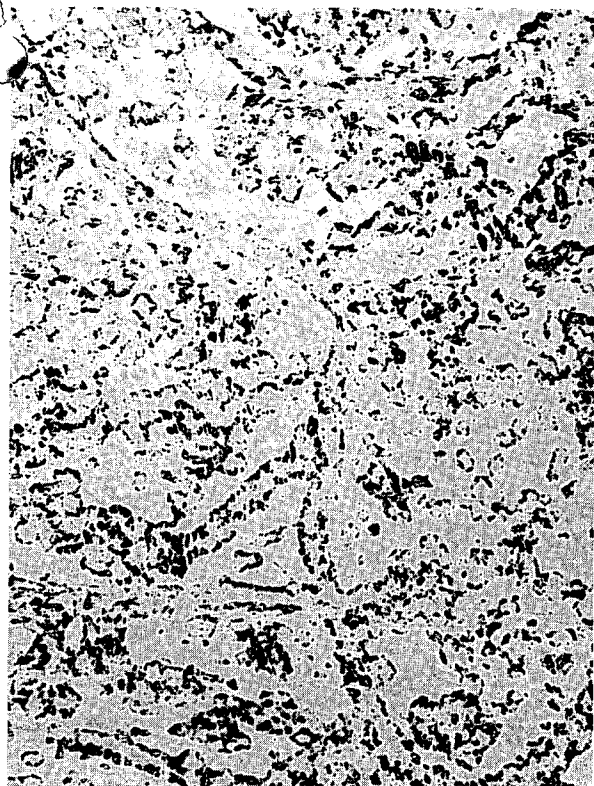
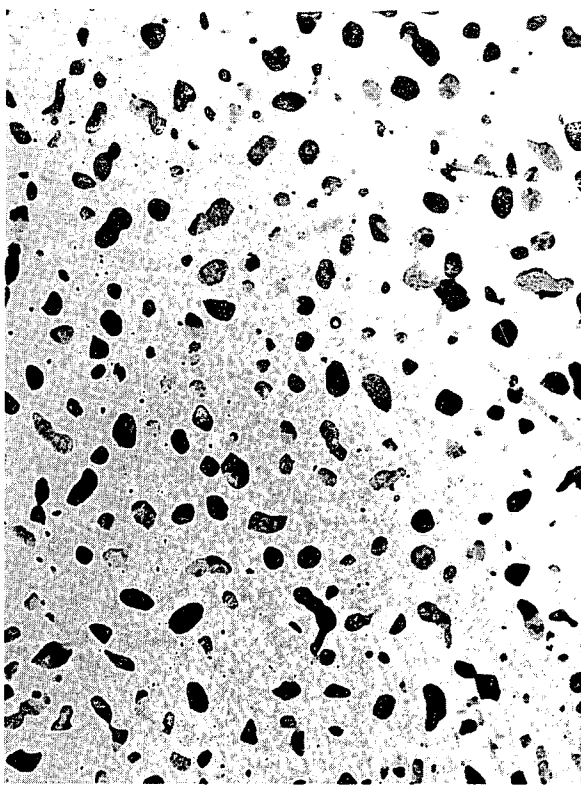


FIG. 24. U - Nb - Zr ISOTHERMAL SECTION AT 600°C.



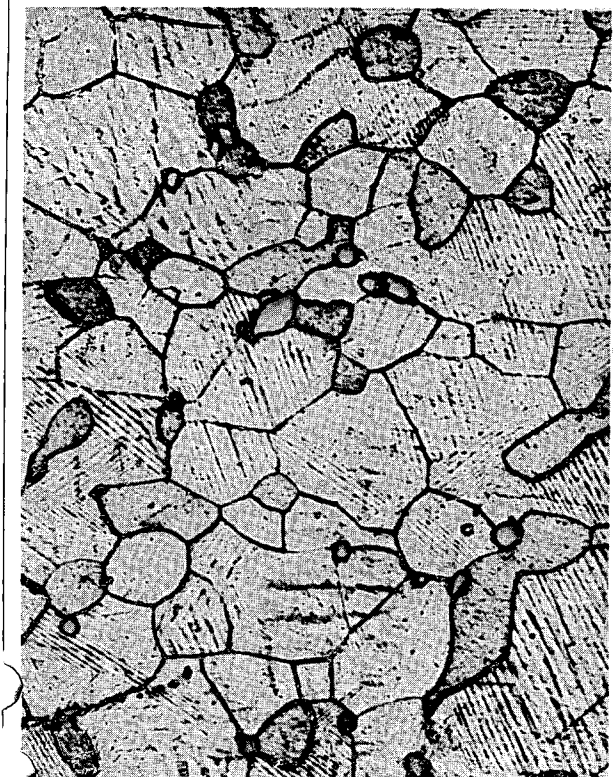
F433

Fig. 25                    x150  
Alloy 19 40 d 700°C w.q.  
polish attack



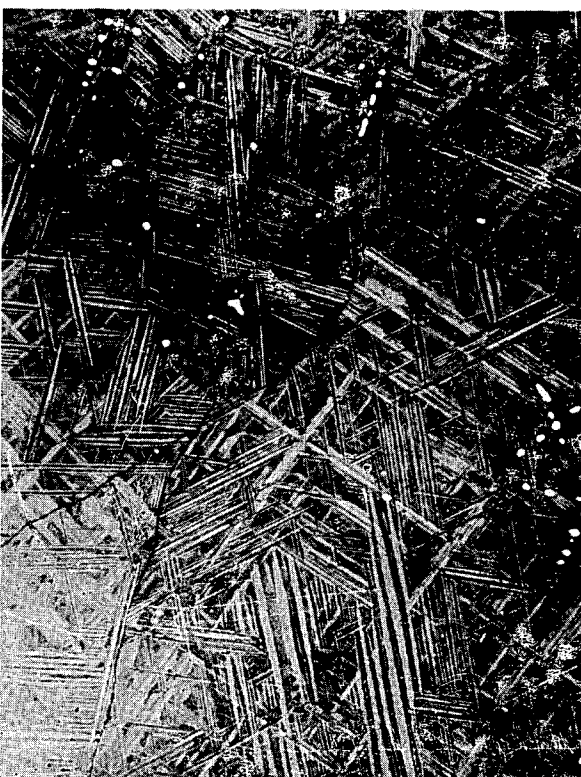
F449

Fig. 26                    x150  
Alloy 21 40 d 700°C w.q.  
atmospheric etch.



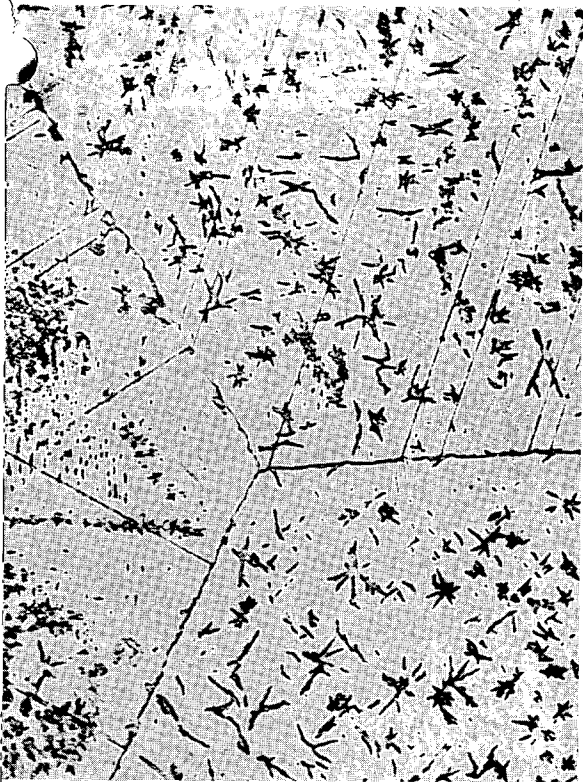
F456

Fig. 27                    x500  
Alloy 21 40 d 700°C w.q.  
oxalic acid etch.



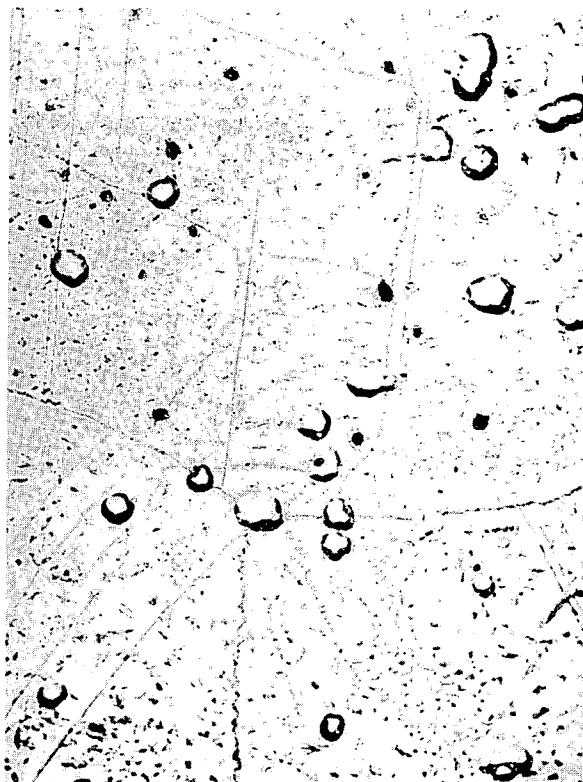
F447

Fig. 28                    x150  
Alloy 22 40 d 700°C w.q.  
oxalic acid etch.



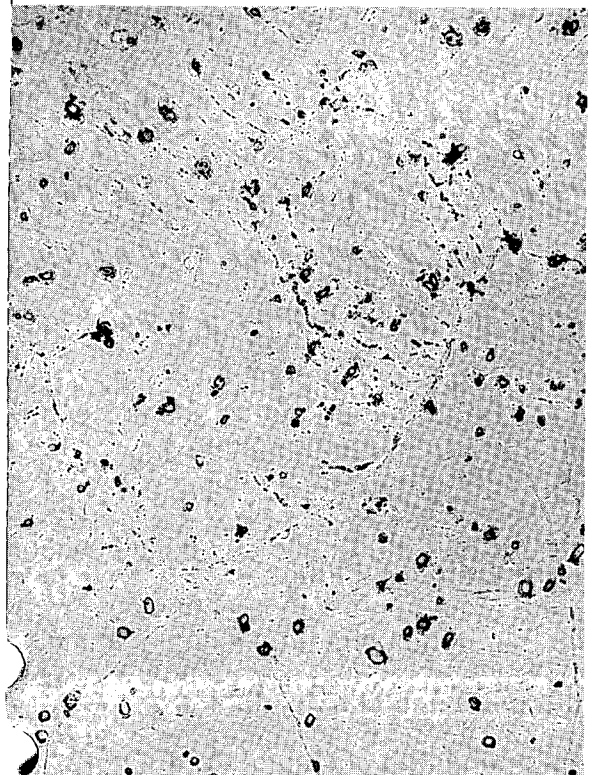
F436

Fig. 29 x150  
Alloy 17 40 d 700°C w.q.  
polish attack



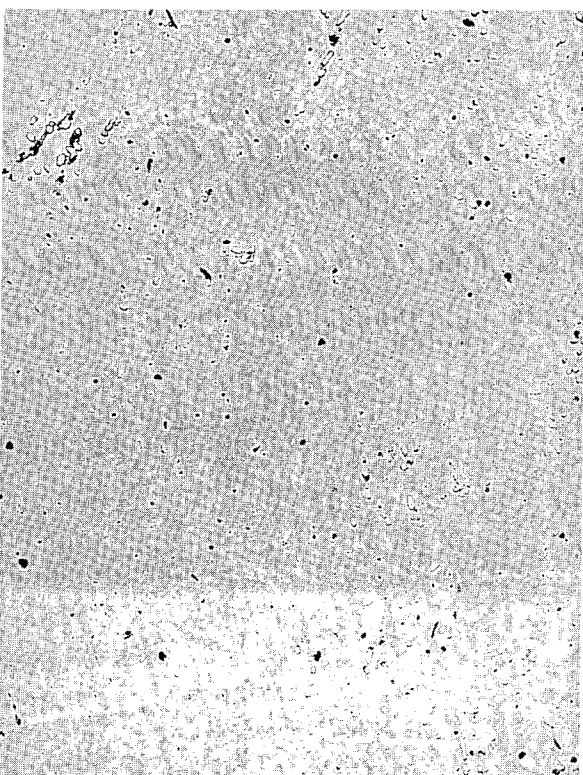
F472

Fig. 30 x150  
Alloy 41 20 d 700°C w.q.  
polish attack



F422

Fig. 31 x150  
Alloy 11. 40 d 700°C w.q.  
polish attack



F452

Fig. 32 x150  
Alloy 24. 40 d 700°C w.q.  
oxalic acid etch.

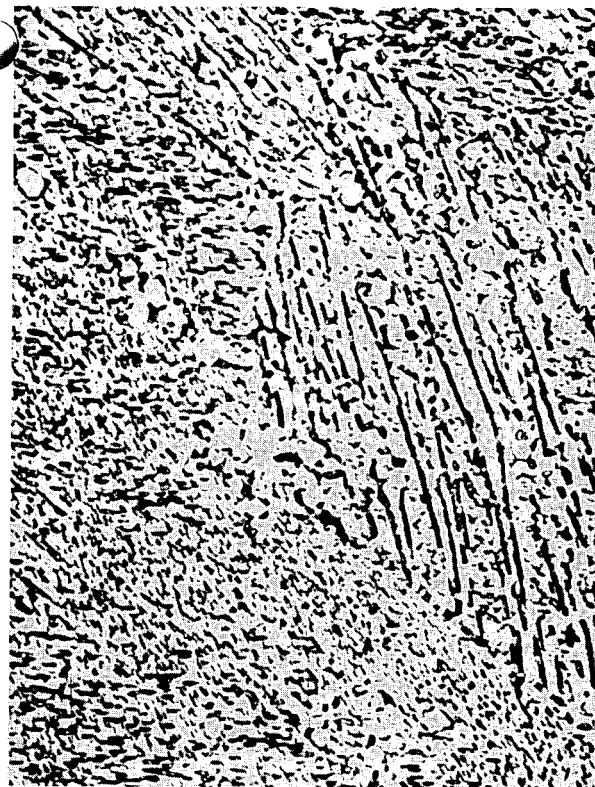


Fig.33

x500

Alloy 14. 51 d.  $650^{\circ}\text{C}$  w.q.  
oxalic acid etch.

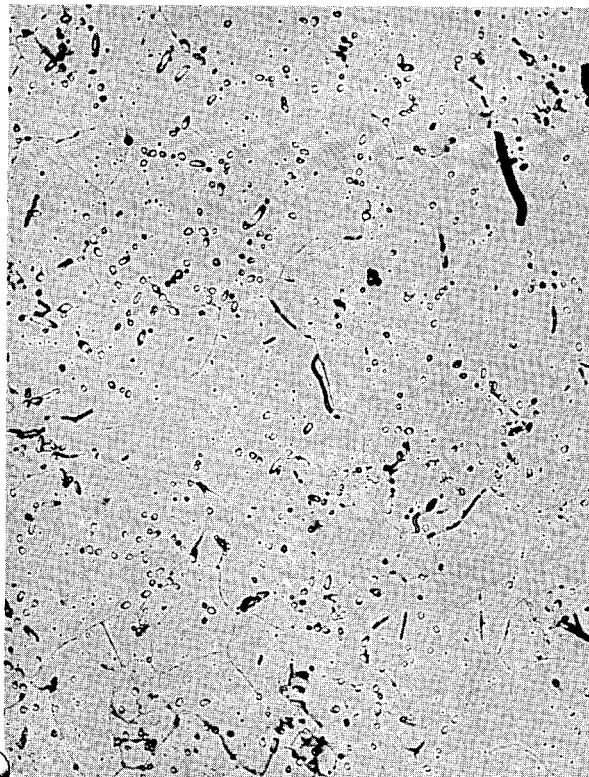


Fig.35

x150

Alloy 23. 51 d  $650^{\circ}\text{C}$  w.q. 0.68  
oxalic acid etch.

F448

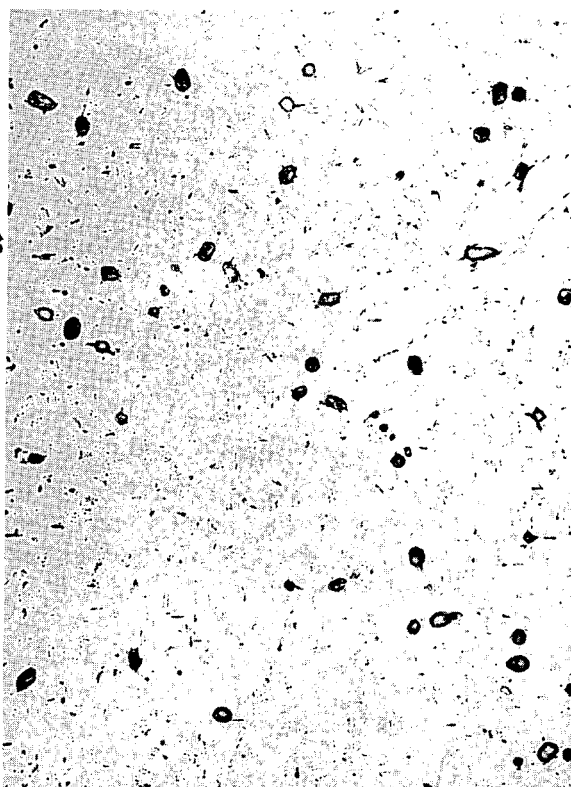


Fig.34

x150

Alloy 13. 20 d  $700^{\circ}\text{C}$  w.q.  
polish attack.

485



F479

Fig.36

x500

Alloy 33. 22 d  $650^{\circ}\text{C}$  w.q.  
oxalic acid etch.

0.33

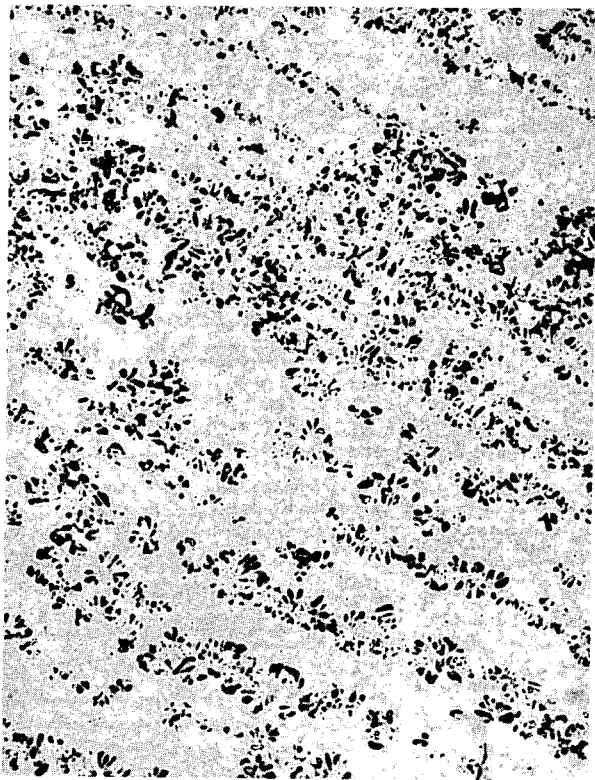


Fig. 37. x500  
Alloy 35. 22 d 600°C w.q.  
polish attack.

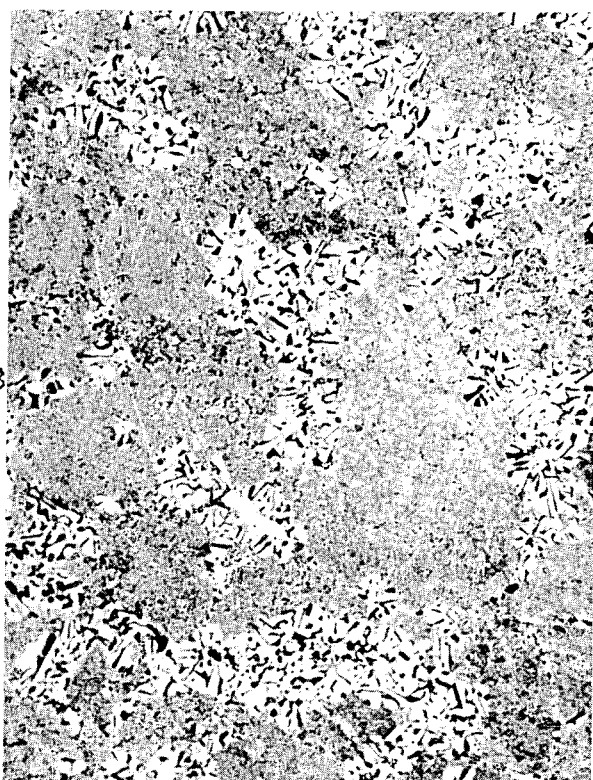


Fig. 38. x500  
Alloy 34. 22 d 600°C w.q.  
oxalic acid etch.

PART B (i)

NATURE AND RANGE OF EXISTENCE OF THE  $\delta$  PHASE

IN THE U-Mo SYSTEM ( $U_2Mo$ )

by

R.S.A. El-Ansari, M.Sc.,

and

G.B. Brook. B.Met.

---

I INTRODUCTION.

The purpose of this research is to study the conditions for the formation and the range of existence of the  $U_2Mo$  or  $\delta$  phase in the U-Mo system. This structure forms from the  $\gamma$  phase by an ordering transformation<sup>1,2</sup> and the cell of the new structure may be considered as being formed from three cells of  $\gamma$  in which U and Mo have preferred sites so that a contraction occurs in one direction to give each pseudo-cube an axial ratio of 0.957. The  $U_2Mo$  cell is thus tetragonal with parameters  $a_0 = 3.427\text{\AA}$ ,  $c = 9.834\text{\AA}$ ,  $c/a = 2.871$  and is of the C 11b,  $\text{MoSi}_2$  type.

The investigation was originally hampered to some extent by uncertainties in the phase relationships in binary U-Mo alloys and therefore some work has been carried out to check the validity of the earlier diagram given by Pfeil and Browne<sup>1</sup> and the recently published modification by Bostrom & Halteman<sup>2</sup> which shows a much narrower range of composition for the  $\delta$  phase. (Fig.1).

The main effort of the research has been devoted to the study of the effects of elements of body-centred cubic structure on the range of composition and structure of the  $\delta$  phase and the effects of Cr, Nb and Zr are described in this report.

In many systems there is a tendency for ordered structures to form where the atomic diameters are neither too similar or so unequal that insufficient solid solubility occurs. This tendency may be observed in uranium alloys where an ordered structure forms at 33 a/o Mo in the U-Mo system (size factor - 10%)<sup>+</sup> but not in U-Cr (size factor - 20%; maximum solid solubility in  $\gamma$  4 a/o) or in U-Nb (size factor - 5% complete  $\gamma$  solid solubility).

It was expected that Cr would increase lattice strain and reduce the overall solubility in uranium thus reducing the extent of the ordered structure but would probably accelerate ordering. As chromium probably exerts the same apparent valency as molybdenum it may allow a separation of effects due to atomic size and electronic factors.

On the other hand the zirconium atom is larger than that of uranium and may allow relief of lattice strain by local ordering of molybdenum atoms around the zirconium ones and may thus inhibit long range order of the  $U_2Mo$  type. It is also possible that zirconium may occupy the uranium lattice sites preferentially and extend the phase field to lower uranium contents.

Niobium, intermediate in atomic size between uranium and molybdenum, would be expected to reduce the tendency to obtain an ordered structure.

Some idea of the effects of these elements may also be obtained from considerations of the relevant binary systems. At temperatures below which  $\gamma$  (U-Mo) orders to  $\delta$  ( $U_2Mo$ ) i.e.  $\leq 560^{\circ}\text{C}$ , cU is in equilibrium with chromium and niobium-rich solid solutions in the U-Cr and U-Nb systems respectively whilst molybdenum forms continuous solid solutions with both chromium and niobium. Hence in the absence of any ternary compounds,

---

<sup>+</sup> All atomic diameters in this report are derived from the closest distance of approach in the BCC form of the element at R.T.

additions of chromium and niobium should terminate the  $\delta$  phase field to form a three phase field of  $\alpha$ U,  $\delta$  and a molybdenum - chromium or niobium - rich solid solution.

On the other hand zirconium forms  $UZr_2$  with uranium and a fairly high melting-point compound  $Zr Mo_2$  with molybdenum. Hence  $\delta$  may form a pseudo-binary system with  $Zr Mo_2$  and/or possibly  $U Zr_2$ .

Since this investigation started, a very abbreviated account of Russian work in this field has been published<sup>4</sup>. Whilst details of various phase fields were not given, the general outline of each diagram was as follows:-

In the U-Mo-Zr system, equilibria were dominated by the high melting point compound  $Zr Mo_2$  which formed pseudo binary systems with  $\delta$  ( $U_2 Mo$ ),  $\alpha$ U and  $\delta$  ( $U Zr_2$ )

In the U-Mo-Nb systems the eutectoid decomposition of  $\gamma$  to  $\alpha + \delta$  of the binary U-Mo alloys became a ternary eutectoid decomposition of  $\gamma$  to  $\alpha + \delta + Mo-Nb$  solid solution at  $565^{\circ}C$ . Similarly in U-Mo-Cr, there was a ternary eutectoid decomposition of  $\gamma$  to  $\alpha + \delta + Mo-Cr$  solid solution at  $570^{\circ}C$ . The small drop in temperature between binary and ternary eutectoid (the binary eutectoid is at  $572^{\circ}C$  according to the Russian authors) indicates that only small ternary additions of Nb and Cr are required and that therefore solubilities of Nb and Cr in  $\delta$  ( $U_2 Mo$ ) would be small.

## II EXPERIMENTAL

### (i) Materials.

The Uranium was supplied as 1" diameter bar, of total impurity content about 350 p.p.m of which carbon was accounted for 250-300 p.p.m.

Johnson-Matthey 'spec-pure' molybdenum rods of purity better than 99.95% Mo were used and contained about 90 p.p.m oxygen 60 p.p.m nitrogen and less than 0.1 w/o C. The niobium was in the form of sheet off cuts containing 2% Ta and having a hardness of 90-150 DPN (corresponding to a mean oxygen and nitrogen contamination of about 0.1 w/o)

Zirconium pellets were prepared by arc melting low hafnium zirconium sponge, the major impurities of which were Fe - 0.02%, N<sub>2</sub> - 0.005%, Cr - 0.002%, Hf - 0.03 ± 25% Al - 510 ppm ± 15%, O<sub>2</sub> - 750 ppm. The hardness after melting was 145 - 150 DPN. The electrolytic flake chromium used contained 0.13% oxide (expressed as Cr<sub>2</sub>O<sub>3</sub>), 0.01% C and 0.01% S.

(ii) Alloy preparation and Heat-treatment.

10 gm buttons of each alloy were melted on a water cooled copper hearth in an argon arc furnace, 10 times on each side to eliminate segregation. Titanium buttons were melted before and after each batch of alloys and hardness tested to check that there was no contamination by oxygen or nitrogen. Microsections through each cast button were used to ensure freedom from segregation. Weight losses were usually 1 - 1.5%.

Samples of each alloy were wrapped in molybdenum foil, sealed in evacuated silica capsules and homogenised for 1 week at 1000°C. Micro examination showed that this was sufficient to remove all coring.

The alloys were then sealed in evacuated silica capsules and annealed at 500°C for four weeks and 400°C for 12 weeks (except for certain alloys containing zirconium which were annealed for five months). These heat treatments were interrupted after two weeks at 500°C and six weeks at 400°C when the alloys were examined metallographically and then returned to the furnace for further heat-treatment.

In view of the lack of agreement between the results of alloys heat-treated for four weeks at 500°C and those reported by Bostrom and Halteman, for binary alloys additional specimens were heat treated for twelve weeks at 400°C (which gave results similar to those of Bostrom and Halteman at 400°C) and were then annealed for one day at 500°C to attain equilibrium at 500°C. The short time at 500°C was considered adequate to redissolve any precipitate formed at 400°C which was not stable at 500°C.

(iii) Metallographic Examination.

After mounting in bakelite, the specimens were polished on silicon carbide papers followed by diamond paste on a revolving pad, and finally electropolished in one of the following solutions:-

Solution 1: orthophosphoric acid ..... 100 ml  
Glycerol ..... 100 ml  
ethyl alcohol (absolute) ..... 100 ml

Solution 2: orthophosphoric acid ..... 50 ml  
concentrated  $H_2SO_4$  ..... 100 ml  
distilled water ..... 100 ml

A stainless steel cathode was used with a cell voltage of about 12 volts. Alternatively some specimens were prepared by polish attack methods using a chromic-nitric acid solution. Etching was carried out either by swabbing the specimens with 1:1 by volume nitric and acetic acid solutions or by electro-etching with solution 1 by reducing the voltage to 2 volts.

The molybdenum solid solution was identified by darkening on etching in 10% potassium hydroxide and 10% ferro-cyanide in water. A solution containing 3% nitric acid and 2% hydrofluoric acid in water darkened  $Zr Mo_2$  without affecting the molybdenum solid solution. As a routine measure, all metallographic specimens were examined by X rays in a solid specimen Debye-Scherrer camera in which the specimen was oscillated and rotated. This allowed identification of minor phases present and indicated whether  $\gamma$  was ordered or not.

**III. MICROSTRUCTURES OBSERVED.**

The microstructures observed in the alloys investigated are:

- i. Grain boundary and nodular precipitate of  $\alpha + \delta$ .  
This type of precipitate shows a eutectoid pattern of  $\alpha + \delta$  at higher magnification as shown in Fig.2.
- ii. Delta phase showing marked anisotropy and "cross-hatching" under polarised light especially after deep etching (Fig.3). This will be referred to as anisotropic delta and denoted as  $a\delta$ .
- iii. Delta phase without cross-hatching and apparently isotropic when examined under polarized light (Fig.4). This will be referred to as isotropic delta and denoted as  $i\delta$ .
- iv. Isotropic  $\delta$  phase with molybdenum solid solution at grain and sub-grain boundaries Figs. 5 and 6.
- v. Delta phase with  $\alpha + \delta + Mo$  solid solution inside grains and along grain boundaries Fig. 7. This is observed only in ternary alloys with Nb or Cr.
- vi. Delta phase with  $Zr Mo_2$  precipitated at grain boundaries (Fig.8). At higher zirconium and molybdenum contents  $Zr Mo_2$  and the molybdenum solid solution co-exist (Fig.9).

**IV. BINARY ALLOYS.**

**(i) Results (Figs. 10 - 12)**

At  $500^{\circ}C$ , the  $\alpha + \delta$  phase field existed to  $26\frac{1}{2}$  a/o Mo at which it was replaced by an apparently single phase  $\delta$  phase with an optically anisotropic structure (Fig.3). With more than 31 a/o Mo, this structure remained single phase but was completely isotropic under polarized light (Fig.4). With 34 a/o Mo, the molybdenum solid solution appeared. After 12 weeks at  $400^{\circ}C$ , alloys with up to 31 a/o Mo contained  $\alpha$  in equilibrium with anisotropic  $\delta$ . At 32 & 33 a/o Mo the  $\delta$  was completely isotropic and molybdenum solid solution first appeared at 34 a/o Mo.

Reheating at 500°C alloys annealed for 12 weeks at 400°C caused no change in the position of the phase boundaries.

Alloys of compositions within the  $\delta$  phase fields as determined by Bostrom and Halteman and Pfeil and Browne respectively have been prepared metallographically by three methods. (1) normal mechanical polish and etch; (2) electrolytic polish and etch; (3) polish-attack using a chromic/nitric acid solution.

In all cases, the alloys supersaturated with uranium according to Bostrom and Halteman's diagram i.e. between dotted line and  $U_2 Mo$  in Fig.1 showed marked optical anisotropy whereas those richer in molybdenum were invariably isotropic. Prolonged etching of the isotropic alloys eventually revealed a faint structure which in bright field illumination looked similar to the anisotropic structure under polarized light of alloys richer in uranium. After 12 weeks at 400°C, the  $\delta$  in two-phase  $\alpha + \delta$  alloys was anisotropic but  $\delta$  in single phase alloys remained isotropic. This suggests the existence of a narrow anisotropic  $\delta$  phase field between 31 and 32 a/o Mo.

(ii) Discussion.

At 400°C the  $\delta$  phase field has been found to extend over the range  $31\frac{1}{2}$  a/o to  $33\frac{1}{2}$  a/o molybdenum which compares well with the range of 31 -  $32\frac{1}{2}$  a/o Mo obtained by Bostrom and Halteman. At 500°C the maximum annealing period of four weeks did not bring about equilibrium. However specimens held for 12 weeks at 400°C did not change in microstructure on reheating to 500°C and it is probable that this treatment represents the true equilibrium at 500°C. In alloys annealed for four weeks at 500°C, the change in microstructure from the anisotropic to the isotropic form of  $\delta$  occurred at between 31 and 32 a/o molybdenum and it appeared that the anisotropic structure was associated with the  $\delta$  phase supersaturated with uranium. However no difference could be found between the X ray structure of isotropic and anisotropic microstructure. For the purpose of the ternary systems, the U-rich limit of the  $\delta$  field in the binary alloys at 500°C has been taken as  $31\frac{1}{2}$  a/o Mo.

V URANIUM - MOLYBDENUM - ZIRCONIUM ALLOYS.

(i) Results (Fig. 10 to 12)

At both 400°C and 500°C, additions of zirconium moved the  $\delta$  phase boundaries to lower uranium contents and had little effect on the width of the phase field. The direction of the boundaries was towards  $Zr Mo_2$  and  $\delta$  formed a pseudo-binary system with that phase the maximum solubility of zirconium in  $\delta$  being about  $2\frac{1}{4}$  a/o. The existence of  $Zr Mo_2$  was confirmed by X ray examination. To the molybdenum-rich side of  $\delta$ , a ternary phase field of  $\delta$ ,  $Zr Mo_2$  and the Mo solid solution existed with zirconium contents above  $2\frac{1}{4}$  a/o.

To the uranium-rich side of  $\delta$  no alloys with more than 2 a/o Zr were examined. At and below 2 a/o, an  $\alpha + \delta$  phase field existed. At 400°C after 12 weeks and 500°C after four weeks a precipitated (as eutectoid) in alloys with up to 32 a/o Mo; in binary alloys of comparable composition no  $\alpha$  was precipitated at 500°C and an anisotropic  $\delta$  resulted.

All the alloys with 2 a/o zirconium or above and the molybdenum-rich alloys with 1 a/o zirconium were not fully ordered after four weeks at 500°C or 12 weeks at 400°C. Prolonging the anneal at 400°C to 20 weeks did not bring about full ordering of the  $\gamma$  phase in these alloys.

On taking alloys annealed at 400°C for 12 weeks and reheating to 500°C, no change in microstructure was observed but X ray examination indicated that alloys with 1 a/o Zr ordered fully.

(ii) Discussion.

The phase boundaries of the  $\delta$  phase were modified by additions of zirconium in such a way as to suggest that two U atoms are replaced by 1 zirconium and 1 molybdenum. Complete replacement of uranium in this manner would of course produce  $Zr Mo_2$  but the  $\delta$  structure (or strictly speaking partially ordered  $\gamma$  structure) will only tolerate the replacement of some 4 to 5% of the uranium atoms. The fact that these small

additions of zirconium delayed ordering appreciably suggests that zirconium does not replace particular U sites preferentially. Insufficient X ray examination was carried out to check this but it is unlikely that such an effect could be detected if present.

Zirconium appreciably reduces the rate of ordering. The observation that the alloy U - 34 a/o Mo - 1 a/o Zr fully ordered on heating at 500°C after a previous anneal for 12 weeks at 400°C had failed to order it, is the only evidence that the zirconium does not reduce the degree of order of  $\gamma$ . Practically full precipitation of  $\alpha$  from  $\gamma$  occurred at 500°C and confirms Bostrom and Halteman's suggestion that once  $\gamma$  has ordered precipitation of any excess uranium as  $\alpha$  is difficult.

VI URANIUM - MOLYBDENUM - NIOBIUM ALLOYS.

(i) Results (Figs 10 - 12)

At both 400°C and 500°C, niobium progressively narrowed the  $\delta$  phase field until it terminated in a three phase field of  $\alpha$ ,  $\delta$  and a molybdenum - niobium solid solution. Alloys brought into equilibrium at 400°C and reheated to 500°C showed no changes in the relative positions of the phase fields and it is probable that there is no difference in the equilibria at the two temperatures. Fig. 11 therefore represents a pseudo equilibrium after four weeks at 500°C.

Between  $1\frac{1}{2}$  and 2 a/o niobium was required to eliminate the  $\delta$  phase field. The composition of the  $\delta$  phase in the ternary eutectoid is estimated at 28.2 a/o Mo, 1.8 a/o Nb 70 a/o U. At the pseudo equilibrium at 500°C this occurred at 27 a/o Mo, 71 a/o U 2 a/o Nb but further precipitation of  $\alpha$  occurred on prolonged annealing. At both temperatures no single phase anisotropic  $\delta$  was found but in the  $\alpha + \delta$  alloys,  $\delta$  was anisotropic.

Ordering was not complete after two weeks at 500°C or 6 weeks at 400°C but all alloys were fully ordered after four weeks at 500°C. After 12 weeks at 400°C ordering appeared complete but there might be some slight disorder in alloys with more than 1 a/o Nb.

(ii) Discussion.

Niobium modified the molybdenum-rich phase boundary of the  $\delta$  phase in such a way as to suggest that 2 atoms of uranium and 1 atom of niobium replaced 3 atoms of molybdenum, the maximum solubility of niobium corresponding to replacement of 15% of the molybdenum atoms. Extrapolation of the molybdenum-rich boundary meets the U - Nb binary system at about 11 a/o Nb. This is within the range of composition over which Dwight and Mueller <sup>5</sup> report evidence of a body centred tetragonal phase (9.5 - 20 at % Nb). Berry <sup>6</sup> obtained a similar structure in a 17.5 a/o niobium alloy whilst in alloys of 11 and 15 a/o niobium he found structures believed by Harding, Waldron and Knight <sup>7</sup> to have transformed from an ordered tetragonal  $\gamma$ . There was evidence to show that the latter existed only below a temperature of about 660 - 680°C. Hence, whilst there is no direct evidence of the existence of an ordered tetragonal phase in U - Nb alloys there is some indirect evidence that the  $\gamma$  phase tends to order to a phase similar to  $\delta$  ( $U_2 Mo$ ) under conditions not yet understood at composition approximating to the extrapolation of the phase boundaries in the U - Mo - Nb system.

Niobium reduced the rate at which  $\gamma$  ordered appreciably but did not appear to reduce the degree of order as far as could be judged from a visual inspection of X ray films. As little as  $\frac{1}{2}$  a/o niobium delayed the onset of ordering sufficiently to allow precipitation of  $\alpha$  at 500°C in alloys containing up to  $30\frac{1}{2}$  a/o molybdenum. In the absence of niobium no precipitation of  $\alpha$  occurred in alloys with 27 - 31 a/o molybdenum before  $\gamma$  ordered to  $\delta$ .

VII URANIUM - MOLYBDENUM - CHROMIUM ALLOYS.

(i) Results (Figs 10 - 12)

In general the effect of chromium resembled that of niobium. At 500°C under conditions of pseudo-equilibrium, the  $\delta$  phase field was identical with that in the U - Mo - Nb system and terminated in a three phase field of  $\alpha$ ,  $\delta$  and a molybdenum-chromium solid solution. However at 400°C appreciable precipitation of  $\alpha$  occurred and the apex of the  $\delta$  phase field was found at 68.6 a/o U, 29.6 a/o Mo and 1.8 a/o Cr. An identical diagram was obtained on re-heating at 500°C alloys in equilibrium at 400°C.

At 400°C no single phase anisotropic  $\delta$  was found but in all  $\alpha + \delta$  bi-phase alloys, the  $\delta$  was anisotropic. However at 500°C after four weeks annealing,  $\gamma$  ordered to  $\delta$  before  $\alpha$  precipitation and an extensive apparently single phase anisotropic  $\delta$  region was obtained as in the binary U - Mo alloys. The  $\gamma$  ordered rapidly at both temperatures i.e. within two weeks at 500°C and six weeks at 400°C.

(ii) Discussion.

Chromium modified the molybdenum-rich boundary of the  $\delta$  phase in such a way as to suggest that 1 atom of uranium and 1 atom of chromium replace 2 atoms of molybdenum the maximum solubility of chromium corresponding to the replacement of about 10% of the molybdenum atoms.

Extrapolation of the molybdenum-rich boundary meets the U-Cr binary at 16 2/3 a/o chromium.

The addition of chromium did not delay the onset of ordering of  $\gamma$  to  $\delta$  which took place at 500°C before a precipitation was complete as in the binary. Whilst this was not established definitely, it appeared that chromium had little effect on ordering.

VIII

GENERAL DISCUSSION.

This investigation has confirmed that precipitation of  $\alpha$  from  $\gamma$  in supersaturated alloys is severely inhibited by the ordering phenomena. Where the third element added, e.g. 1% Zr, delayed or reduced the rate of ordering, it was possible to obtain almost complete precipitation of  $\alpha$  from  $\gamma$  before ordering began and the phase boundaries obtained at 500°C were the same whether the alloys were annealed directly at 500°C for four weeks or reheated at 500°C after three months at 400°C. More complete precipitation of  $\alpha$  was obtained too with niobium additions but these reduced the onset or rate of ordering less and complete precipitation of  $\alpha$  was not obtained in four weeks at 500°C. On the other hand, with chromium additions  $\alpha$  precipitation was delayed as in the binary alloys.

In binary alloys, the anisotropic  $\delta$  phase was observed whenever  $\delta$  was supersaturated with respect to uranium. The isotropic structure was obtained in the single phase  $\delta$  field at 400°C and whenever  $\delta$  was in equilibrium with molybdenum. In ternary alloys whenever  $\delta$  co-existed with any phase but  $\alpha$ , its microstructure was optically isotropic. However whenever  $\alpha$  was present the  $\delta$  phase became optically anisotropic in both bi - and tri - phase alloys at both temperatures. Hence it is probable that the anisotropic structure of  $\delta$  is associated with some supersaturation with respect to  $\alpha$  uranium and that even after three months at 400°C the uranium rich  $\delta + \alpha$  alloys are not completely in equilibrium.

The cause of the anisotropy is not clear. As it was only found in alloys believed to be supersaturated with  $\alpha$  when ordering took place, it might be a manifestation of the effect of excess uranium atoms on the mechanism of ordering or on the ordered structure or the result of some pre precipitation form of  $\alpha$ . X ray examination could detect no differences in structure between the two microstructural forms of  $\delta$ . A detailed examination of the ordering process would be required before this is understood fully. Nevertheless the examination of the ternary alloys particularly those with zirconium supports the suggestion that the anisotropic form of  $\delta$  is supersaturated with respect to uranium and that the limits of the isotropic phase represent the  $\delta$  phase boundaries.

The effects of the three elements on the  $\delta$  phase field differed markedly. Zirconium replaced uranium in the proportion of 1 Zr to 2U. In small quantities, it is probable that zirconium took uranium sites in the  $\delta$  structure but as zirconium reduced the amount of order attained under the experimental conditions, zirconium replaced uranium atoms at random. The effect of zirconium on the  $\gamma$  or  $\delta$  phase field at 400°C and 500°C is a measure of the dominance of the ternary system by the high melting point compound Zr Mo<sub>2</sub> (forming peritectically at 1880°C). The Russian work suggests that Zr Mo<sub>2</sub> forms pseudo binary systems with all phases in the ternary system and the solubilities of Mo and Zr in the ternary system are markedly decreased in the manner characteristic of cases where the solid solution is in equilibrium with an intermetallic compound of low free energy. Zr Mo<sub>2</sub> has a Laves

phase structure (C 15 structure  $Mg Cu_2$  type) which is a particularly close packed structure occurring when the ratio of the interatomic distances of the two components is approximately 1.2:1. Relative atomic sizes are the main factor in deciding the stability of this structure and it can be constructed by the correct packing of hard spheres of the correct relative sizes, the smaller atoms being at the corners of tetrahedra round each large atom and the large atoms forming a lattice similar to that of diamond. Hence it is probable that addition of zirconium to alloys of  $\delta$  phase composition causes short range order of this type with molybdenum atoms and thus hinders the establishment of long range  $U_2 Mo$  order.

On the other hand, whilst reducing the rate of ordering, niobium had the opposite effect on the phase boundaries of the  $\delta$  phase, one atom of niobium replacing three of molybdenum. No ternary compounds were found and the  $\delta$  phase formed a ternary eutectoid with a U and a niobium - molybdenum solid solution. Extrapolation of the  $\delta$  phase boundary met the U - Nb binary at 11.1 a/o Nb which is within the range of composition in which there is evidence of ordering within the  $\gamma$  phase. In view of the effect of  $\sim 2$  a/o niobium on the ordering of  $\gamma$  (U - Mo), very long annealing times would be necessary to establish any ordering of the  $U_2 Mo$  type in U - Nb alloys and an ordered structure in U - Nb is probably never stable but may form as a transitional metastable structure under certain conditions.

The significance of this extrapolation can be considered from another point of view. The uranium-rich  $\gamma$  (U - Nb) phase is not stable below about  $640^{\circ}C$  on account of the monotectoid decomposition. However the hypothetical solubility of niobium in  $\gamma$  uranium at  $400^{\circ}C$  can be estimated from the extrapolation of the  $\gamma$  immiscibility loop to lower temperatures. There is some lack of agreement in the form of this curve but as a matter of convenience the curve determined by Berry<sup>6</sup> at F.R.I. has been used. This is a parabola and fits approximately the equation  $t = -0.625x^2 + 52.5x - 92.5$  where  $t$  is the temperature in  $^{\circ}C$  and  $x$  the atomic fraction of niobium. This gives a hypothetical solubility at  $400^{\circ}C$  of 10.8 a/o Nb in the  $\gamma$  phase which agrees well with the extrapolated  $\delta$  phase boundary. The molybdenum-rich boundary of the  $\delta$  phase in U-Mo lies very close to the maximum metastable solubility of molybdenum in  $\gamma$  before ordering takes place as would be expected from the

similarity of structures and it can therefore be seen that the direction of the molybdenum-rich phase boundary of  $\delta$  is approximately that expected if the probable metastable  $\gamma$  phase boundaries in the two binary systems were joined by a straight line. In other words the effect of niobium on the  $\delta$  phase boundary is more or less what would be expected from the relevant binary systems and the limitation of the  $\delta$  phase field is a consequence of the monotectoid and eutectoid decompositions.

Both niobium and molybdenum affect the lattice parameter in the same sense, molybdenum providing the greater reduction. (The ratio of the distortions produced by equal atomic percentages of molybdenum and niobium is 3:1 taking the low niobium part of the lattice parameter curve for U - Nb<sup>8</sup>). Where the distortions produced by two solutes are in the same sense and one is much greater than the other, Hume-Rothery<sup>9</sup> has pointed out that in copper - and silver base solid solutions, the solid solubility isothermal is not a straight line from one binary system to the other but is concave to the solvent-rich corner. If this was applicable to uranium solid solutions, the U - Nb - Mo isothermal should be somewhat concave. However the suggestion above that the latter is a straight line is based on sufficient assumptions and extrapolations for a slight concavity not to be detected. Also the main divergence from a straight line would be expected at the niobium-rich end. Secondly in the copper and silver-base alloys the ternary isothermals usually lie along lines of constant electron/atom ratio except where differences in size factor cause small divergences from this. It seems unlikely at first sight that the U - Nb - Mo ternary isothermal correspond to lines of constant electron/atom ratio. Assuming that lattice distortion did not affect the c/a of the isothermal, it would be necessary to postulate a valency for niobium of 10 assuming that U had valency of 4 and Mo its group valency of 6. However, Hume-Rothery and Andrews<sup>10</sup> have shown that in copper-rich alloys, the deviations from a constant electron/atom ratio were directly related to the lattice distortion, the greater the lattice distortion produced, the lower the electron/atom ratio of the solubility limit.

As the relative lattice distortions produced by molybdenum and niobium in uranium are approximately 3:1 respectively, this would require a higher valency still for niobium. There is however some evidence that the valency of uranium may be higher in alloys with small amounts of niobium<sup>8</sup>, as in dilute alloys of uranium in palladium<sup>11</sup>. If U did exert a higher valency in alloys containing niobium, the normal group valency of 5 for niobium would be possible. The purpose of this conjecture is to show the need for further work on the measurement of physical properties and solubility limits of the uranium-rich solid solutions.

The effect of chromium on the  $\delta$  phase boundary is much less than that of niobium, one atom of chromium replacing two of molybdenum. No ternary compounds were formed. This is somewhat surprising for several reasons. Extrapolation of the phase boundary meets the U - Cr binary system at 16 2/3 a/o Cr which is well outside the maximum solubility of chromium in  $\gamma$  U at any temperature. As chromium causes greater distortion of the  $\gamma$  uranium lattice than does molybdenum then by analogy with Hume - Rothery's arguments on solubility limits in copper-base alloys, one would expect the solubility limit of a stabilized  $\gamma$  phase in U - Mo - Cr to be markedly convex to the U corner. Hence small amounts of chromium would have been expected to reduce the  $\delta$  phase field more rapidly to higher uranium contents than does niobium. As chromium would be expected to exert the same group valency as molybdenum, no electronic effects would be expected in this system unless small amounts of chromium modify the uranium valency.

IX CONCLUSIONS.

1. In binary U-Mo alloys, the  $\delta$  phase was located at 31 1/2 a/o Mo to 33 1/2 a/o Mo at 400°C and 500°C which is in reasonable agreement with Bostrom and Halteman<sup>2</sup>. On annealing directly at 500°C only partial precipitation of  $\alpha$  occurred before ordering of  $\gamma$  took place and a pseudo  $\delta$  phase boundary at 26 1/2 a/o Mo at 500°C and 31 1/2 a/o Mo at 400°C which agree with the position of the U-rich boundary determined by Pfeil & Browne.

The optical anisotropy of the  $\delta$  phase was found to depend on composition and it is concluded that the optically anisotropic alloys are supersaturated with respect to uranium. Whilst the reason for the optical anisotropy is not known it may be a result of excess U atoms on the mode of transformation. X ray analysis by powder and single crystal methods has not shown any difference between the two types of metallographic structure.

2. Zirconium dissolved in the  $\delta$  phase (or partially ordered  $\gamma$ ) to a maximum of  $2\frac{1}{4}$  a/o and moved the phase boundaries to lower uranium contents in the proportion of 1 Zr and 1 Mo replacing 2 U atoms. The  $\delta$  phase formed a pseudo-binary system with Zr Mo<sub>2</sub> a Laves phase which dominated the whole ternary system. Zirconium delayed the onset and reduced the rate of ordering to such an extent that the 2 a/o Zr alloys were not fully ordered after 5 months at 400°C. It is suggested that short range order of Mo atoms around each Zr inhibited the formation of the long range U<sub>2</sub> Mo order.

3. Niobium also delayed the onset and reduced the rate of ordering but not to the same extent as zirconium did. A maximum solubility of 1.8 a/o niobium terminated the ternary  $\delta$  phase field in a three phase field of a U,  $\delta$  and a niobium-molybdenum solid solution. The phase boundaries were moved to higher uranium contents in the proportion of 1 Nb + 2 U atoms replacing 3 Mo atoms. The molybdenum-rich boundary extrapolated to cut the U - Nb binary system at about 11 a/o Nb which is approximately the maximum solubility of Nb in  $\gamma$ U when extrapolated to 400°C. This suggested that the  $\gamma$  ( $\delta$ ) solubility isothermal at 400° would be approximately a straight line in the absence of the eutectoid and monotectoid transformations and may well be so at higher temperatures (> 640°C)

4. Chromium had little effect on the rate of ordering as far as can be seen and moved the phase boundaries to higher uranium contents less severely than niobium did, 1 atom of Cr + 1 atom of U substituting for each 2 Mo atoms. This is unexpected as Cr increases distortion in uranium and has a much lower solid solubility than would be expected from extrapolation of the  $\delta$  phase boundary.

5. It is considered that useful information about the alloying behaviour of BCC elements in uranium would be obtained from studies of solubility isothermals in  $\gamma$  uranium. Further work on the effect of alloying elements on the ordering of the  $\gamma$  phase to  $\delta$  is also required.

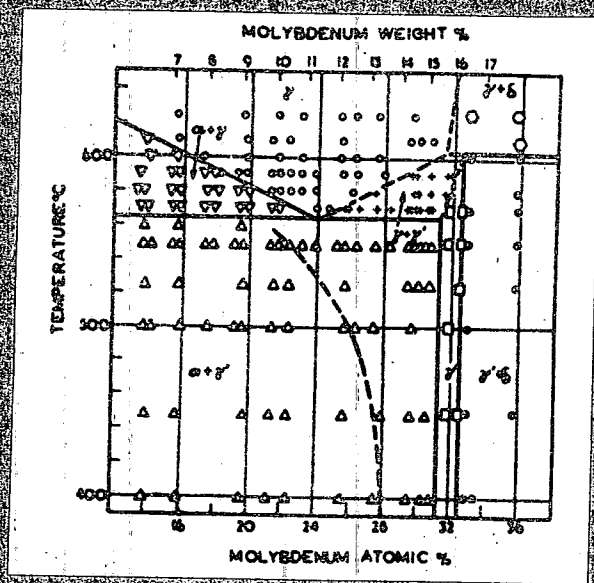
RSELA/GBB/AK.  
12/6/69.

068 051

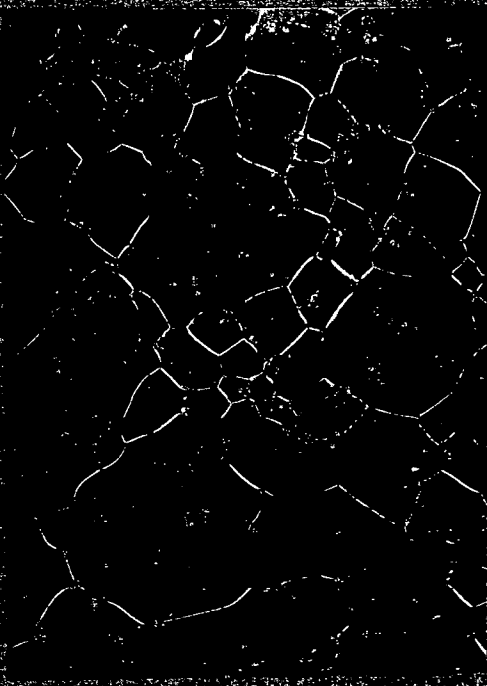
R E F E R E N C E S .

1. Pfeil, P.C.L. and Browne, J.D. A.E.R.E. Report M/R1333, 1954.
2. Bostrom, W.A. and Halteman, E.K. 2nd Nuclear Eng. & Sci. Conf., March 1957, Paper No.57-NESC-12.
3. Halteman, E.K. Acta Cryst. 1957, 10, 166.
4. Ivanov O.S. & Badajeva T.A. 2nd U.N. Int. Conf. Peaceful Uses of Atomic Energy. A/Conf/15/P/2043.1958.
5. Dwight A.E. & Mueller M.H. U.S. AEC Document ANL 5581. 1957.
6. Berry. B.S. F.R.I. Report R126/3. 1958.
7. Harding A.G. Waldron M.B. and Knight C. A.E.R.E. Report M/R 2673A 1958.
8. Pfeil P.C.L. Williamson G.K. and Browne J.D. A.E.R.E. Report M/R 2498. 1958
9. Hume - Rothery. W. Phil. Mag. 1936 [7] 22 1013
10. Andrews K.W. & Hume-Rothery W. Proc.Roy.Soc. 1941 [A] 178 464
11. Catterall.J.A. Phil.Mag. 1957 [8] 2 491.

-----oo-----



068-057



068 - 054



668-055

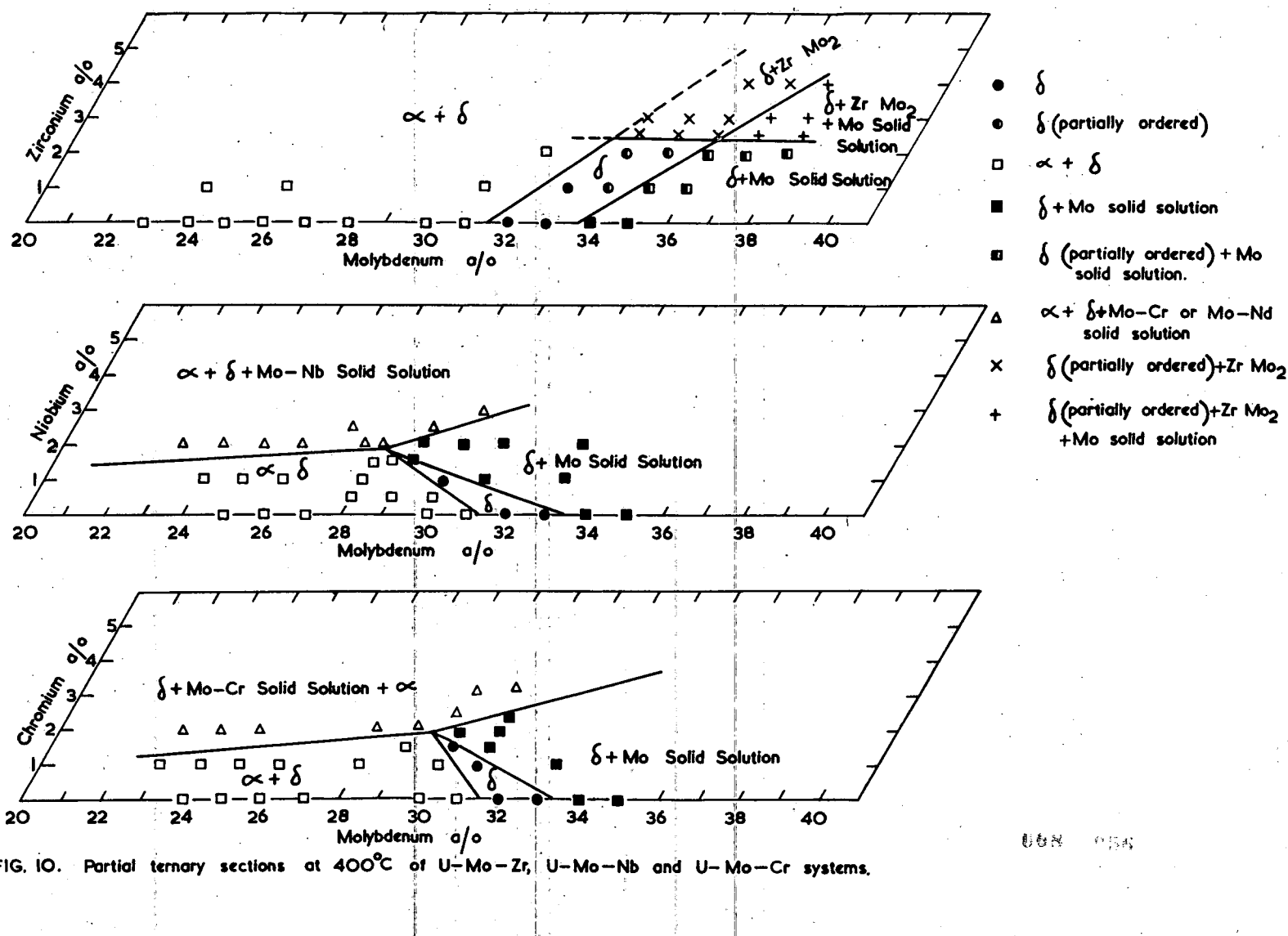


FIG. 10. Partial ternary sections at 400°C of U-Mo-Zr, U-Mo-Nb and U-Mo-Cr systems.

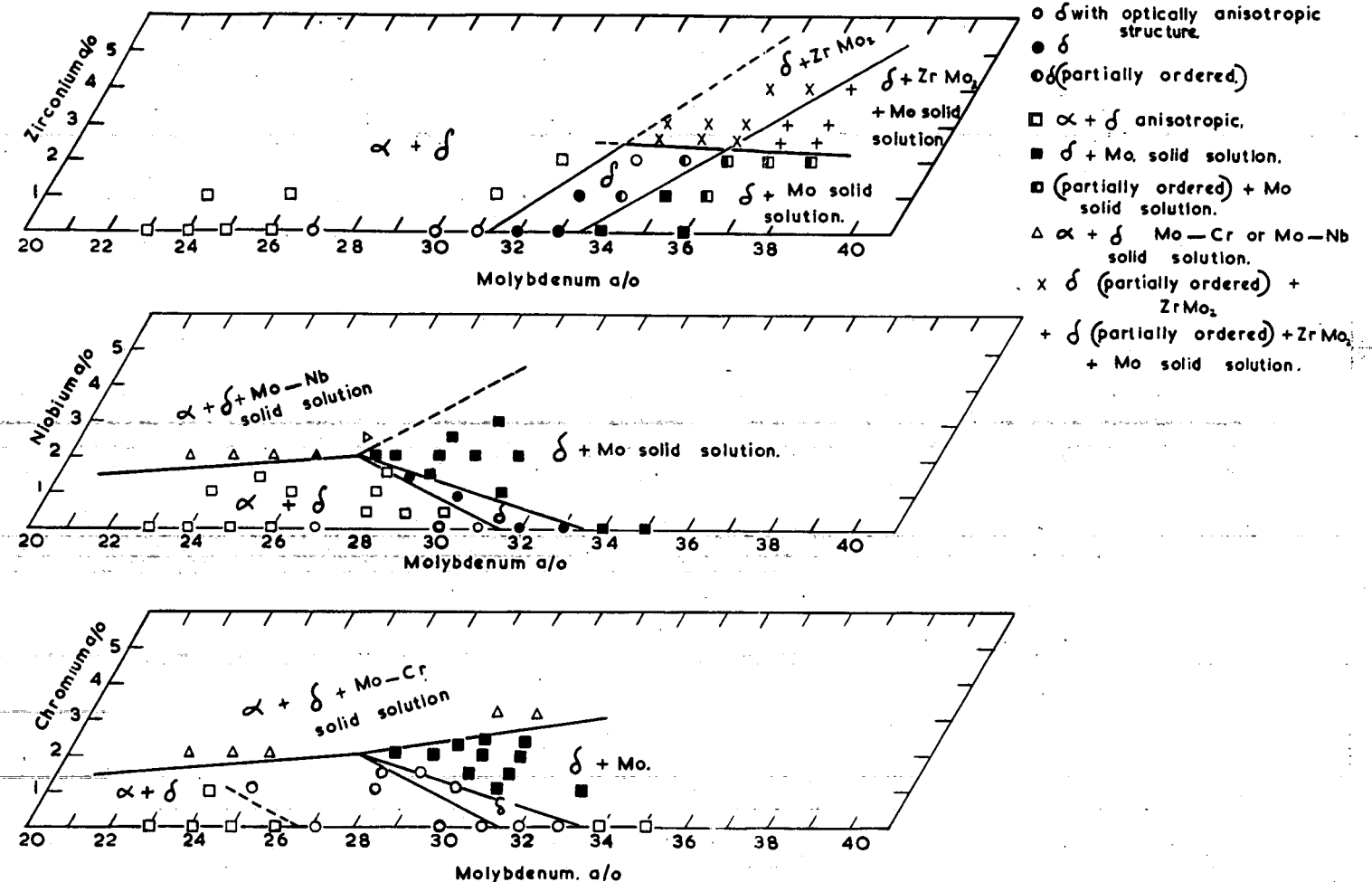


Fig II Partial ternary sections of U—Mo—Zr, U—Mo—Nb, and U—Mo—Cr systems showing phases present after 4 weeks at 500°C

068-057

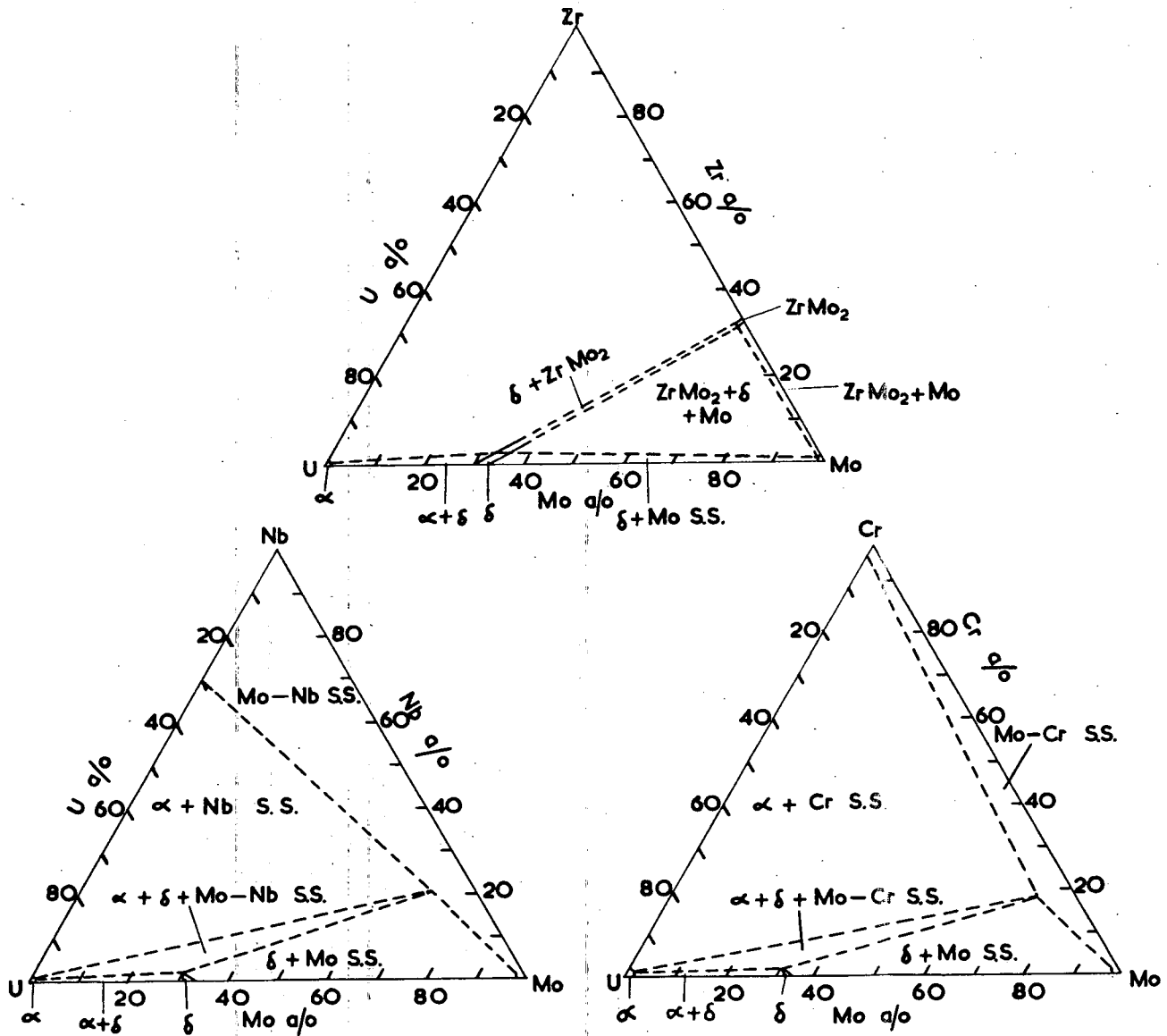


Fig. 12. Hypothetical Phase Sections at 400°C for the U-Mo-Zr, U-Mo-Nb and U-Mo-Cr systems.

PART B (ii).

X-RAY EXAMINATION OF THE  $\delta$  PHASE

by

H. Lynton, B.Sc., Ph.D.

I. DEBYE-SCHERRER METHODS

Three specimens of coarse grain size have been examined in detail. These are:-

Specimen a) U-25 At.% Mo

This had been homogenized for 1 week at  $1000^{\circ}\text{C}$ , water quenched and annealed for 2 weeks at  $500^{\circ}\text{C}$ . The microstructure showed large grains of the  $\delta$  phase with  $\alpha + \delta$  precipitate at the grain boundaries and within the grains. Under polarized light the matrix had a cross-hatched appearance. Debye-Scherrer type photographs of the block specimen with filtered CoKa radiation indicated the presence of the  $\delta$  phase only.

Specimen b) U-31 At.% Mo 1% Cr

This had been homogenized for 1 week at  $1000^{\circ}\text{C}$ , water quenched and annealed for 2 weeks at  $500^{\circ}\text{C}$  followed by 4 weeks at  $400^{\circ}\text{C}$ . Microstructure showed a fine precipitate at the grain boundaries with weak cross-hatched appearance of the grains under polarized light. Debye-Scherrer photographs indicated  $\delta$  only.

Specimen c) U-33 At.% Mo 1% Cr

The heat treatment was the same as for b). Large grains of  $\delta$  phase only were observed and these were isotropic under polarized light. Debye-Scherrer photographs confirmed that these were  $\delta$  phase.

As the Debye-Scherrer type photographs of normal exposure time did not show the presence of the small quantities of  $\alpha$ U precipitate seen visually in specimens a) and b), extra long exposure photographs were taken. Faint additional lines appeared on the films but these can all be explained as due to weak  $K\beta$  radiation passing the filter. No  $\alpha$ U structure lines appeared and no detectable difference was seen between the isotropic and cross-hatched specimens. Without the further refinement of using crystal monochromatized radiation to reduce the background scatter and remove the  $K\beta$  lines, it is unlikely that either small differences or the presence of small quantities of  $\alpha$ U will be detected.

## II. SINGLE CRYSTAL EXAMINATION

Single crystal photographs have been taken with a Unicam Weissenberg goniometer using  $CuK\alpha$  filtered radiation. Large single grains in all the three specimens were examined by mounting the whole block on the goniometer and directing the X-rays through a small collimator on to a single grain. With the 25 At.% Mo specimen, a large grain was also cut out of the block and mounted alone.

Zero and higher layer equi-inclination photographs confirm the ordered  $U_2Mo$  structure proposed by Halteman and give unit cell dimensions of  $a = 3.44 \text{ \AA}$ ,  $c = 9.82 \text{ \AA}$  in good agreement with the values  $a = 3.427 \text{ \AA}$ ,  $c = 9.834 \text{ \AA}$  published. Intensities from the isolated grain of the 25 At.% Mo specimen, estimated visually into one of seven groups, agree very well (apart from a difference in scale) with those given by Halteman. These intensities are listed in Table 1 and the agreement shown graphically in Figure 1 where the full line gives Halteman's data and the broken line the writer's.

Five very weak reflections 1.1.4, 2.0.4, 0.0.10, 1.1.10 and 2.0.10, not observed by Halteman, were seen and two further strong ones 1.1.12 and 2.1.11 at the limit of  $CuK\alpha$  radiation. A parameter of  $z = 0.328$ , assuming space group  $D_{4h}^{17}$  -  $I\bar{4}/mmm$  is consistent with the observed data.

The additional weak lines reported in the previous progress report No. 2 were very probably due to foreign radiation as they do not appear with the radiation from a new Cu X-ray tube.

It has been suggested that the cross-hatched appearance under polarized light of the  $\delta$  grains in some specimens may be due to either the preprecipitation of  $\alpha$ U or a stage in the ordering process. This could be investigated using crystal monochromatized x-radiation by following the annealing of a single  $\gamma$  grain.

HL/DS

068 061

TABLE 1

Plane	<u>I<sub>L</sub></u>	<u>I<sub>H</sub></u>	Plane	<u>I<sub>L</sub></u>	<u>I<sub>H</sub></u>
002	not obs	w	208	m	w
101	w	mw	314	-	-
004	not obs	-	305	w	vw
110	vs	s	0.0.10	vvw	-
103	vs	vs	226	not obs	m
112	m	mw	321	vw	vw
114	vw	-	323	vs	m
200	vs	m	1.1.10	vvw	-
105	m	w	316	s	m
006	s	m	219	s	m
202	w	w	307	not obs	-
211	w	vw	1.0.11	m	mw
204	vvw	-	228	not obs	w
213	vs	m	400	vs	m
116	vs	m	325	not obs	w
107	-	-	2.0.10	vvw	-
008	m	vw	402	vw	vw
220	vs	m	411	vw	vvw
215	m	vw	0.0.12	s	m
206	s	m	318	m	vw
222	w	vw	404	-	vvw
301	vw	vw	330	vs	m
118	m	vw	413	vs	m
224	not obs	-	332	v	vw
310)	m	-	309	s	m
303)	vs	m	327	not obs	-
312	w	w	1.1.12	s	not obs
109	s	m	2.1.11	m	not obs
217	-	-			

not obs - not within range of photographs

vs - very strong

s - strong

m - medium (mw - medium weak)

w - weak

vw - very weak

vvw - very very weak

- - no detectable intensity

I<sub>H</sub> - intensities observed by HaltemanI<sub>L</sub> - " " " " writer

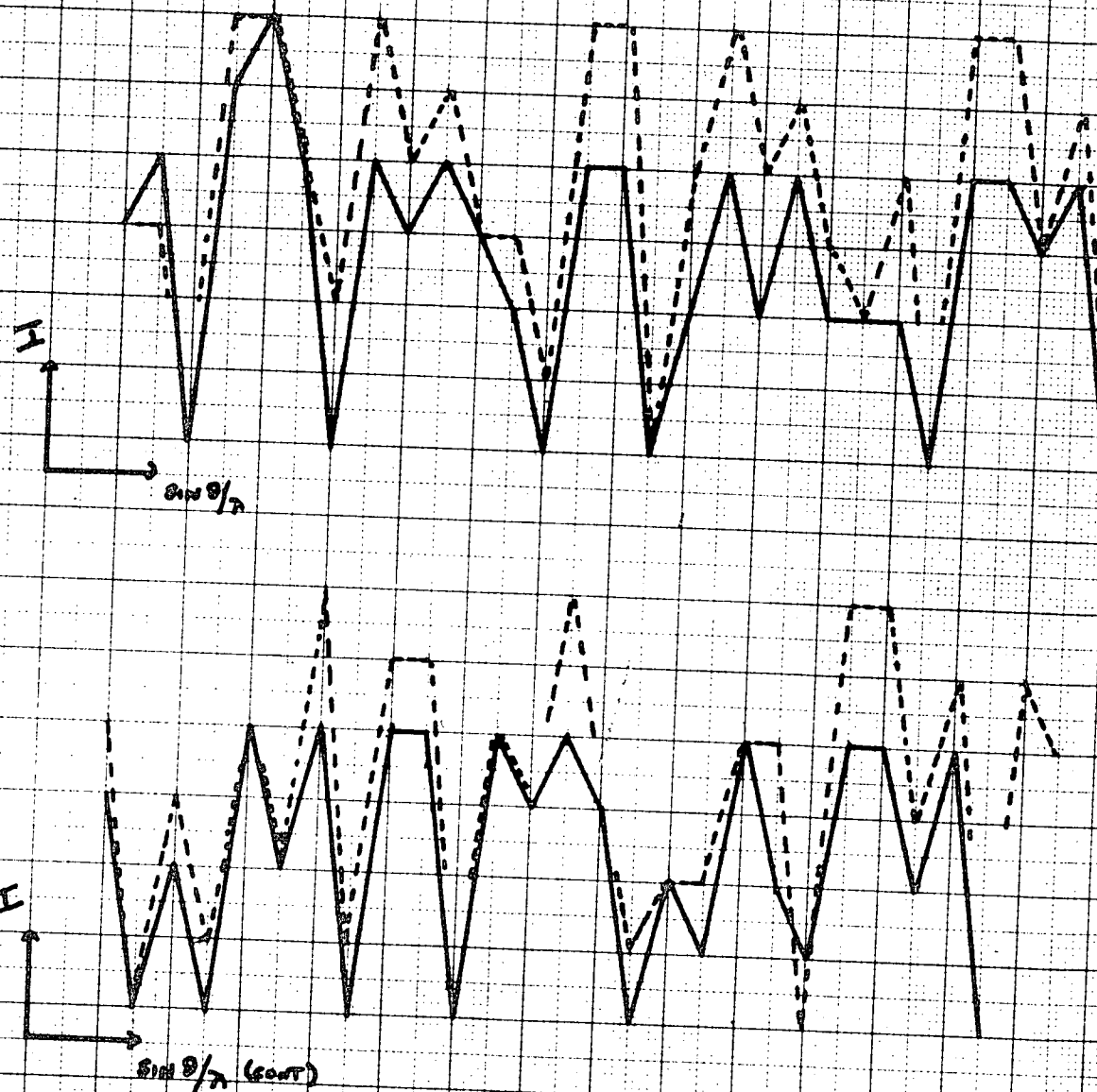


Fig. 1a. Agreement between the intensities observed by Halteman and those observed by the writer.

PART C.

KINETICS OF TRANSFORMATION FROM THE  $\gamma$  PHASE OF URANIUM ALLOYS.

THE EFFECT OF THIRD ELEMENTS ON TRANSFORMATIONS  
IN URANIUM MOLYBDENUM ALLOYS.

by

G.B. Brook., B. Met.

E.H. Welch., L.I.M.

and

D.H. Désy., B.Sc., M.Met.E., Eng.Sc.D.

---

I. INTRODUCTION.

Many transitional elements form solid solutions in the  $\gamma$  phase of uranium but only those of titanium, zirconium, niobium and molybdenum are at all extensive and it is from the alloy systems with these elements that the useful  $\gamma$  phase alloys are to be found. In all four systems the gamma phase can be retained on quenching from high temperatures on the addition of sufficient alloying element, and much attention has been devoted to the stability of the retained  $\gamma$  phase on reheating. In general the effectiveness of the alloying element in stabilising gamma increases in the order titanium, zirconium, niobium, molybdenum and it is therefore alloys of the uranium-molybdenum system which have received most attention. These are being considered as high temperature fuel elements and it is therefore of practical as well as theoretical interest to study the manner in which small ternary additions can affect the isothermal decomposition of the gamma phase. If elements can be found which delay the nucleation of the precipitating phase and/or diffusion, the metastable  $\gamma$  phase may be rendered more stable at higher temperatures, or the use of alloys of higher uranium content may be possible without decreasing thermal stability.

In alloys containing less than about 31 a/o molybdenum, the ultimate decomposition product of the  $\gamma$  phase below about  $500^{\circ}\text{C}$  is  $\alpha$ -uranium and an ordered phase corresponding to  $\text{U}_2\text{Mo}$  and known variously as  $\gamma'$  or  $\delta$ . The transformation of different alloys on quenching from the  $\gamma$  phase field has been investigated widely<sup>1 - 3</sup> both by quenching to room temperature and tempering, and by quenching direct to the tempering temperature (stepped quench) and all have shown that decomposition takes place by precipitation of lamellar  $\alpha$  + enriched  $\gamma$  at the boundaries and within the grains. The  $\gamma$  subsequently orders to the  $\gamma'$  or  $\delta$  phase. Since this work was begun, Van Thyne and McPherson<sup>4</sup> have reported a limited amount of work on the influence of niobium and platinum on the start of decomposition of  $\gamma$  phase in U-8 w/o Mo alloys and showed that 1.5 w/o niobium delayed precipitation at all temperatures whilst 3 w/o niobium had little effect at about  $500^{\circ}\text{C}$  but delayed precipitation appreciably at  $400^{\circ}\text{C}$ . The effect of 1 w/o platinum was less marked than 1.5 w/o niobium. In a more extensive survey, Storhok, Bauer and Dickinson<sup>5</sup> have shown that at  $500^{\circ}\text{C}$ , the stability of the  $\gamma$  phase in U - 7.5 w/o to 12 w/o Mo alloys is a maximum for critical niobium contents. Ruthenium was more effective in delaying decomposition of  $\gamma$ , zirconium had an adverse effect whilst chromium and vanadium were reported to have little effect.

The purpose of this investigation has been to study the transformation of a uranium - 10 a/o molybdenum alloy in detail using dilatometry, metallographic techniques and hardness measurements supported by X-ray examination and to study the effect of ternary additions selected to throw light on the basic principles by which the transformation can be influenced.

Basically, a ternary addition can influence the decomposition of a solid solution in four ways:-

- A. by reducing the free energy of the solid solution it can extend its range of stability. As this will normally require large ternary additions or only be applicable where the total change in free energy required is small this probably cannot be applied to the U - Mo alloys. However small amounts of ternary addition can change the free energy of the solid solution sufficiently to alter the kinetics of transformation so that precipitation may be accelerated or retarded appreciably. This is because the activation energy which has to be supplied in forming a nucleus of precipitate or segregate of critical size is inversely proportional to the square of the free energy change.

- B. The activation energy for nucleation is proportional to the cube of the interfacial energy of the nucleus. This includes the coherency strains holding the lattice of the precipitate in register with that of the matrix and it has been shown, in aluminium copper alloys, how very small ternary additions, (0.1%), may influence markedly the nucleation of a particular phase<sup>6</sup>.
- C. The activation energy for nucleation is also inversely proportional to the square of the strain energy due to volume changes. This is not likely to be altered significantly by small ternary additions.
- D. The initial rate of precipitation usually follows a relationship of the form  $I = K \exp [ - (A + Q) / RT ]$  where the constant A is a composite activation energy for nucleation and Q the activation energy for diffusion. At low temperatures A becomes small in comparison with Q and precipitation becomes primarily, though not entirely, dependent on diffusion. Hence it would be possible to affect precipitation at temperatures below the nose of the TTT curve by altering the activation energy for diffusion.

Although D (effect on diffusion) is known to occur, little is known of the mechanism other than that certain elements may associate with vacancies thereby reducing the number available for diffusion. Many examples of the effect of trace additions of ternary elements on precipitation in aluminium alloys have been attributed to the effect on interfacial energy<sup>7</sup> and it has been possible to correlate similar effects with size factor of the ternary element added to magnesium-lead alloys<sup>8</sup>. However it is not possible yet to use this hypothesis to guide the choice of ternary addition for uranium-base alloys.

Nevertheless it is possible to estimate qualitatively the way in which ternary additions might modify the free energy of the  $\gamma$  phase as follows. If the interaction energies between unlike atoms,  $V_{AB}$ , is equal to the mean of the interaction energies of like atoms,  $\frac{V_{AA} + V_{BB}}{2}$  i.e. the internal energy,  $E_0$  is proportional to the amount of each component the free energy / composition curve shows a minimum and is convex to the composition axis and a complete range of solid solutions is obtained. (Fig.1a) If  $V_{AB} < \frac{V_{AA} + V_{BB}}{2}$  i.e.  $\Delta V$  is negative, a more pronounced minimum is obtained (Fig.1(c)) and if  $\Delta V$  is negative and large superlattice formation within the solid solution may occur and in the extreme, stable compounds may form and

reduce mutual solubility in the primary solid solutions. A negative  $\Delta V$  is usually associated with negative heats of solution in the liquid state and with high melting point compounds. If  $\Delta V$  is positive i.e.  $V_{AB} > \frac{V_{AA} + V_{BB}}{2}$ , an inflected curve is obtained part of which is concave to the composition axis and this results in phase separation and a miscibility gap (Fig.1(b)). If  $\Delta V$  is small and positive, as the temperature increases, the entropy term,  $TS$ , becomes relatively more important and at a certain temperature (given by  $\frac{KT}{Z\Delta V} = 0.5$ , where  $K$  is Boltzmann's constant and  $Z$  the co-ordination number) is so large that the maximum in the free energy curve, due to the increase in internal energy is counteracted and the curve becomes convex to the composition axis and the miscibility gap is closed. If  $\Delta V$  is large and positive this condition may not be reached below the melting point and two separate solid solutions will be obtained up to the solidus. A positive  $\Delta V$  is generally associated with a positive heat of solution in the liquid state.

The theory on which this is based assumes that the relative sizes of the atoms are the same. As the relative size factor is increased, there will be an increasing tendency to phase separation and restricted solid solubilities i.e. to decrease the stability of  $\gamma$ .

Little has been published on the thermodynamic properties of uranium alloy systems but a guide to the relative values may be obtained from a study of the phase diagrams. That for uranium-molybdenum is characteristic of a system in which  $\Delta V$  is positive and moderately large. Whilst ordered structures are usually associated with a negative internal energy ( $\Delta V$  negative), the ordered phase,  $U_2Mo$ , is not typical as the structure comprises layers of atoms, every third layer of which is composed of molybdenum atoms which is consistent with a positive  $\Delta V$ . Hence the free energy/composition curve for the  $\gamma$  U-Mo phase can be regarded as an inflected curve similar to Fig.1(b) with a maximum towards the molybdenum rich side of the diagram. The rather unfavourable size factor of - 9% for molybdenum in uranium would also contribute to the high internal energy. Hence in order to reduce the free energy of the  $\gamma$  U-Mo solid solution, the ternary addition should have a negative  $\Delta V$ , i.e. negative heat of solution, with uranium and also with molybdenum. On the other hand for an increase in free energy, to give more rapid precipitation, the ternary addition should have a positive  $\Delta V$  with uranium but a negative  $\Delta V$  with molybdenum.

It is not known how important the effect of size factor would be, or if it can be distinguished but it seems likely that for greater stability the size of the ternary atom should be such as to reduce lattice strain and vice versa.

The three additions chosen represent three different types of equilibrium diagram with uranium. Tantalum and uranium have very limited mutual solid solubility<sup>10</sup> and therefore  $\Delta V$  would be expected to be large and positive. The molybdenum-tantalum system consists of a continuous solid solution the lattice parameters of which show a slight negative deviation from Vegard's law. This suggests a  $\Delta V$  close to zero and probably negative. Hence additions of tantalum to uranium-molybdenum alloys would be expected to decrease the stability of the metastable  $\gamma$  phase. Whilst the size factor of tantalum with respect to uranium is about -5%,<sup>\*</sup> the stabilising effect of this change is unlikely to compensate such a marked effect as that of the large positive  $\Delta V$ .

The second addition, niobium, also has a phase diagram indicating a positive heat of solution but as the miscibility gap is closed at  $\sim 900^{\circ}\text{C}$ <sup>10</sup> it suggests that  $\Delta V$  though positive is small. The molybdenum-niobium system forms a continuous range of solid solution with lattice parameters showing a slight negative deviation from Vegard's law<sup>11</sup>. This suggests a  $\Delta V$  close to zero and probably negative. Hence additions of niobium would not be expected to increase the stability of gamma but the decrease in stability would be less marked than with tantalum additions. The size factor of niobium with respect to uranium is about -5% being similar to that of tantalum, and this would be expected to increase its stabilising effect. Therefore the effect of niobium is of particular interest and it is possible that the stabilising effect of size factor and opposite effect on internal energy may either balance or vary with composition as the work of Van Thyne and McPherson<sup>4</sup> and Storhok et al<sup>5</sup> has indicated.

---

<sup>\*</sup> This is based on the interatomic distances in the pure metal and to that extent is open to question.

At the other extreme, rhenium forms a very stable high melting point compound  $URe_2$  of C 14 (Mg Zn<sub>2</sub> type) Laves phase structure (at elevated temperatures).<sup>12</sup> This type of structure is a geometrically close packed solutions and shows great stability in metastable solid structure e.g. Mg Zn<sub>2</sub> in Al-Mg-Zn alloys. From this it is fairly certain that in uranium rhenium alloys,

$\Delta V$  is strongly negative. The mutual solubilities of molybdenum and rhenium in each other are fairly high (42 a/o Re and 14 a/o Mo) and the terminal solid solutions are separated by two high melting point compounds. Again this is strong evidence that  $\Delta V$  is negative and fairly large. Together these factors indicate that rhenium should increase the stability of the ternary  $\gamma$  phase. The size factor of -11% is fairly close to that of molybdenum in uranium.

The important factor in determining the stability of  $\gamma$  phase is the difference in free energy between the  $\gamma$  phase and its decomposition products and so far the effect of the third element on the latter has not been considered. The phases formed are  $\alpha$  and a Mo - enriched  $\gamma$ . The free energy of enriched  $\gamma$  is probably affected in the same way as the homogeneous  $\gamma$  stable at the higher temperature and it is unlikely that the free energy of  $\alpha$  will be altered much as the solubilities of all the solutes in  $\alpha$  are small. Hence the difference in free energy between the metastable  $\gamma$  and the equilibrium phase mixture will be decreased by an addition which lowers the free energy of metastable  $\gamma$  and vice versa.

Therefore the effect has been compared of additions of 1 a/o tantalum, niobium and rhenium to a U-10 a/o molybdenum alloy to illustrate three possible effects on transformation rates.

II. EXPERIMENTAL.

(a) Materials and Alloy Preparation.

The details of materials are given in Table 1.

TABLE 1.

<u>Metal.</u>	<u>Remarks.</u>
Uranium	Ca reduced rolled bar. Main impurity C ( $\sim$ 300 ppm)
Molybdenum	H.P. rod. Main impurity Fe (40 ppm)
Niobium	Sheet off-cuts. Hardness on re-melting, 90-150 DPN
Rhenium	Pre-melted potassium reduced sponge.
Tantalum	Sheet off cuts.

Alloys of analysed compositions shown in table II were melted in an arc furnace with a water cooled copper hearth in an atmosphere of argon at 15 cm pressure.

TABLE II

Alloy No:	Use	Composition (a/o)					Homogenising treatment.
		U (by diff)	Mo	Nb	Ta	Re	
Mo 1	Dilatometry	89.40	10.60	-	-	-	15 days $1030^{\circ}\text{C}$
Mo 2	Metallography	89.47	10.53	-	-	-	7 days $1020^{\circ}\text{C}$
Nb 1	Dilatometry	88.87	10.05	1.08	-	-	14 days $1000^{\circ}\text{C}$
Nb 2	Metallography	88.67	10.31	1.02	-	-	7 days $1020^{\circ}\text{C}$
Ta 1	Dilatometry	89.11	10.04	-	0.85	-	14 days $1000^{\circ}\text{C}$
Ta 2	Metallography	89.48	9.50	-	1.02	-	7 days $1020^{\circ}\text{C}$
Re 1	Dilatometry	89.03	9.98	-	-	0.99	14 days $1000^{\circ}\text{C}$
Re 2	Metallography	89.50	9.70	-	-	0.80	7 days $1020^{\circ}\text{C}$

After homogenising for the times given above the elongated buttons of each alloy were hot-rolled to 0.040" thick sheet using intermediate heating in a eutectic lithium-potassium carbonate bath at 775°C. Specimens for both dilatometry and metallography were cut to shape by a precision abrasive wheel.

(b) Dilatometry.

The transformation characteristics of the binary U-Mo alloy and ternary alloys containing Nb, Ta or Re were determined using the recording dilatometer described in F.R.I. Report R126/3.

The specimens in the form of sheets  $1\frac{1}{4}$ " x  $\frac{1}{4}$ " x 0.04" were first heated in the  $\gamma$  phase region for  $\frac{1}{2}$  hour at 900°C then quenched directly to the transformation temperature and allowed to transform to completion. The time taken to cool from 900°C to within 5°C of the transformation temperature was 1- $1\frac{1}{2}$  mins. A complete record of expansion and contraction was obtained for each run. The mean of several satisfactory transformation curves was taken for each temperature.

(c) Metallographic Examination.

Specimens  $1/16$ " x  $\frac{1}{4}$ " x 0.04" were sealed in small evacuated silica capsules to avoid attack by the heating medium and to simulate conditions in the dilatometer. These were then heated for 15 mins at 900°C in a lead bath and quenched directly to a second lead bath at the transformation temperature. The time to attain the temperature of the second bath was less than 30 seconds. After holding for appropriate times the specimens were quenched into water. After mounting in a cold setting resin microsections were prepared in the usual manner finishing by diamond dust and "attack polishing" using  $\gamma$  alumina with a solution of 50 gms  $\text{CrO}_3$  and 10 ml  $\text{HNO}_3$  in 100 ml water. Where appropriate, specimens were lightly electropolished in a solution of 50 ml phosphoric acid, 100 ml. sulphuric acid and 100 ml water. Specimens were examined under polarised light, after etching in 10% oxalic acid in water and after tarnishing for several days in air. All hardness measurements were made on the metallographic specimens using a Vickers diamond indenter at 5Kg load.

### III. RESULTS.

#### A. Dilatometric Measurements.

The isothermal transformation diagrams obtained from the dilatometric measurements are shown individually in Figs. 2-5 and compared in Fig. 6.

The binary alloy (Fig. 2) gave a normal C curve with rather a flat nose at about 525°C. The lines for 20, 40, 60 and 80% transformation showed slight irregularities with temperature but could not be interpreted as evidence of a double nose. The C curves for all the ternary alloys were double nosed, the upper one being at about 525-550°C and the lower at 450-475°C. These varied in prominence, being relatively weak in the alloy with rhenium and more pronounced in the alloys with niobium and tantalum. The nearest corresponding feature in the binary alloys was the rather flat nose at 500-550°C which might possibly be interpreted as two almost overlapping noses. The relative prominence of these features are compared in Table III in which the comparable incubation times are given for binary alloy at 525°C, 500°C and 475°C.

TABLE III.  
Comparison of Incubation Times to Start of Transformation.

Alloy	Upper Nose		Lower Nose		Maximum Incubation time between noses	
	Time (min)	Temp °C	Time (min)	Temp °C	Time (min)	Temp °C
U-Mo-Ta	3.3	530	6.0	450	8.0	485
U-Mo-Nb	3.4	535	6.0	475	7.6	500
U-Mo-Re	11.0	535	14.0	475	16.0	500
U-Mo *	4.6	525	7.7	475	5.0	500

\*For the binary alloy, the incubation times are given for temperatures corresponding to those of the noses and maximum incubation time in the ternary alloys.

Otherwise the main features were the acceleration of the whole transformation by niobium and tantalum at all temperatures except those close to 500°C and the delay in transformation by rhenium.

In all experiments the total contraction on quenching, transforming, and cooling to room temperature was the same, about 0.014", as the total expansion on reheating to 900°C for the next experiment within an experimental error of 13%.

#### B. Analysis of Dilatometric Transformation Curves.

Numerous analyses of rates of transformation at constant temperature have been made and these have been discussed at length in the literature, e.g. see 13. Several of these have been examined and the dilatometric transformation curves show most satisfactory correlation when the rate of transformation is set as

$$\frac{da}{dt'} = K_1 (1 - a)^{m-1}$$

where  $t'$  is the growth time,  $(1 - a)$  allows for interference between particles and depleted areas and  $K_1$  and  $m$  are constants.

Integration gave

$$\begin{aligned} \ln (1 - a) &= - \frac{K_1}{m} t'^m \\ \text{or } a &= 1 - \exp \left[ - \frac{K_1}{m} t'^m \right] \\ &= 1 - \exp \left[ - \left( \frac{t'}{\gamma} \right)^m \right] \text{ where } \frac{K_1}{m} = \gamma^{-m} \end{aligned}$$

and  $\gamma$  is a constant with dimensions of time.

For plotting graphically this is more conveniently expressed as

$$\frac{1}{1 - a} = \exp \left[ \left( \frac{t'}{\gamma} \right)^m \right]$$

$$\text{taking logs } \ln \ln \left( \frac{1}{1 - a} \right) = m \ln t' + n \ln \gamma$$

From the slope of the plot of  $\ln \ln \frac{1}{1-a}$  and  $\ln t'$  can be determined  $m$  which is usually found to be 1.5 to 2.5 depending on the shape of the nucleus of precipitates. The transformation curves were plotted in this way and gave straight lines over the range 20% to about 80% transformation. Values for the slope are given below.

TABLE IV.

Values of  $m$  taken from plots of transformation

curves according to the equation  $a = 1 - \exp \left[ - \left( \frac{t'}{\gamma} \right)^m \right]$

Temp. °C	ALLOY			
	U-Mo	U-Mo-Ta	U-Mo-Nb	U-Mo-Re
565	2.0	-	-	1.8
550	2.2	2.0	1.6	2.1
525	2.5	1.6	2.2	2.0
500	2.1	1.4	1.8	1.7
475	1.7	1.8	1.8	1.8
450	1.7	1.4	1.7	1.8
400	1.0	1.5	1.3	1.9
Mean	1.9	1.6	1.7	1.9

Only in the rhenium alloy was the agreement at all satisfactory and the mean value for  $m$  was approximately 2. Values about 2 were obtained at the higher temperatures in the binary and over the range 525-475°C in the niobium alloy. The reason for the variation in the other alloys is probably that some precipitation started during cooling past the nose, particularly in the alloy with tantalum and this has introduced an error in the estimation of the start of the transformation. The results of the alloy with rhenium are the only ones on which complete reliance can be placed.

C. Metallographic Examination.

Hardness and metallographic examinations were carried out on the same specimens. Where desirable the structure of the specimen was determined by a glancing angle X-ray technique.

On transforming at each temperature, the hardness, measured after quenching to room temperature, remained constant for a short incubation period and then increased in proportion to the logarithm of time and reached a maximum value beyond which the hardness remained constant. It is probable that had the heat-treatments been continued a slight fall would have been experienced. Typical curves for the U-Mo-Ta alloy are shown in Fig.7 and all are summarised in Fig.8. The hardness as quenched from 900°C and the hardness before transformation started at each temperature were virtually the same:- 160 DPN for the binary alloy and the one with Ta; 145 DPN for that with Nb and 120 DPN for that with Re. With the exception of the tantalum alloy, the difference in as quenched hardness is proportional to the analysed molybdenum content.

In the binary and the rhenium alloy the maximum hardness increased with decreasing transformation temperature to the highest values of 530-550 DPN at 450°C. The rhenium alloy was some 40 points harder at 550°C but the difference decreased to 20 DPN at 475°C and was reversed at 450°C. The hardnesses at 450°C and 475°C were higher than would be expected from extrapolation of the values at 550°-500°C. The niobium and tantalum alloys had similar hardnesses to the binary over the range 550-500°C but had much lower hardnesses over the range 450-475°C. Those of the tantalum alloy lay on a straight line from 450°C-550°C but there was a discontinuity in the curve for the niobium alloy at 475°C.

The hardness changes can be correlated with metallographic observations. These are summarised in Figs. 9-12 and also plotted for comparison are the TTT curves taken from the incubation time and time to maximum hardness, and from the dilatometric studies.

In the binary alloy, the first change detected at all temperatures was the formation of a grain boundary precipitate, which in larger quantities in specimens transformed at 500-550°C, could be resolved as a lamellar eutectoid-like structure, (Fig.13). At lower temperatures, it was not resolvable optically but from the similar general appearance it is inferred that the lamellar structure is formed at all temperatures. On quenching to room temperature, the matrix transformed by shear to a slightly lenticular banded structure of hardness  $\sim$  160 DPN identified by X-rays as  $\alpha''$  (Fig.14). On isothermal treatment of samples at all temperatures, the lamellar structure grew from nuclei at the grain boundaries at the expense of  $\gamma$  ( $\alpha''$  at room temperature). The hardness rise started some 2-5 minutes after the first appearance of the lamellar structure, and the TTT curves for the start of precipitation and hardening both formed continuous and parallel curves over the range of temperature 550°C-450°C with no sign of any discontinuity. Hence it can be inferred that over this temperature range the phase from which the lamellar structure precipitates is the same, that is, metastable  $\gamma$ , and that the shear transformation to  $\alpha''$  must occur at below 450°C.

At 500-550°C the growth of the lamellar structure continued until all  $\gamma$  had been consumed and no  $\alpha''$  was found on quenching to room temperature. Over this range of temperature (500-550°C) the TTT curves derived from hardness and metallography agreed reasonably well, the maximum hardness corresponding to the complete decomposition of  $\gamma$  to the lamellar structure. Dilatometric measurements gave rather later TTT curves but it is clear from the metallographic work that some precipitation of the lamellar structure probably occurred during cooling to the transformation temperature and this would affect the detection of the start of the transformation.

At 475°C and 450°C, after 15-22 minutes, and 32-48 minutes respectively, the lamellar structure ceased to grow and the matrix ceased to transform to  $\alpha''$  on quenching. The matrix was faintly anisotropic and had an irresolvable internal structure which might be very fine precipitation or an optically active variation in structure (Fig.15). X-ray examination indicated that this was retained  $\gamma$ . The pattern was rather

diffuse but was identified as one of the slightly tetragonal modifications. No further growth of the lamellar structure was observed within the limits of the treatments (4 hours) and the maximum hardness was attained at logarithmically equal times after the retention of  $\gamma$  was first observed. It is quite probable that longer heat-treatment times would have led to either further growth of the lamellar structure or precipitation of  $\alpha$  within the retained  $\gamma$ .

The addition of 1 a/o tantalum accelerated the whole transformation, (Fig.10), and caused much finer precipitation. At the minimum time examined, 1 minute after quenching at 500-525°C and 2 minutes at 450-475°C, precipitation at grain boundaries had started. Fortunately it was possible to detect the start of the hardness increase and, as, in the early stages the hardness and metallographic changes could be correlated in the binary alloy, it is reasonable to suppose that this is true for the ternary. The whole transformation was completed rapidly and, at all temperatures,  $\gamma$  ( $\alpha''$  on quenching to room temperature) transformed isothermally completely to the lamellar structure. The time for the rise to maximum hardness agreed well with the completion of the metallographic change. The end of the transformation at 475°C and 450°C occurred after 7-10 mins and 21-32 mins, less than the time required for the development of the mechanism by which  $\gamma$  was retained at 475°C and 450°C in the binary alloy. The transformation detected dilatometrically started later and finished much later than that examined metallographically.

In the niobium-bearing alloy, all samples showed signs of the grain boundary precipitate at the shortest times examined and no satisfactory curve for the start of the transformation can be given. However, the precipitate grew only slowly and the start of the hardness increase occurred at roughly the same time as in the binary alloy, and was completed a little more rapidly. Except at 500°C the start of the transformation as determined dilatometrically was close to that obtained from hardness measurements. The transformation followed the same course as in the binary alloy with the exception that in one sample at 500°C (15 minutes) the stabilised  $\gamma$  structure was

obtained but was later absorbed by growth of the lamella eutectoid. At 475°C and 450°C, the stabilised  $\gamma$  structure appeared at the same time as in the binary alloy, but the lamellar complex continued to grow and at 475°C completely absorbed the  $\gamma$  phase in about 1½ hours.

As in the binary alloy the hardness change reached its maximum shortly after the absorption of all the original  $\gamma$  phase at the higher temperatures and at logarithmically equal times after the stabilisation of  $\gamma$  at the lower temperatures. The end of the dilatometric change occurred somewhat later than the metallographic change but the form of the TTT curve was similar to that of metallographic and hardness changes at 500-550°C.

The effect of rhenium was of special interest in that it delayed appreciably the decomposition of the  $\gamma$  phase, e.g. the shortest time for precipitation to start at the grain boundaries was 2 minutes at 500°C instead of <1 minute in the binary and it took 12 minutes at 450°C instead of 3 minutes in the binary. The shortest time to maximum hardness was 15 minutes (525°C) in the binary but 70 minutes (525°0) in the rhenium alloy.

The course of transformation was, however, the same as in the binary with the following exceptions. The growth of the lamellar complex was slower and at 500°C after 70 minutes, (a time at which the transformation was complete in the binary),  $\gamma$  was stabilised and no longer transformed to  $\alpha''$  on quenching. At 475°C  $\gamma$  was stabilised some 20 minutes later than in the binary alloy, and at 450°C in the same time as in the binary. The time required to develop maximum hardness did not bear the same relationship to the time to stabilise  $\gamma$  as in the binary; progressively longer times were needed as the temperature fell. The TTT curves determined dilatometrically agreed fairly well with those determined from the hardness tests except that the latter gave no support for the slight double nose form of the former.

#### IV. DISCUSSION.

This examination has confirmed results of earlier workers in that the mechanism of the decomposition of the  $\gamma$  phase in U-10 a/o Mo is by the growth of a lamellar structure comprising plates of  $\alpha$  in a matrix of enriched  $\gamma$ . The latter, given sufficient time, would no doubt have transformed to the ordered  $\gamma'$  or  $\delta$  ( $U_2Mo$ ). At  $500^{\circ}$ - $550^{\circ}C$  the lamellar structure grew at the expense of  $\gamma$  which transformed by shear to  $\alpha''$  on quenching until, ultimately, complete formation of  $\alpha$  + enriched  $\gamma$  had occurred and no  $\alpha''$  could be detected. However, at  $450$ - $475^{\circ}C$ , this type of transformation was interrupted suddenly by the apparent retention of the  $\gamma$  phase after a certain time. This was not a gradual process and at no time were the  $\alpha''$  and  $\gamma$  phases present together. Subsequently no further growth of the lamellar complex was detected. The maximum hardness attained was higher than would have been expected from the transformation at  $500$ - $550^{\circ}C$ .

There are three possible reasons for the retention of  $\gamma$ :-

- (i) during growth of the lamellar eutectoid, the residual  $\gamma$  might be progressively enriched until such a composition is attained that a variant of  $\gamma$  is retained. This may be discarded for two reasons. In the first place this should occur quite readily at  $500$ - $550^{\circ}C$  also, and secondly a composition gradient would be established so that both  $\alpha''$  and retained  $\gamma$  would be expected in the same specimen and that the transition from one to the other would occur gradually with time. This was not observed.
- (ii) a very fine precipitate or submicroscopic aggregation of U or Mo atoms akin to G.P. zones in aluminium alloys might have formed and prevented the shearing necessary to form  $\alpha''$  on quenching. This is feasible and might explain the unresolved structure in Fig.15 and the higher maximum hardness but not necessarily the complete inhibition of the lamellar structure.

(iii) The first stage of ordering of  $\gamma$  to  $\gamma'$  or  $U_2Mo$  might have started and prevented the transformation to  $\alpha''$  by shear. This would account for the higher hardness and also for the inhibition of further precipitation of  $\alpha$  as it has been established<sup>9</sup> that  $\alpha$  precipitation from the ordered  $\gamma$  is much slower than from the disordered  $\gamma$ . The X-ray evidence of a diffuse  $\gamma$  pattern does not contradict this. Whilst it is true that no extra diffractions were observed, it is possible that the first stage of ordering could be the development of tetragonality and extra diffractions would not be observed until later.

The ternary addition of tantalum increased nucleation of  $\alpha$  and accelerated the whole decomposition. At all temperatures  $\gamma$  decomposed to  $\alpha +$  enriched  $\gamma$  completely and no retained  $\gamma$  was detected. At 450°C and 475°C the transformation was complete before the time required for  $\gamma$  retention in the binary alloy had elapsed. On the other hand, whilst niobium accelerated nucleation slightly, the rate of decomposition was about the same as in the binary. At 450° and 475°C,  $\gamma$  was retained on quenching after times comparable to those in the binary. Of particular interest is the observation that although niobium did not interfere with the mechanism by which untransformed  $\gamma$  was retained on quenching, the growth of the lamellar  $\alpha + \gamma$  structure was not inhibited, with the result that at 475°C complete decomposition of  $\gamma$  occurred and was almost complete at 450°C. The only tentative explanation of the retention of  $\gamma$  which accounts for the inhibition of  $\alpha$  precipitation is that the retention of  $\gamma$  is a consequence of the early stages of the process culminating in ordering of the  $\gamma$ . It is known that niobium appreciably reduces the rate of formation of the ordered phase  $\delta$  in alloy of U-25 to 33 a/o Mo and that complete precipitation of  $\alpha$  occurs at 500°C and 400°C before ordering takes place with as little as 0.5% niobium present<sup>14</sup>.

Hence the available evidence suggests that whilst niobium delays the completion of the formation of the ordered structure ( $\gamma'$ ,  $\delta$  or  $U_2Mo$ ), it does not stop the first stages of

ordering of  $\gamma$  which lead to the retention of a distorted, probably slightly tetragonal,  $\gamma$ . However the presence of niobium alters the manner in which the first stage takes place so that a precipitation on the form of the lamellar eutectoid is not prevented in any way. It appears likely that the ordering of  $\gamma$  is a two stage process, firstly the development of tetragonality which is not affected by niobium and the ordering of U and Mo atoms which is inhibited by niobium. Clearly further work is required on this topic.

Rhenium delayed nucleation of  $\alpha$  and reduced the whole process by a factor of 2 - 5 depending on temperature. By reducing the rate of decomposition of  $\gamma$ , rhenium allowed more time for the  $\gamma$  stabilisation mechanism to operate with the result that stabilised  $\gamma$  was obtained at 500°C as well as 450°C and 475°C. The times for the development of stabilised  $\gamma$  at 450°C and 475°C were about the same or a little longer than in the binary. This suggests the important technological possibility that by the optimum addition of rhenium and/or other similar elements it might be possible to delay or reduce a precipitation until the reaction which stabilizes  $\gamma$  starts.

These results are in general agreement with the conclusions reached in the introduction namely that

- (a) tantalum would markedly accelerate the decomposition of  $\gamma$  because it would be expected to increase the free energy of  $\gamma$  relative to that of  $\alpha$ .
- (b) niobium would probably have the same effect but would be less marked and that its effect might well vary with temperature and composition. In fact it was found that niobium reduced the incubation time but that thereafter the rate of transformation was little faster than that of the binary i.e. the net effect on the stability of the  $\gamma$  phase was small.
- (c) rhenium would increase the stability of the  $\gamma$  phase by decreasing the free energy of  $\gamma$  relative to  $\alpha$ .

These findings add support to the general hypothesis that in order to increase the stability of a quenched solid solution in a system displaying positive heats of solution i.e.  $\Delta V$  positive, the ternary addition should have a negative heat of solution with the solvent ( $\Delta V$  negative, complete solid solubility or strong intermetallic compound formation) and a negative heat of solution or  $\Delta V$  with the solute. To accelerate isothermal decomposition of the quenched metastable solid solution, the ternary addition

should have a positive heat of solution with the solvent ( $\Delta V$  positive, strong miscibility gap preferably extending through the solidus and no intermetallic compound formation) and a negative heat of solution with the solute. This hypothesis needs further confirmation but suggests the most useful additions to be made for either effect.

Of particular importance is the further investigation of the relative importance of size factor on changes in internal energy. For instance it appeared to be of little importance in the case of tantalum and rhenium but might have been almost of equal importance in the alloy with niobium. However this is of importance as it is possible that additions of critical size factors may in fact assist or inhibit nucleation by altering the interfacial energies as has been observed in magnesium-base alloys.<sup>8</sup> It is possible that for U - Mo alloys a size factor of -5% with respect to uranium may assist nucleation. For example the lamellar structure was much finer in the alloy with tantalum.

In the alloys which decomposed fully to eutectoid (ternaries with Ta and Nb) the maximum hardness was roughly inversely proportional to temperature. In those in which  $\gamma$  was retained, (binary and ternary with Re) the hardness was higher than in those in which  $\gamma$  decomposed fully i.e. the hardness of retained  $\gamma$  is greater than that of the  $\alpha +$  enriched  $\gamma$  complex.

From the dilatometric measurements, the transformation followed the equation  $a = 1 - \exp [-(\frac{t}{T})^m]$  where  $m$  was approximately 2. According to Zener<sup>14</sup> this would be expected from a reaction which involved precipitation in the form of cylinders whereas the probable form of precipitate in this case was plate-like. This would require a constant  $m$  of  $\sim 2.5$ . It is probable that the conditions of growth in this alloy are not comparable with those for which this constant was derived.

The main value of the dilatometric technique was the speed with which the transformation curves were obtained, the ability to repeat these to check reproducibility of the transformation and the fact that the same specimen could be used repeatedly. In practice it is necessary to ensure that the dilatometric technique is measuring the same transformation as is being studied by other techniques. In the U - Mo system, this was so and in general it agreed well with the results of more tedious metallographic and hardness examinations. However there were differences in detail in that the dilatometric results gave evidence of a double nosed curve in three of the alloys. There was no evidence of a change in

the manner of the early stages of decomposition metallographically which would account for this. It was noted that the rate of cooling in the dilatometer was such that in all but the rhenium alloy some transformation would have taken place during quenching. Nevertheless a genuine start of transformation was detected and it is probable that dilatometrically the first appearance of precipitate caused no detectable change. Alternatively at the slower cooling rate in the dilatometer fewer vacancies might have been retained and nucleation consequently be more difficult.

Since this research was undertaken Hills et al<sup>3</sup> have published an account of a complementary examination of U - Mo alloys in which they cooled specimens from 900°C to 600°C - 450°C and held the samples for varying periods. In general, the slower cooling rate which they used gave a slower transformation than in this investigation e.g. in the 10 a/o Mo alloy at 550°C a peak hardness of 390 DPN was attained in 8 - 10 hours at which an  $\alpha$  +  $\gamma$  structure was obtained compared with 35 mins in this work. At 500°C the peak occurred at 5 - 10 hours (compared with 22 minutes) the micro-structures being  $\alpha$  +  $\gamma$  with some  $\gamma'$  (detected in the Harwell work). At 450°C at 30 minutes Hills et al found lamellar  $\alpha$  +  $\gamma$  in a matrix of  $\alpha''$ . After about 8 hours a peak hardness of 570 DPN was attained (560 DPN at 2 hours in this work) and the structure comprised lamellar structure in a matrix which corresponded to retained  $\gamma$  in this work. Hence the agreement is quite good taking into account difference in rate which could have been a consequence of the rate of cooling. There is a difference in interpretation of the results at 450°C however. The existence of  $\alpha''$  before the peak at 450°C in the paper by Hills et al is interpreted as evidence that 450°C is below the  $M_s$  whilst it is clear from the more detailed examination in this report that this is unlikely to be so.

Hardening in U - 10% Mo did not start before visible precipitation of  $\alpha$  +  $\gamma$  was observed and was complete when the eutectoid formation was complete. In this it differs from the U - 10 a/o Ti alloy in which hardening occurred before any precipitate was resolvable optically. The appearance of the eutectoid at grain boundaries was associated with overageing and softening in the U-10 a/o Ti alloy.

R E F E R E N C E S.

1. Saller, H.A. Bauer, A.A. U.S. A.E.C. Report. B.M.I. 957. 1954.  
& Rough, F.A.
2. Van Thyne, R.J. Trans. ASM. 1957, 49, 598.  
& McPherson, D.J.
3. Hills, R.F. Harris, D.R. A.E.R.E. Report 2840. 1959.  
Hodkin, D.J. & Waldron, M.B.
4. Van Thyne, R.J. & Trans. A.S.M. 1957, 49.  
McPherson, D.J.
5. Storhok, V.W. Bauer, A.A. U.S.A.E.C. Report.  
& Dickerson, R.F. B.M.I. 1278. 1958.
6. Silcock, J.M. Heal, T.J. J. Inst. Met. 1955 - 56, 84, 23.  
& Hardy, H.K.
7. Hardy, H.K. J. Inst. Met. 1955 - 56, 84 429.
8. Brook, G.B. Unpublished Information.
9. Bostrom, W.A. 2nd Nucl. Eng. & Sci. Conf. 1957,  
& Haltemann, E.K. Paper 57 - NESC-12.
10. Rough, F.A. & Bauer, A.A. U.S.A.E.C. Report. B.M.I. 1300.
11. Hansen, M. & Anderko, K. Constitution of Alloys.  
New York, McGraw Hill. 1958.
12. Hatt, B.A. F.R.I. Report R53/19, 1955.
13. Hardy, H.K. & Heal, T.J. Progress in Metal. Physics 1954, 8, 143.
14. El-Ansari, R.S. & This Report part B(i)  
Brook, G.B.
15. Zener, C. J. Appl. Phys. 1949, 20, 950.

---

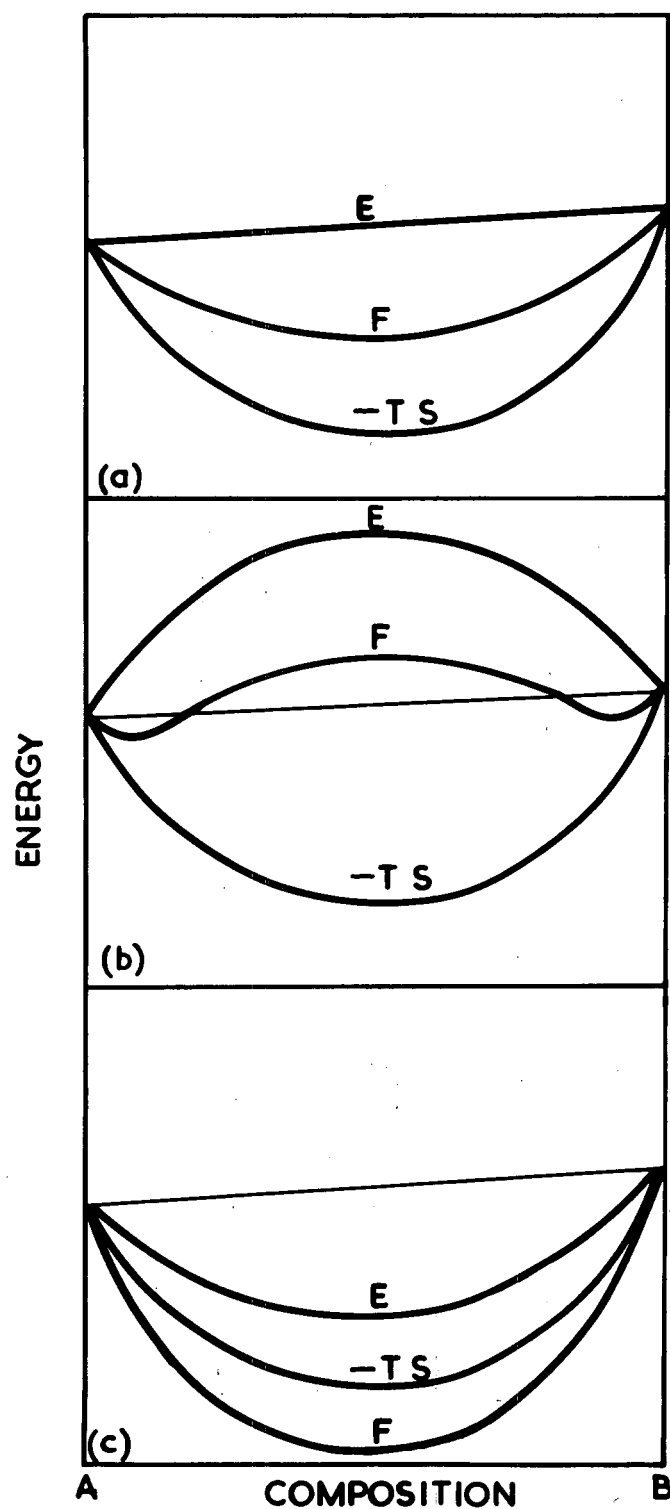


Fig. 1. Hypothetical Free Energy / Composition Curves where

$$(a) V_{AB} = \frac{V_{AA} + V_{BB}}{2}$$

$$(b) V_{AB} > \frac{V_{AA} + V_{BB}}{2}$$

$$(c) V_{AB} < \frac{V_{AA} + V_{BB}}{2}$$

668 785

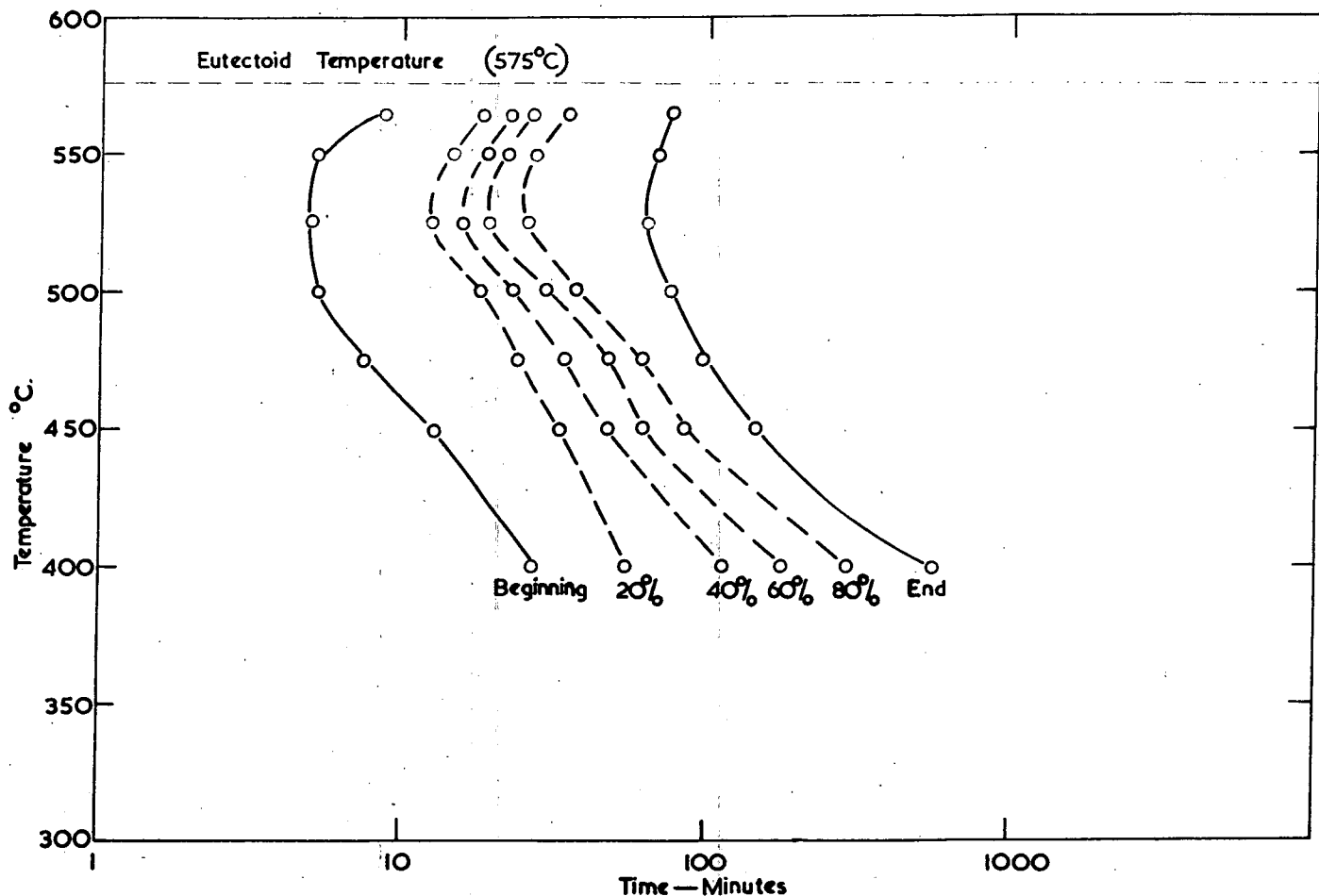


Fig.2. Isothermal Transformation diagram for U-10.6% Mo obtained dilatometrically.

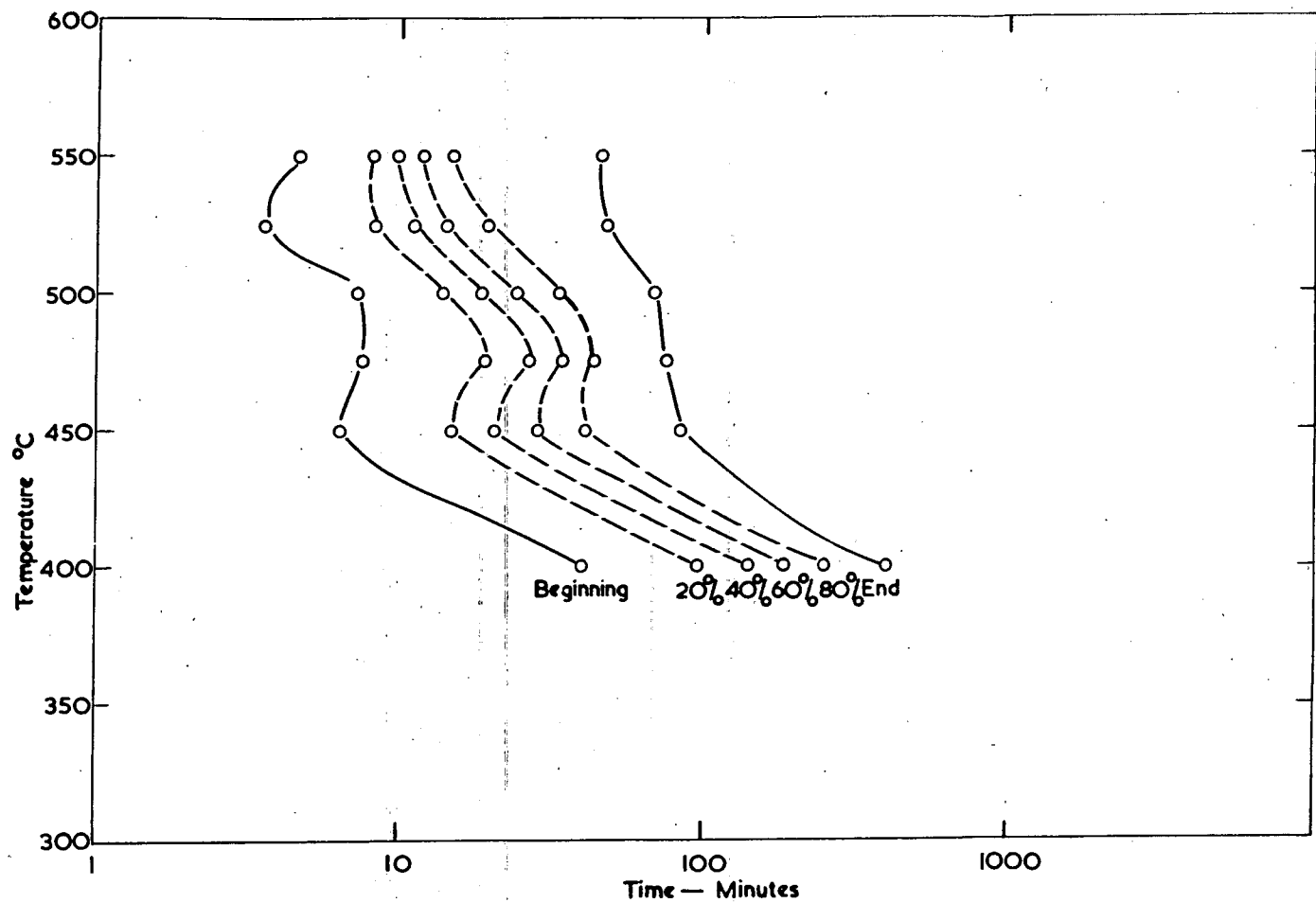


Fig. 3. Isothermal Transformation diagram for U-10.04 a/o Mo-0.85 a/o Ta obtained dilatometrically.

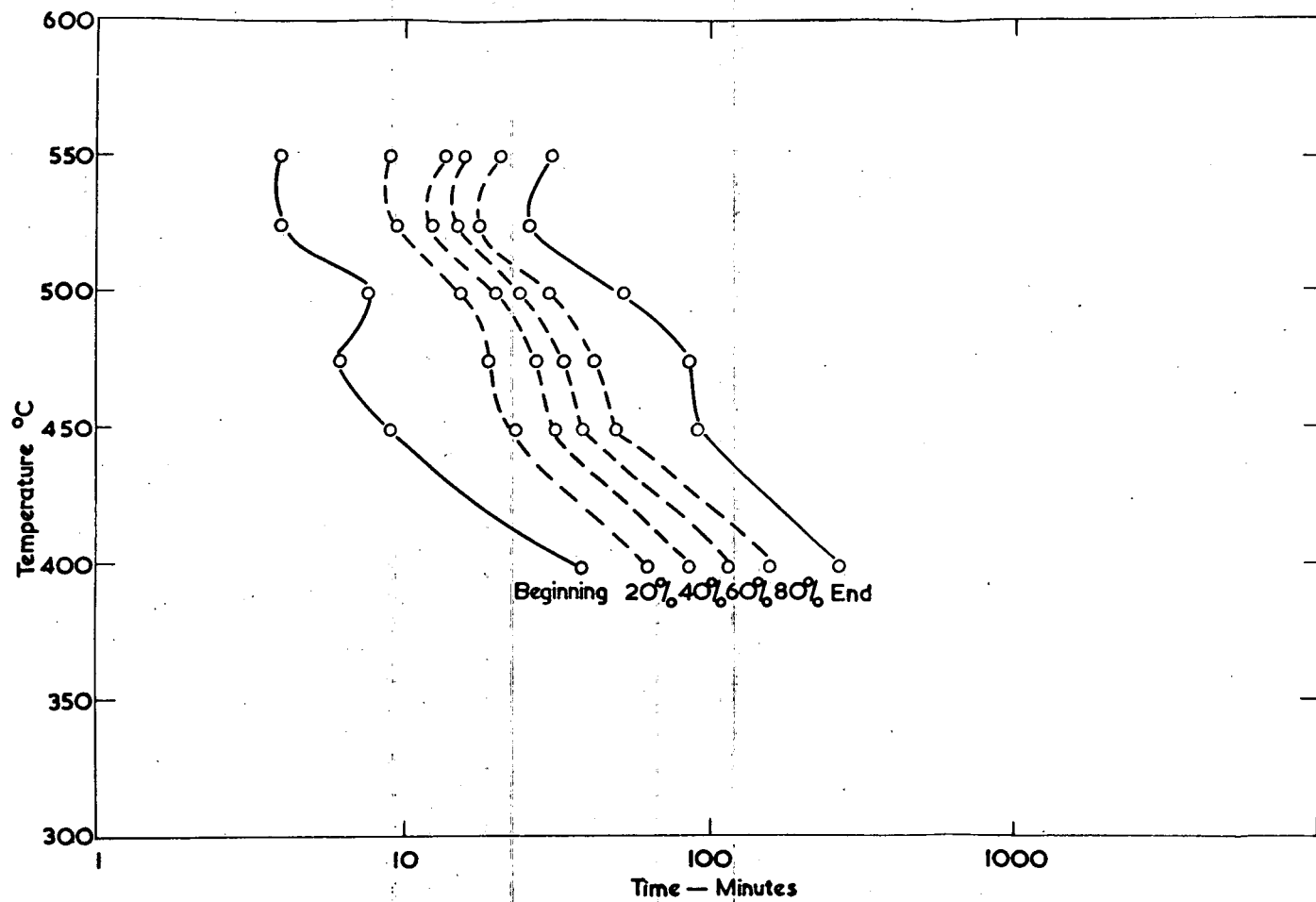


Fig. 4. Isothermal Transformation diagram for U-10.05 a/o Mo-1.08 a/o Nb obtained dilatometrically.

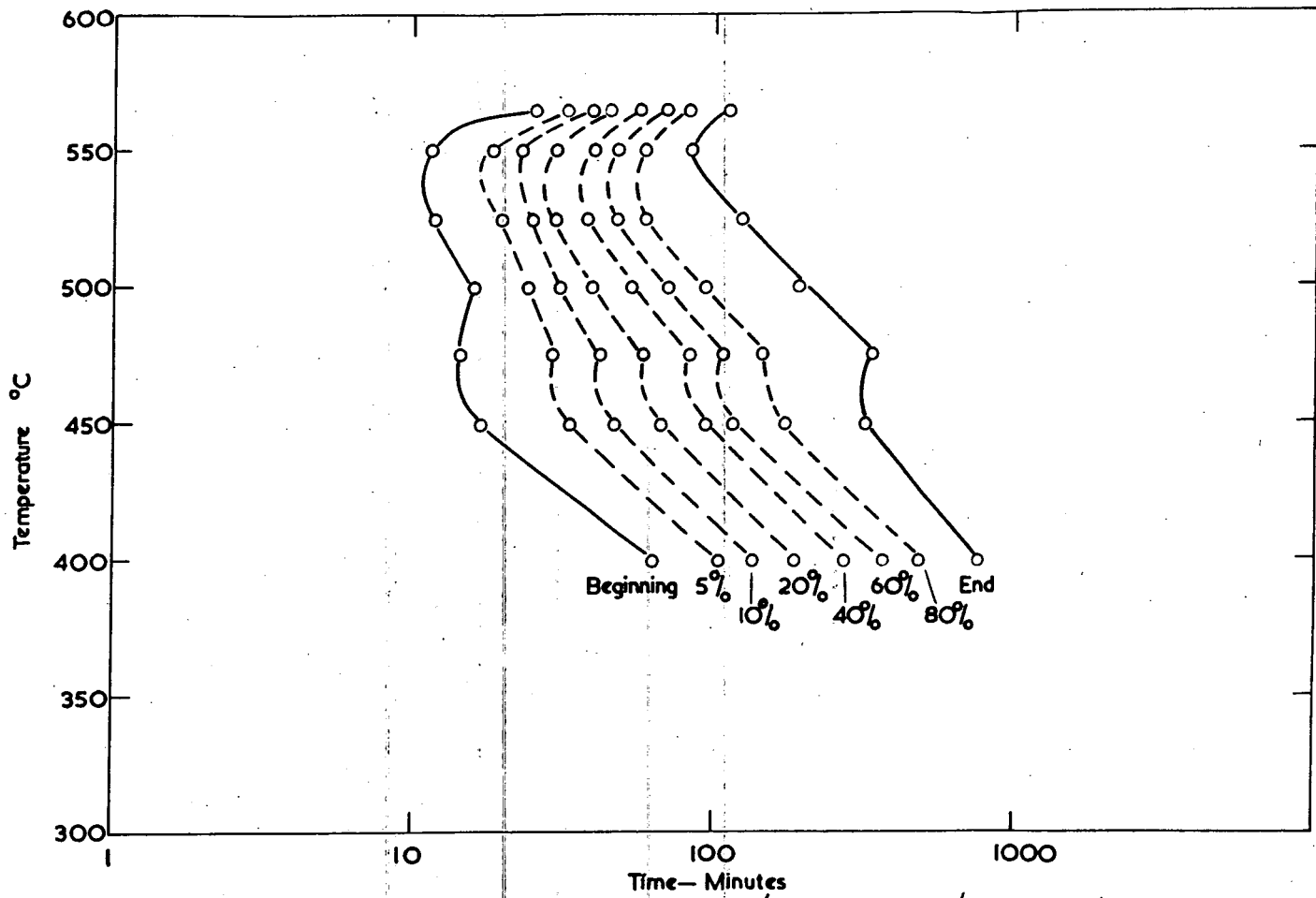


Fig. 5. Isothermal Transformation diagram for U-9.98 a/o Mo-O-995 a/o Re obtained dilatometrically.

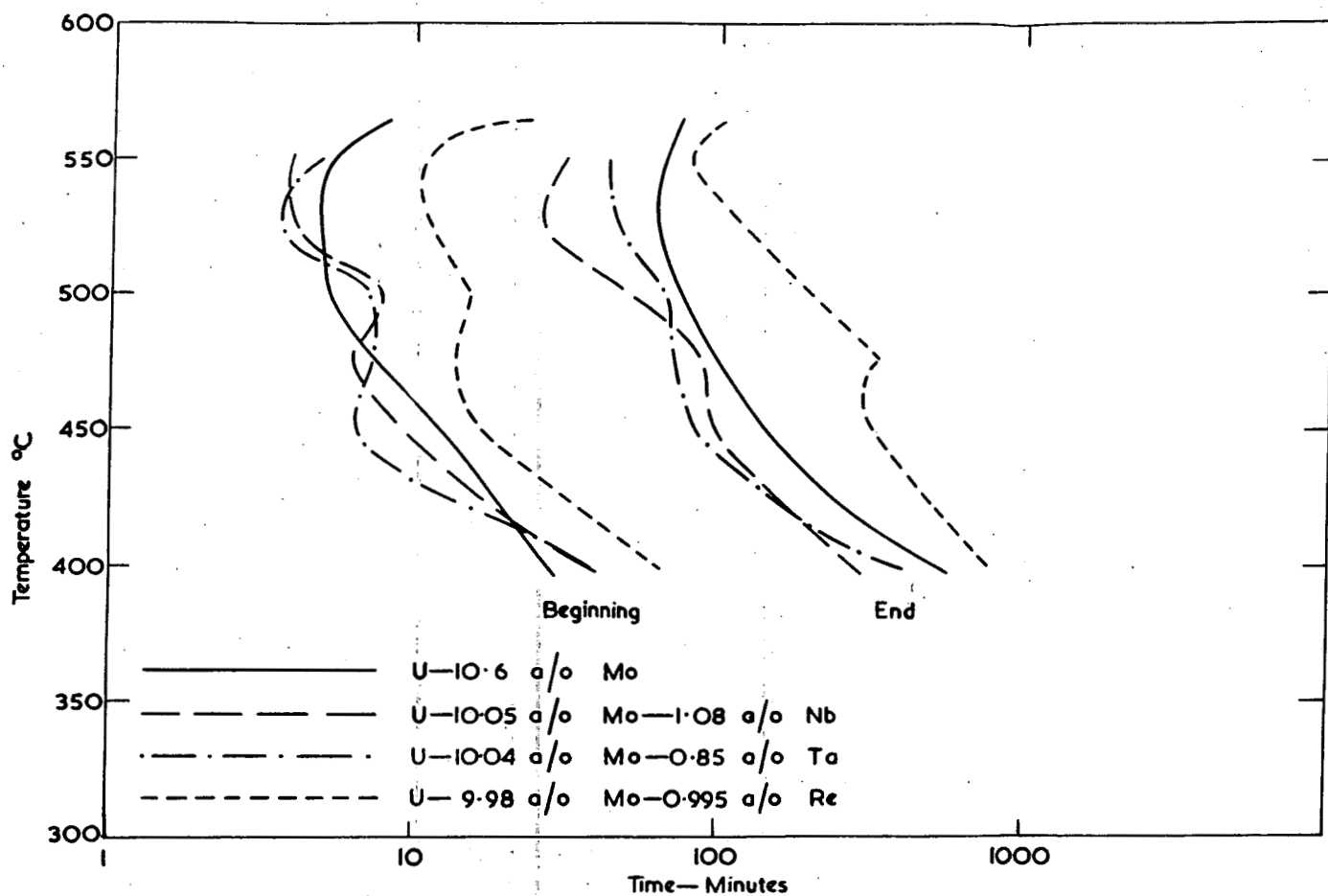


Fig. 6. Comparison of beginning and end of the binary U-Mo alloy and ternary alloys containing Nb, Ta or Re.

684 090

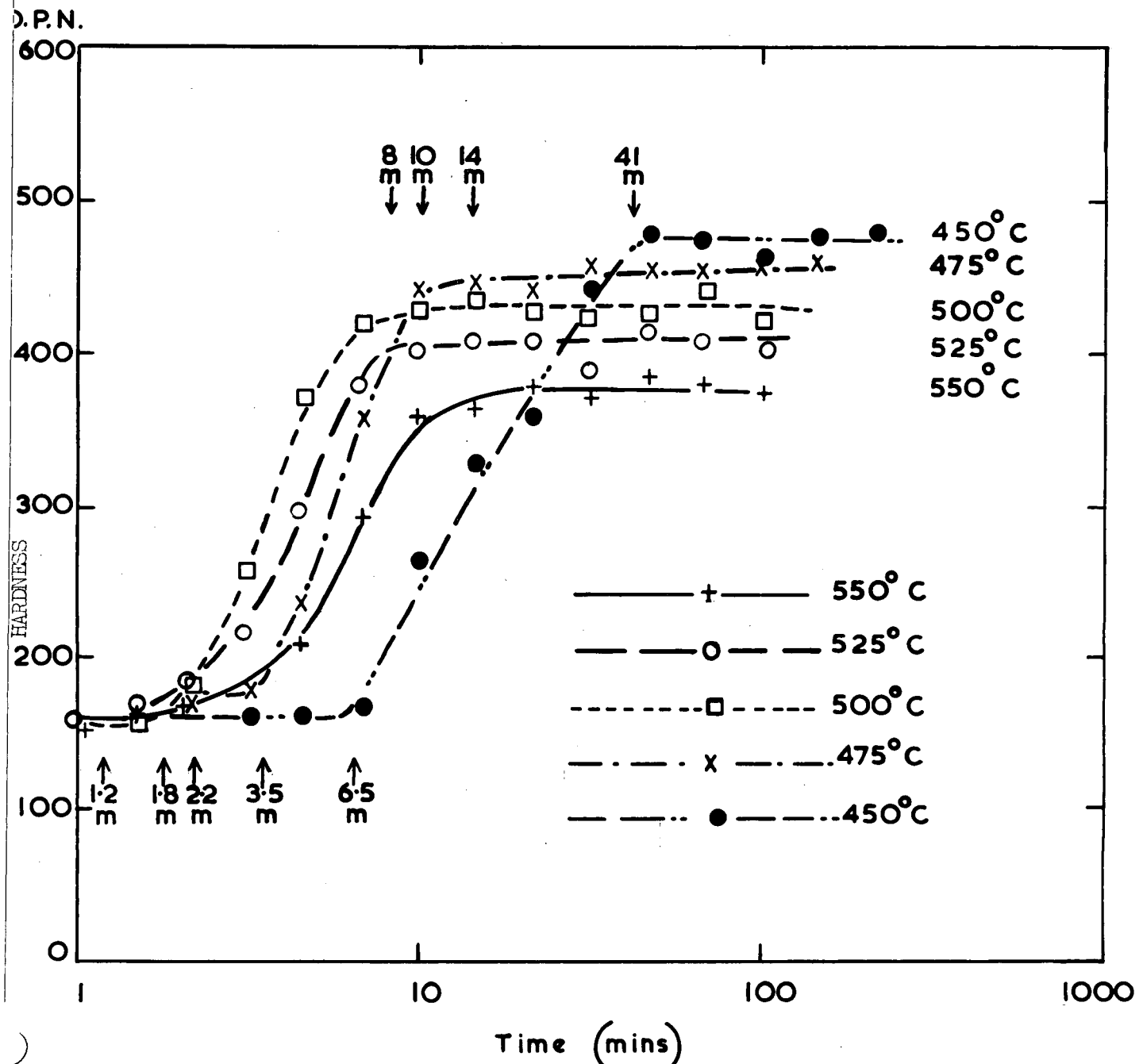


Fig. 7. Isothermal hardness ageing curves for U-Mo-Ta alloy quenched from 900°C to 450°C - 550°C

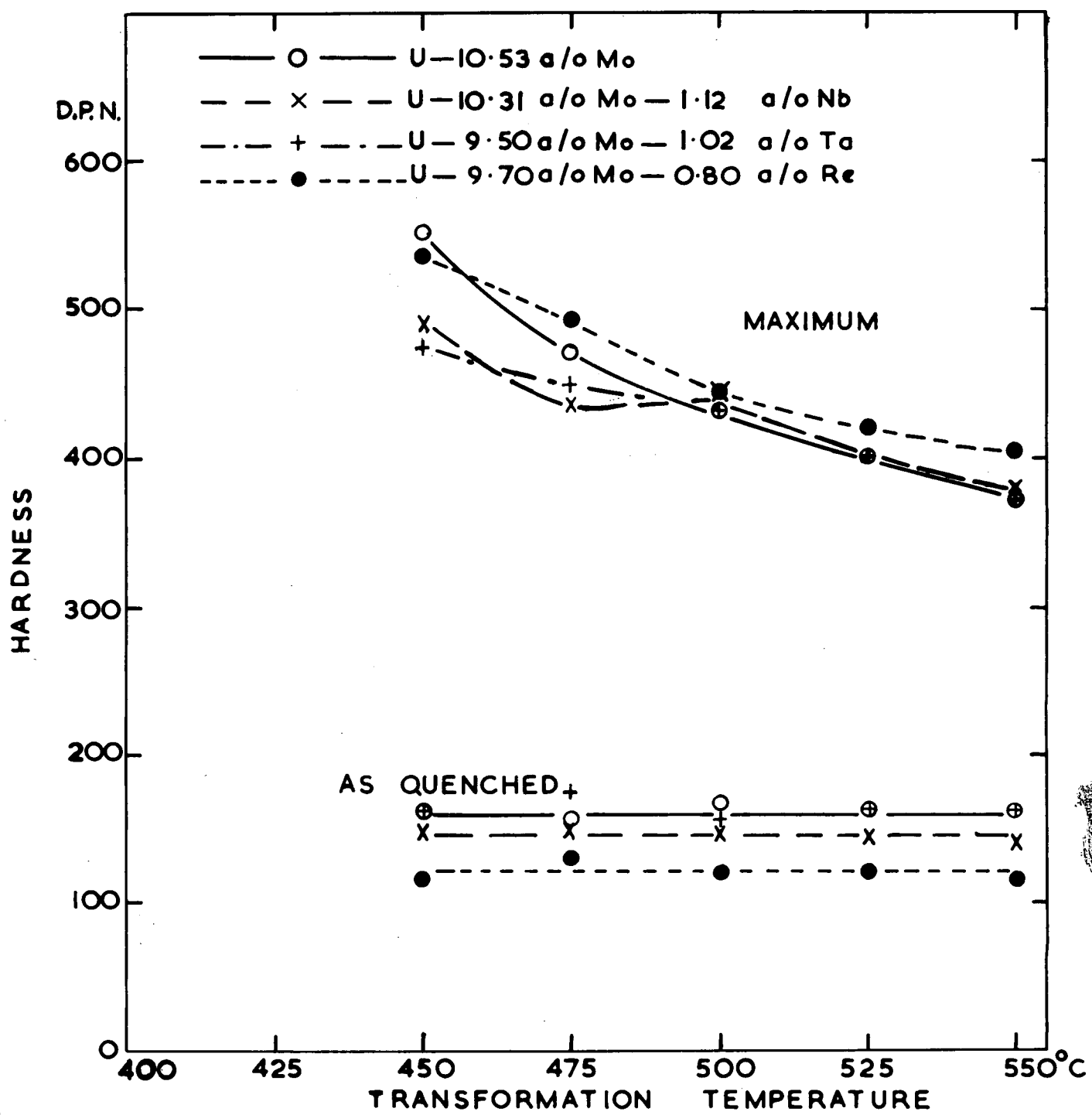


FIG. 8. Hardness temperature relationships for U-Mo base alloys.

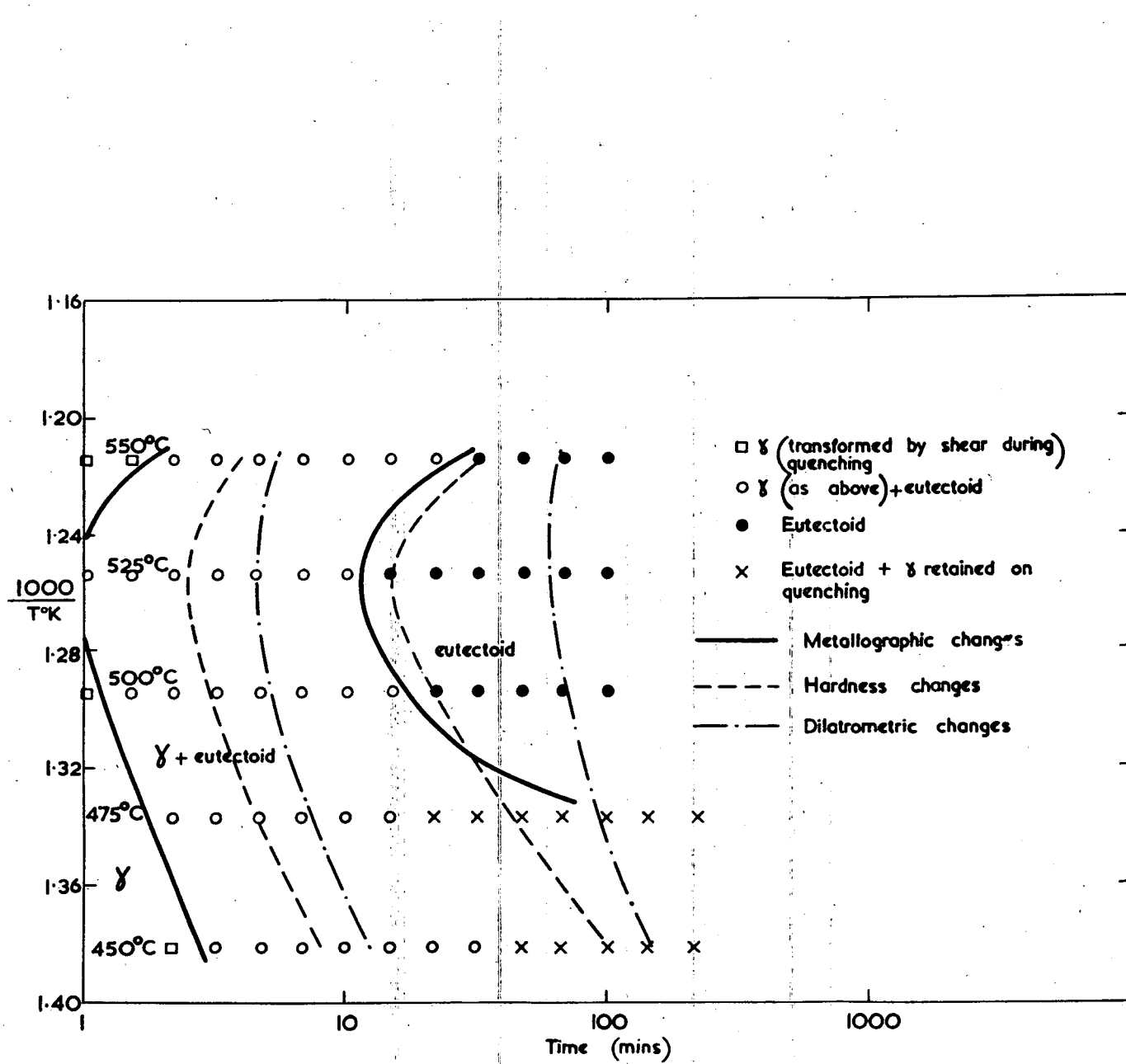


Fig. 9. Time-Temperature-Transformation Diagram of U-10.5% Mo alloy showing metallographic changes in relation to hardness and dilatometric T.T.T. curves.

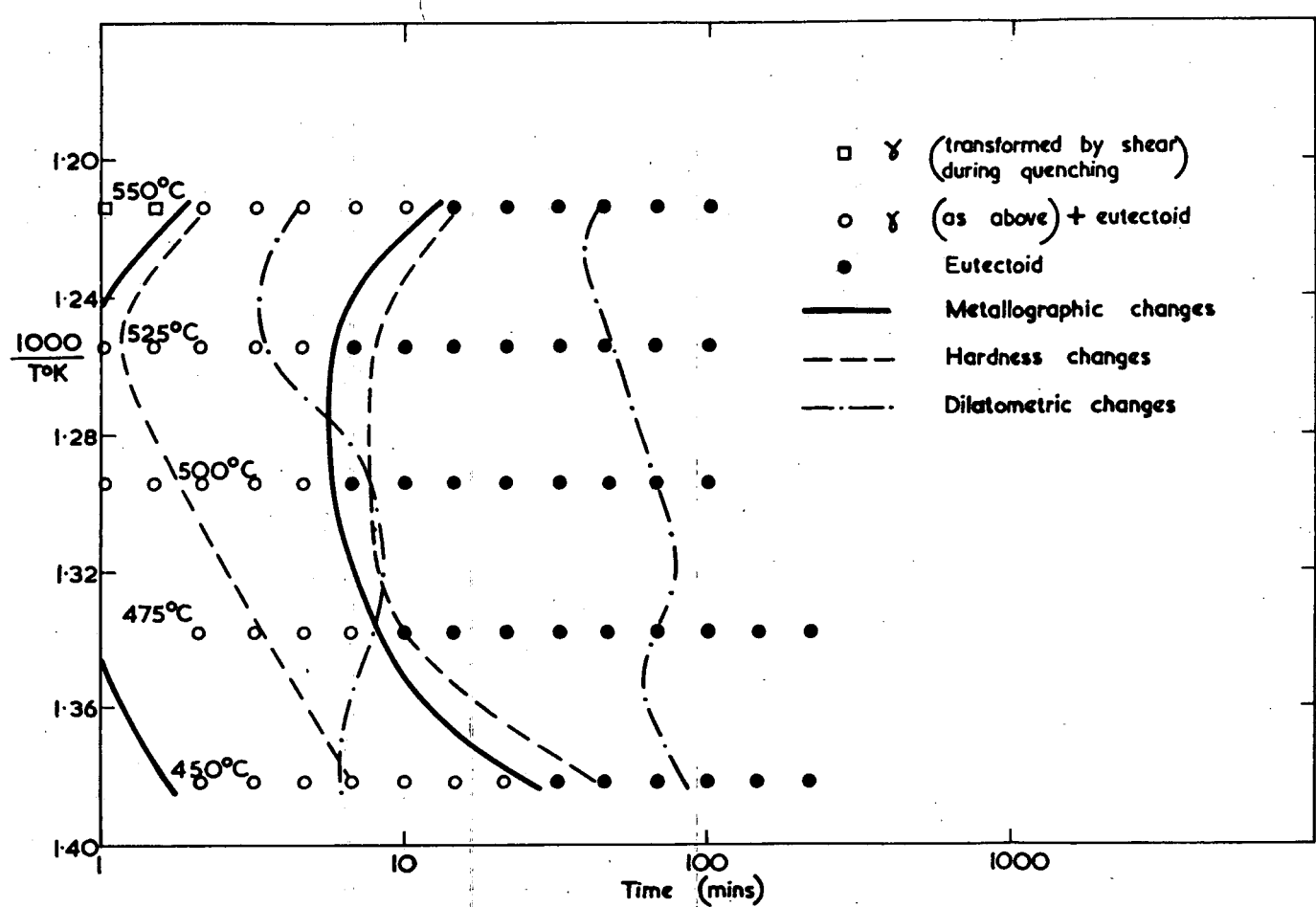


Fig. 10. Time-Temperature-Transformation Diagram of U-9.5 a/o Mo-1.0 a/o Ta alloy showing metallographic changes in relation to hardness and dilatometric T.T.T. curves.

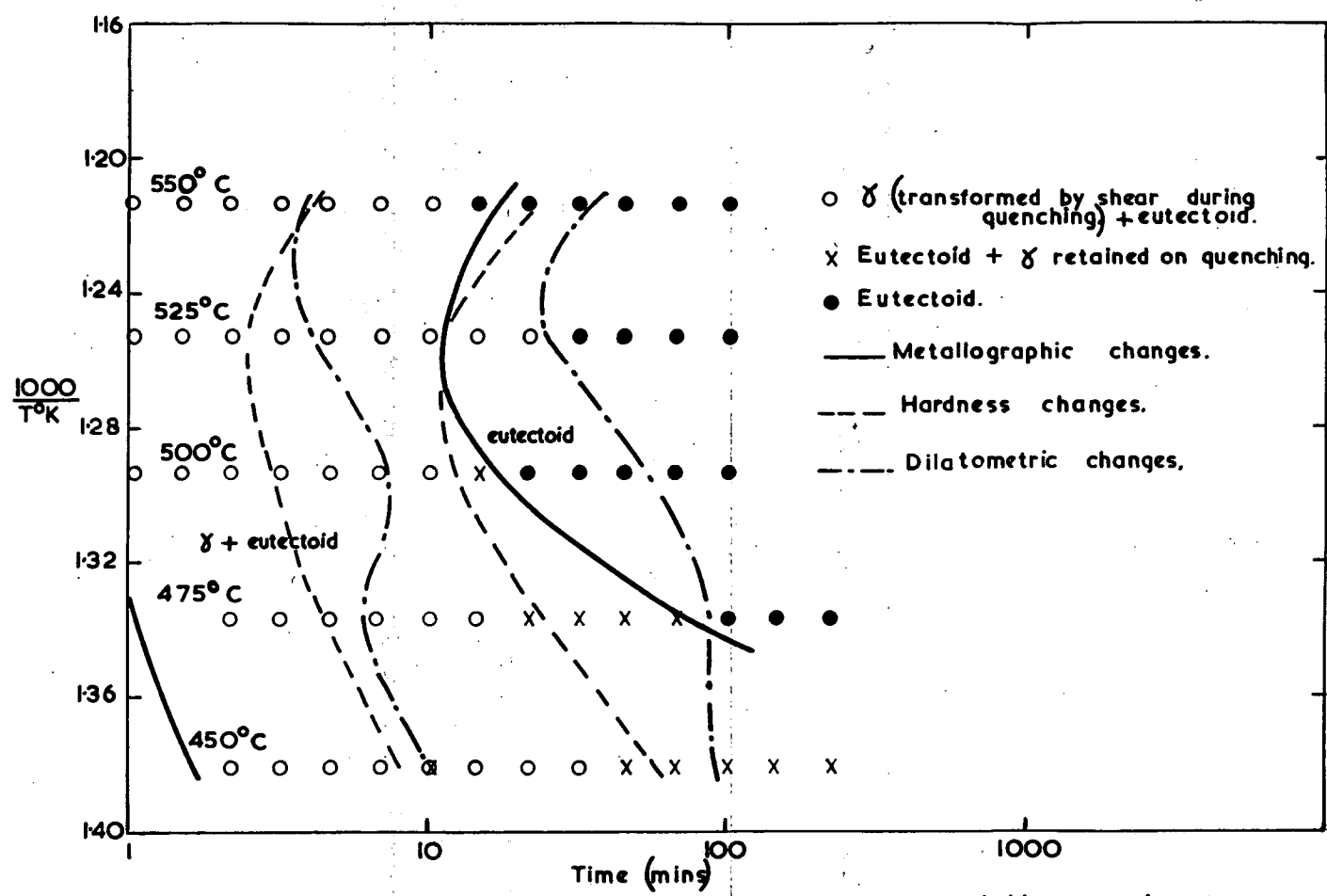


Fig. 11. Time-Temperature-Transformation diagram of U-10.3 a/o Mo - 11 a/o Nb alloy showing metallographic changes in relation to hardness and dilatometric T.T.T. curves.

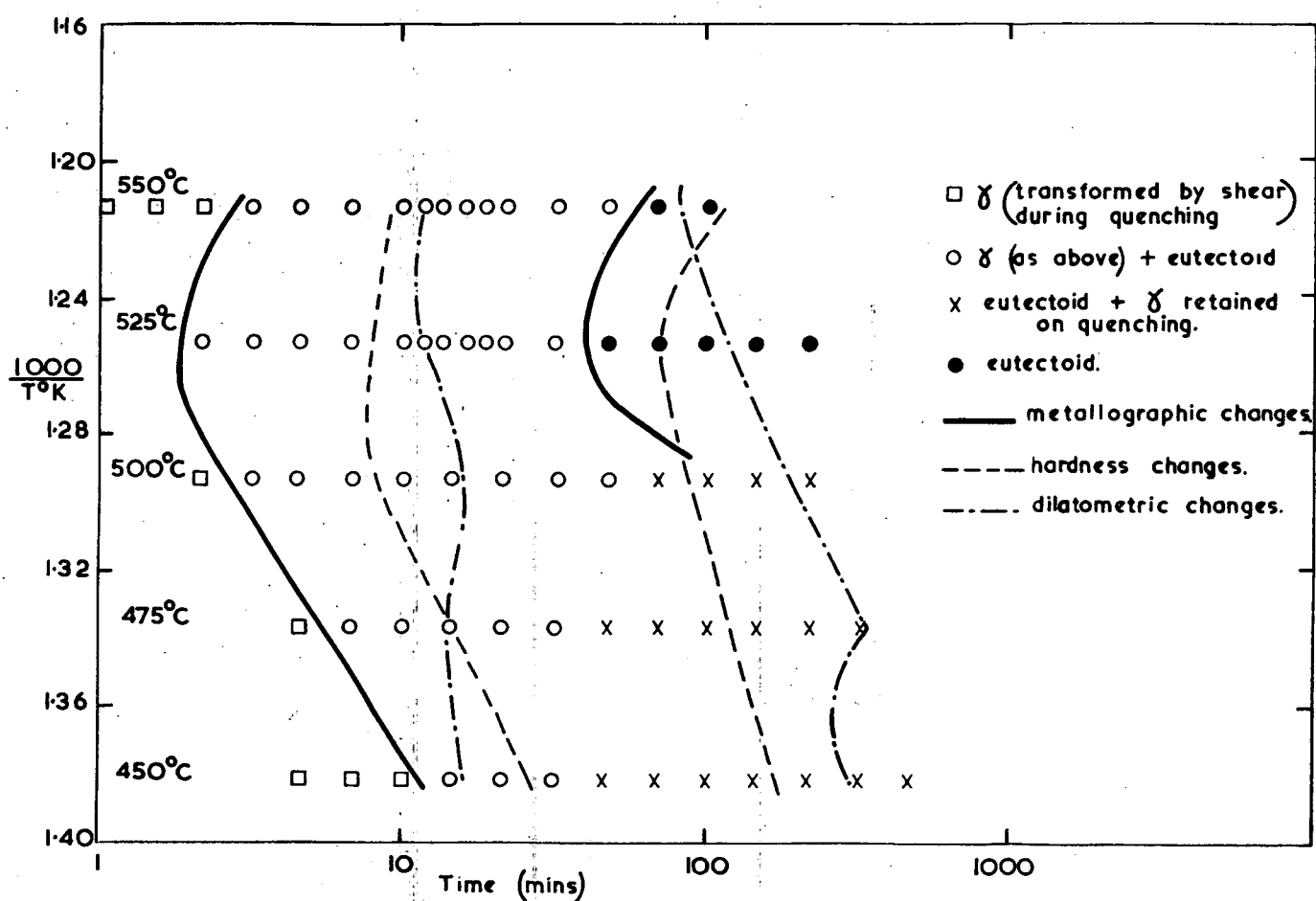
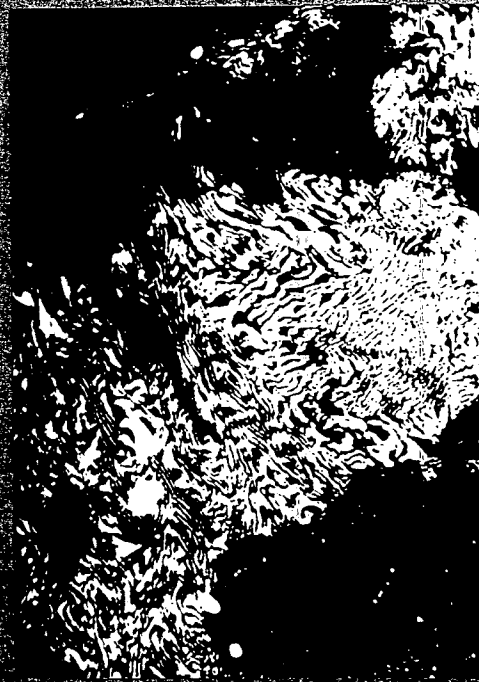


Fig. 12. Time — Temperature — Transformation diagram of U-9.7 at/o Mo-0.8 at/o Re alloy showing metallographic changes in relation to hardness and dilatometric T.T.T. curves.



068-096  
J-10137-16 Mo quenched from the  
Y region and held 15 mins at 450°C X-ray Y

068-097  
J-10137-16 Mo quenched from the  
Y region and held 50 mins 450°C X-ray Y



068-098  
J-10137-16 Mo quenched from the  
Y region and held 2.5 mins at 450°C X-ray Y

068-097

R. 126/1/1959